1994-09

Environmental forcing of ambient noise in the Nansen and Amundsen Basins of the Arctic Ocean

Feller, David

Monterey, California. Naval Postgraduate School

NPS - OC - 94 - 05

NAVAL POSTGRADUATE SCHOOL
Monterey, California

THESIS

Environmental Forcing of Ambient Noise in the Nansen and Amundsen Basins of the Arctic Ocean

by
David Feller

September, 1994

Thesis Co-Advisors: Robert H. Bourke
James H. Wilson

Approved for public release; distribution is umlimited

Prepared for:
Naval Oceanographic Office
Stennis Space Center, MS 39529-5000

NAVAL POSTGRADUATE SCHOOL
Monterey, California 93943

Rear Admiral T. A. Mercer
Superintendent

This thesis was prepared in conjunction with research sponsered in part by the Naval Oceanographic Office under contract number N6230693PO3011.

Released by:

P.J. MARTO, Dean of Research

REPORT DOCUMENTATION PAGE

Form Approved OMB No. 0704-0188

1. AGENCY USE ONLY *(Leave blank)*	2. REPORT DATE	3. REPORT TYPE AND DATES COVERED
	22 September, 1994	Master's Thesis

4. TITLE AND SUBTITLE Environmental Forcing of Ambient Noise in the Nansen and Amundsen Basins of the Arctic Ocean

5. FUNDING NUMBERS

6. AUTHOR(S) David Feller

7. PERFORMING ORGANIZATION NAME(S) AND ADDRESS(ES)
Naval Postgraduate School
Monterey CA 93943-5000

8. PERFORMING ORGANIZATION REPORT NUMBER
NPS - OC - 94 - 05

9. SPONSORING/MONITORING AGENCY NAME(S) AND ADDRESS(ES)

10. SPONSORING/MONITORING AGENCY REPORT NUMBER

11. SUPPLEMENTARY NOTES The views expressed in this thesis are those of the author and do not reflect the official policy or position of the Department of Defense or the U.S. Government.

12a. DISTRIBUTION/AVAILABILITY STATEMENT
Approved for public release; distribution is unlimited.

12b. DISTRIBUTION CODE
A

13. ABSTRACT *(maximum 200 words)*

The AREA 1992 experiment inserted three ANMET buoys on separate ice floes about 600 km north of Franz Josef Land. The buoys drifted in unison for most of the experiment and provided 12-19 months of hourly ambient noise data between 5 and 4000 Hz while obtaining limited weather data. The drift pattern was neatly divided into five legs of nearly uniform ice velocities in response to major changes in the wind field.

The annual median spectra of each buoy were nearly identical at or above 200 Hz but diverged below 200 Hz. The largest differences were recorded between the two closest buoys. The annual spectra were 10 dB greater than the long term Eurasian Basin median spectra at all frequencies. The annual median spectra was 6-7 dB greater than the CEAREX 1988/89 median spectra below 100 Hz but was quieter than CEAREX above 100 Hz.

Persistent extreme noise levels above the 95th or below the 5th percentiles were rare. Sustained 95th percentile noise levels were caused by the ice field convergence resulting from storms passing near the buoy cluster. Sustained noise levels near the 5th percentile occurred during periods of slow, steady winds.

Temporal coherency of the year-long record ranged from 12-23 hours at all frequencies, comparable to other reported data. Significant energy was found at synoptic periods of 16-148 hours and near the tidal/inertial 12 hour period at all three buoys, implying the same forcing mechanisms were important in spite of buoy separations up to 300 km. Spatial coherency between the buoys showed the highest correlation between the closest buoy pair. Differences in correlation coefficients were smaller at higher frequencies due to the increased importance of local effects at higher frequencies.

Ice speed was the best environmental correlate with ambient noise from 5-10 Hz, wind speed was best from 32-100 Hz, and wind stress was best above 100 Hz.

Three periods of extreme noise levels (two loud, one quiet), each lasting for several days, were investigated in detail to establish the role of wind forcing on ambient noise generation. Periods of loud noise were associated with periods of high wind/ice speed coupled with rapid changes in direction, i.e., loud noise levels are the result of large ice convergence and shearing moment. Quiet periods occur when the buoy drift speed is slow. One of the loud noise events showed that periods of ice convergence on nearby land will increase the noise level, even during times of moderate wind speeds.

14. SUBJECT TERMS Oceanography, Ambient Noise, Arctic,	15. NUMBER OF PAGES 185
	16. PRICE CODE

17. SECURITY CLASSIFICATION OF REPORT	18. SECURITY CLASSIFICATION OF THIS PAGE	19. SECURITY CLASSIFICATION OF ABSTRACT	20. LIMITATION OF ABSTRACT
Unclassified	Unclassified	Unclassified	UL

Approved for public release; distribution is unlimited.

ENVIRONMENTAL FORCING OF AMBIENT NOISE IN THE NANSEN AND AMUNDSEN BASINS OF THE ARCTIC OCEAN

by

David Feller
Lieutenant United States Navy
B.S., Auburn University, 1987

Submitted in partial fulfillment of the
requirements for the degree of

MASTER OF SCIENCE IN METEOROLOGY AND PHYSICAL OCEANOGRAPHY

from the

NAVAL POSTGRADUATE SCHOOL
September, 1994

Author: [redacted]
David Feller

Approved By: [redacted]
Robert H. Bourke, Thesis Co-Advisor

[redacted]
James H. Wilson, Thesis Co-Advisor

[redacted]
Robert H. Bourke, Chairman,
Department of Oceanography

ABSTRACT

The AREA 1992 experiment inserted three ANMET buoys on separate ice floes about 600 km north of Franz Josef Land. The buoys drifted in unison for most of the experiment and provided 12-19 months of hourly ambient noise data between 5 and 4000 Hz while obtaining limited weather data. The drift pattern was neatly divided into five legs of nearly uniform ice velocities in response to major changes in the wind field.

The annual median spectra of each buoy were nearly identical at or above 200 Hz but diverged below 200 Hz. The largest differences were recorded between the two closest buoys. The annual spectra were 10 dB greater than the long term Eurasian Basin median spectra at all frequencies. The annual median spectra was 6-7 dB greater than the CEAREX 1988/89 median spectra below 100 Hz but was quieter than CEAREX above 100 Hz.

Persistent extreme noise levels above the 95th or below the 5th percentiles were rare. Sustained 95th percentile noise levels were caused by the ice field convergence resulting from storms passing near the buoy cluster. Sustained noise levels near the 5th percentile occurred during periods of slow, steady winds.

Temporal coherency of the year-long record ranged from 12-23 hours at all frequencies, comparable to other reported data. Significant energy was found at synoptic periods of 16-148 hours and near the tidal/inertial 12 hour period at all three buoys, implying the same forcing mechanisms were important in spite of buoy separations up to 300 km. Spatial coherency between the buoys showed the highest correlation between the closest buoy pair. Differences in correlation coefficients were smaller at higher frequencies

due to the increased importance of local effects at higher frequencies.

Ice speed was the best environmental correlate with ambient noise from 5-10 Hz, wind speed was best from 32-100 Hz, and wind stress was best above 100 Hz.

Three periods of extreme noise levels (two loud, one quiet), each lasting for several days, were investigated in detail to establish the role of wind forcing on ambient noise generation. Periods of loud noise were associated with periods of high wind/ice speed coupled with rapid changes in direction, i.e., loud noise levels are the result of large ice convergence and shearing moment. Quiet periods occur when the buoy drift speed is slow. One of the loud noise events showed that periods of ice convergence on nearby land will increase the noise level, even during times of moderate wind speeds.

TABLE OF CONTENTS

LIST OF FIGURES

ACKNOWLEDGEMENTS

The author would like to thank Professors Robert H. Bourke and James H. Wilson for their support and guidance while researching and preparing this thesis. In addition, the following individuals provided much needed assistance and guidance: Professors R.T. Williams and F.R. Williams, and Mary Jordan, Mark Boothe and Dr. Peter Guest of the Meteorology Department, Naval Postgraduate School; Michael Cook, Arlene Guest and Peter Braccio of the Oceanography Department, Naval Postgraduate School; the Naval Postgraduate School Computer Center consultants; Mr Matthew Barron and Dr. Nelson Letourneau of the Acoustics Division, Naval Oceanographic Office; and Peggy Bruehl of Unidata Corporation. A special thank you is due to LCDR A. Rost Parsons, United States Navy, who saved me from much wasted effort while performing this research with his assistance whenever asked. Finally, I would like to gratefully thank my wife, Linda, for her unwavering support during my long hours of work.

I. INTRODUCTION

A. HISTORY

Using the ocean environment to maximum advantage has always been, and continues to be, a major consideration in the development of strategy and tactics for employment by the United States submarine force. The world ocean is made up of widely varying acoustic environments which must be studied independently. The environments that have received the most attention in the past have naturally been those in which the Navy expects to fight in wartime.

Development of nuclear propulsion technology by the former Soviet Union has led to deployments of Soviet, and now Russian, nuclear ballistic missile submarines within the Arctic basin which continue at the present time. This threat requires United States submarines to be proficient at operating within the Arctic Ocean.

United States submarines have been deploying under the ice-covered Arctic Seas since the USS Nautilus (SSN-571) made its historic voyage to the North Pole in 1958. The presence of Soviet (now Russian) ballistic missile submarines within the Arctic, and particularly under the ice pack, has made the Arctic a high priority operational region for the United States submarine force. Scientific study of the acoustic environment in the Arctic Ocean is necessary to support submarine operations in the Arctic basin. The under-ice acoustic environment presents unique sonar system problems that have yet to be solved. A major concern is the lack of an accurate Arctic ambient noise prediction model in spite of years of research devoted to measuring and analyzing ice-generated noise. In the Arctic, unlike the mid-latitude open ocean areas, ambient noise variations dominate detection and tracking performance by sonar

systems. Arctic ambient noise can vary by 20 dB to 30 dB over several hours, with associated large variations in detection ranges.

The goal of most Arctic ambient noise research projects in the past has been to determine the dominant noise generating mechanisms and to characterize the noise generated by each mechanism in terms of its spectra, and temporal and spatial variability. Several attempts have been made to correlate Arctic ambient noise based on long (monthly, seasonal, yearly) (Buck and Clark, 1989)(Lewis and Denner, 1987 and 1988) and short (hourly, daily, weekly) (Dyer, 1988) measurement records with local environmental parameters, such as wind speed and ice speed, measured directly above the noise measurement sites. All of these efforts have failed (with especially poor performance at frequencies below 300 Hz) to generate a high enough correlation level between local environmental parameters and ambient noise to confidently create an ambient noise prediction system. This failure is primarily due to the fact that a significant portion of the low frequency noise is generated at distant locations and propagates to the measurement site. The research in this thesis addresses only the storm-generated noise since its presence or absence is believed to be the cause of both very loud and very quiet noise events, respectively.

Oard (1987) proposed dominant noise generation mechanisms for various frequency ranges. A glance at a few of the major mechanisms and their characteristic spectra such as ridging (10 - 50 Hz), rafting (40 - 400 Hz), lead formation (20 - 3000 Hz) and wind (100 - 1000 Hz) demonstrates the difficulty of pinning down the exact characteristics of a broad band spectrum, especially when the spectra is not exactly the same for each event observed.

The problem of multiple sources contributing to the ambient noise field at every sample frequency is not a new phenomena. This problem is a major stumbling block in attempting to model the ambient noise field due to the difficulty in attributing measured ambient noise to the correct combination of sources.

The ambient noise measured at any point is the sum of the contributions from all noise generating phenomena at surrounding points, taking into account the initial source levels and propagation loss effects. The size of the region which can affect the measured ambient noise depends on the noise source levels and the acoustic propagation environment. Knowledge of the remote, as well as local, forcing is required to increase the correlations and predictive accuracy.

As a first step in deriving a complete ambient noise model, this thesis will focus on noise statistical properties and on storm event analysis for those occasions where the noise field is exceptionally loud or quiet. These occasions have great strategic and tactical implications on submarine operations. Previous preliminary studies (Bourke and Parsons, 1993)(Parsons, 1992) suggest that loud conditions are closely associated with the passage of a storm front, and quiet conditions with the near absence of atmospheric gradients (i.e., winds) (Poffenberger, Bourke and Wilson, 1988).

The paramount concern regarding ambient noise levels on sonar performance relates to detection ranges. A loud noise period results in shorter detection ranges, requiring a submarine to be closer to its objective. Conversely, a quiet environment results in longer detection ranges, allowing a submarine to remain farther away. The large, rapid variations in ambient noise levels could cause the

submarine to lose contact while at relatively long ranges, or much worse, be counter detected while at very short ranges. Submarines also have recurring housekeeping chores that can generate considerable self noise. The ability to routinely perform these tasks while the ambient noise environment is loud, and avoid them while the ambient noise environment is quiet, would be a significant tactical advantage to the submarine commander.

B. PURPOSE

The dual needs of the scientific community and the submarine force led to two goals for this research.

The first goal was to characterize the ambient noise field measured in the Arctic basin during the AREA 1992 experiment by three ambient noise/meteorological (ANMET) buoys. These buoys were placed in the central Arctic ice pack and drifted through areas of the Nansen and Amundsen Basins where few previous ambient noise measurements have been made.

The second goal was to examine the correlation between observed environmental parameters and the ambient noise measured under the ice pack. A key part of this second goal was to study in detail the impact of synoptic scale weather systems on the observed noise field. Storms and their associated frontal passages are known to be major causes of ambient noise levels exceeding the 95^{th} percentile (Parsons, 1992). This study will attempt to more closely relate extreme noise events (noise levels above the 95^{th} and below the 5^{th} percentiles) to known, forecastable atmospheric events.

II. AMBIENT NOISE, METEOROLOGICAL, AND POSITION RECORDS

The ambient noise, meteorological and position records from the three ambient noise/meteorological (ANMET) buoys used in this study were installed in the central Arctic ice pack north of Franz Josef Land in April 1992. The buoys used in this study were Buoys 12813, 12815 and 12819, which will be referred to as Buoys 13, 15 and 19, respectively, for brevity. The three buoys were placed in an approximately isosceles triangular pattern 600 km north of Franz Josef Land. The long sides were approximately 180 km and the short side approximately 100 km. Figure 1 shows the region surveyed by the AREA 1992 experiment. Figures 2, 3 and 4 show the three buoy drift patterns relative to a gridded reference frame as well as the boundaries of the drift legs and the locations of the three synoptic events, which will be discussed later.

The buoys were installed between 17-20 April 1992 (Barron, personal communication, 1993). The first full day of data acquisition for all three buoys was 21 April 1992, and the records were truncated to begin on that date. Buoy 15 sank on 28 August 1993 after its ice floe got too close to Svalbard and broke up. Buoy 19 sank on 23 December 1993 and Buoy 13 sank on 8 January 1994, when their respective ice floes broke up.

The noise records from Buoys 13 and 15 had to be truncated before the buoys sank because they drifted into shallow water (305 m) and their hydrophones ran aground. Their records were trimmed to end just before the time of the first grounding of the hydrophone. The records vary in length between 376 days (Buoy 15) and 592 days (Buoy 19).

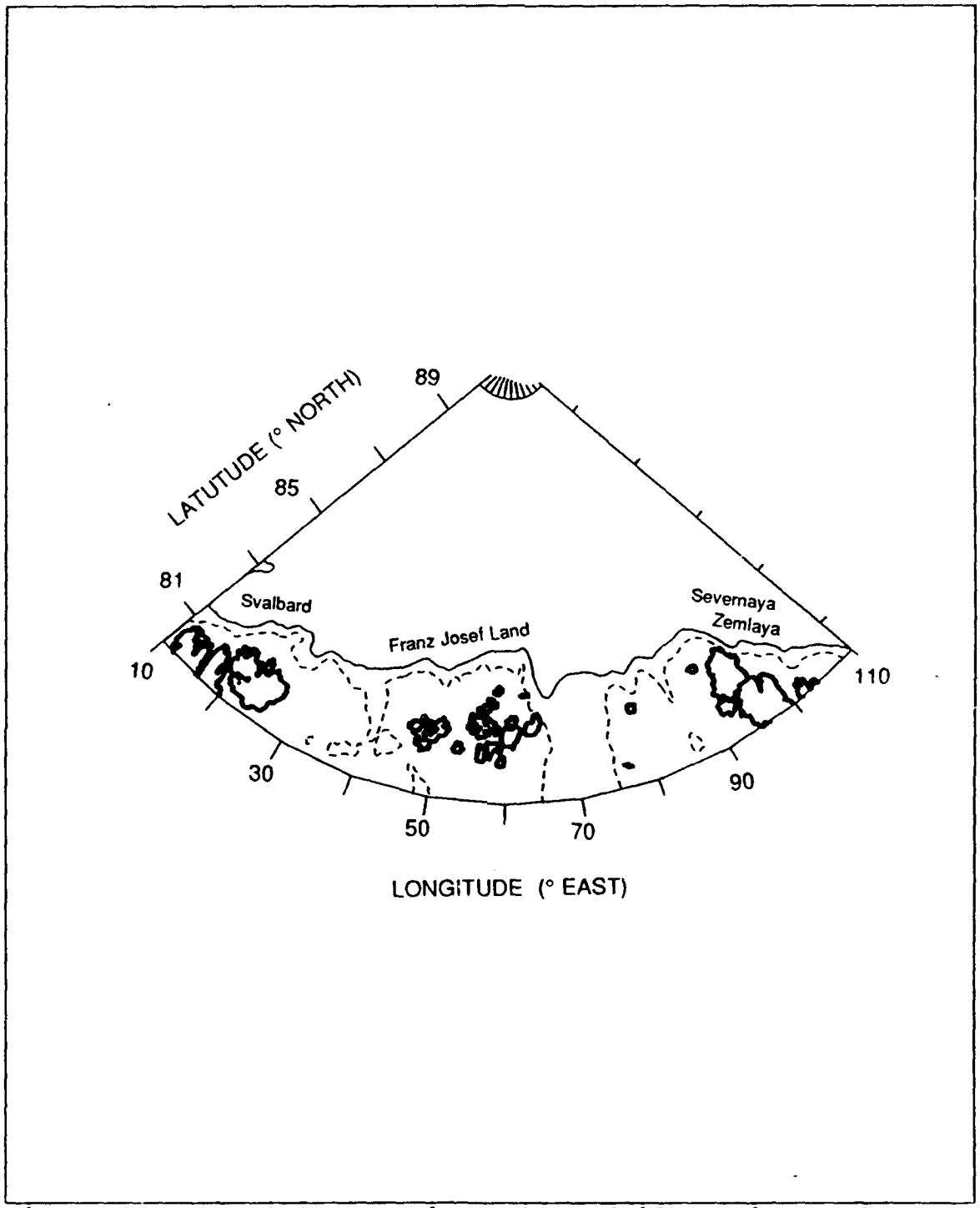

Figure 1. AREA 1992 experiment buoy drift region. The solid line is the 1000 m isobath. The dashed line is the 305 m isobath, which was the depth of the buoy hydrophones.

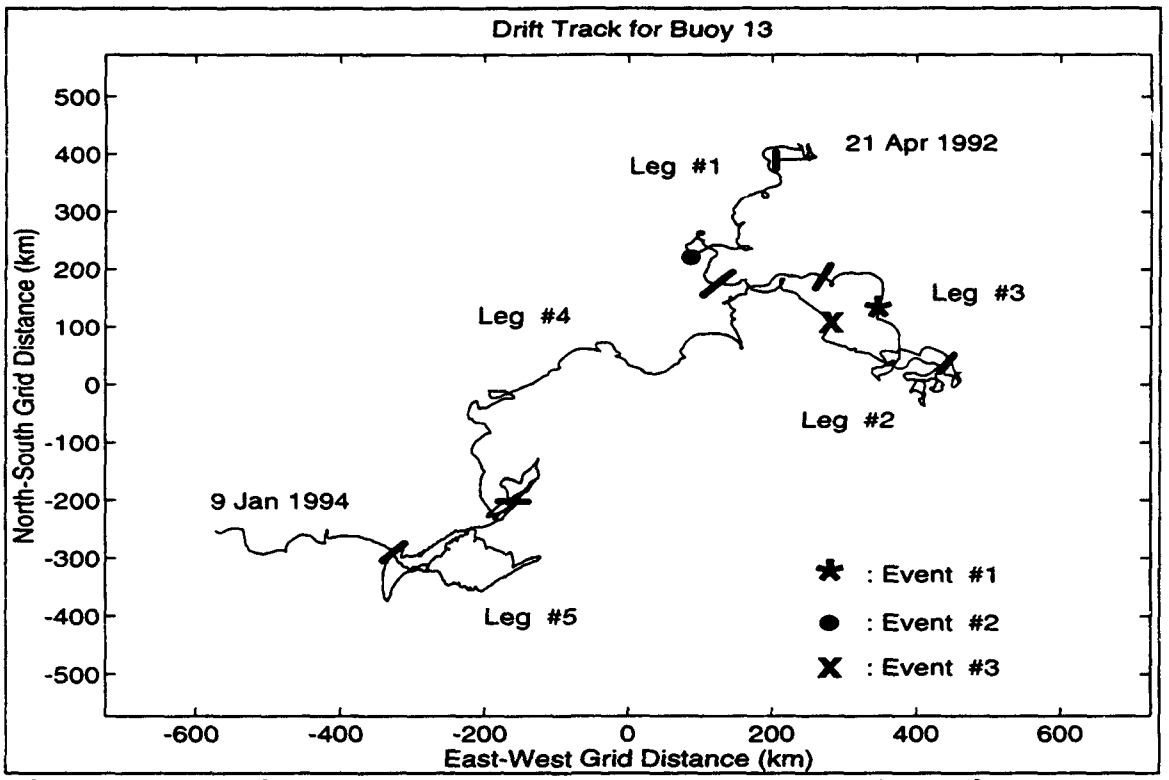

Figure 2. Drift track for Buoy 13 shows the locations of the drift leg boundaries (bars) and the three analyzed synoptic events.

The data were provided by Mr. Matt Barron and Dr. Nelson Letourneau of the Naval Oceanographic Office.

A. ANMET BUOY CHARACTERISTICS AND BACKGROUND

The ANMET buoys were first deployed in 1988 and were a significant improvement over previous Arctic buoys (Buck and Clark, 1989) in that they record noise measurements hourly instead of every three hours, and also measure a larger number of frequencies. The buoys measure the noise field at eleven frequency bands centered at 5, 10, 20, 32, 50, 100, 200, 500, 1000, 2000 and 4000 Hz. The bandwidth of each band is 25% of the center frequency. Noise measurements were made on the hour, with a frequency-dependent sample time selected for each band to maintain a constant time-

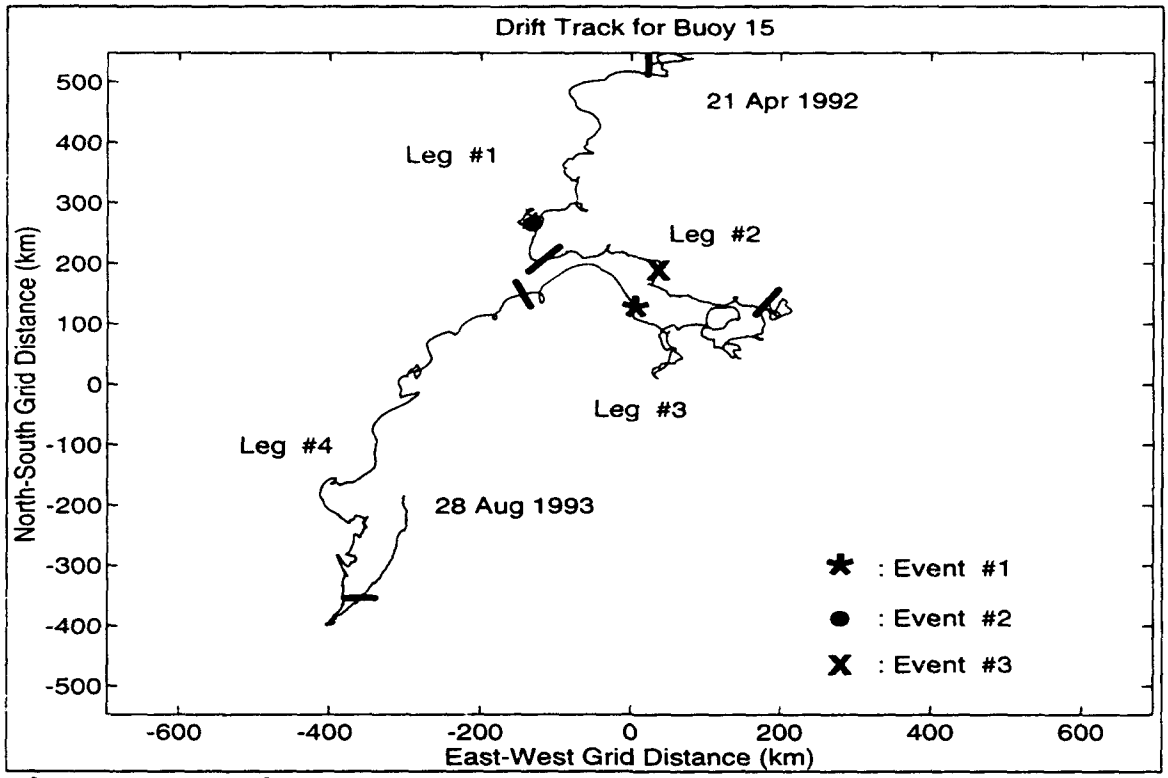

Figure 3. Drift track for Buoy 15 shows the locations of the drift leg boundaries (bars) and the three analyzed synoptic events.

bandwidth product of 40 Hz-seconds. This acquisition procedure implies that the recorded noise field is a snapshot in time that is expected to be representative of noise conditions present during the preceding and following 30 minute intervals. The maximum allowable self-noise of the ANMET buoy is frequency-dependant as shown in Table I. These self-noise limits are well below the lowest measured Arctic ambient noise levels. The ANMET buoy's acoustic measurements are performed by a single hydrophone suspended 305 m below the ice.

As discussed by Parsons (1992), low frequency data at 5 Hz and 10 Hz has sometimes been contaminated by cable strum in earlier buoy designs. The hydrophone cable for the

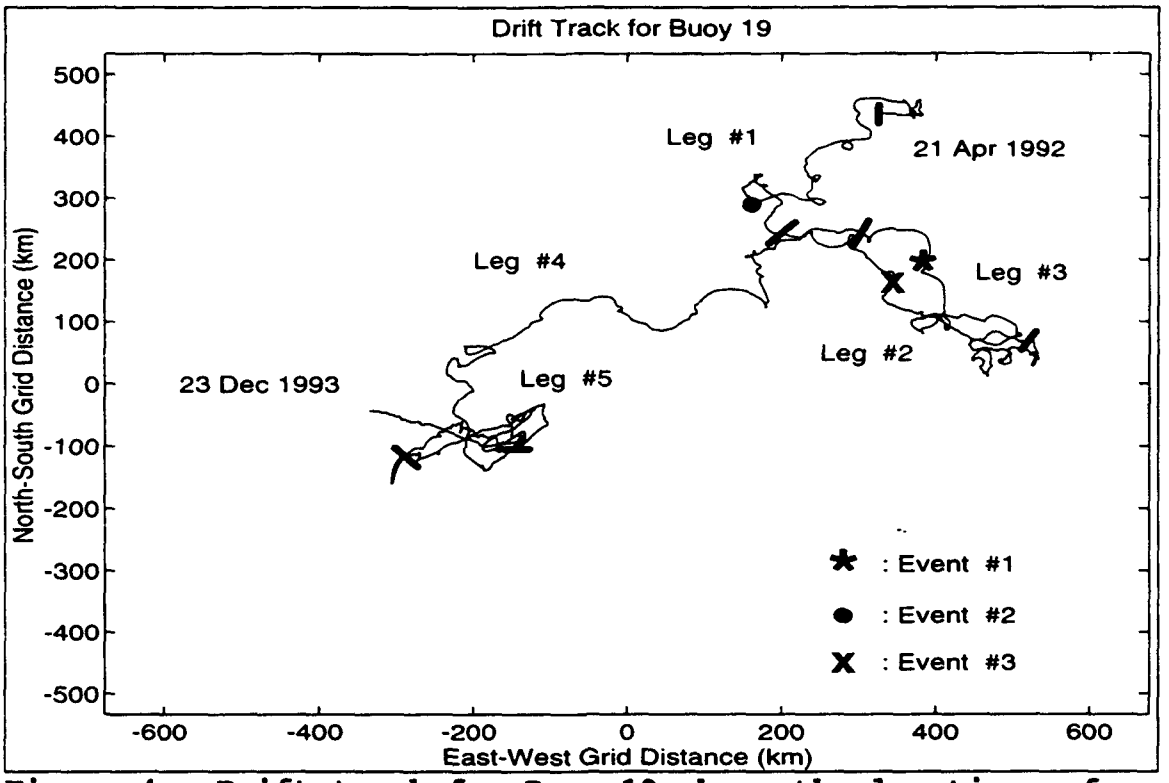

Figure 4. Drift track for Buoy 19 shows the locations of the drift leg boundaries (bars) and the three analyzed synoptic events.

current generation of ANMET buoys has been designed to minimize cable strum contamination (Barron, personal communication, 1993) and hence are presumed to be uncontaminated by cable strum.

The meteorological measurements of air temperature and pressure and ice temperature were made every 15 min. The air and ice temperature sensors each have a range of -50°C to +10°C, a resolution of 0.25°C, and an accuracy of +/- 1°C. The barometric pressure sensor has a range of 950 to 1050 mb, a resolution of 0.1 mb, and an accuracy of better than 1.0 mb in a wind of 30 m/s.

All data were telemetered via the ARGOS satellite system, which also tracked the position of the buoys. The

Center Frequency (Hertz)	Maximum Acceptable System Noise (Decibels re 1 $\mu Pa^2/Hz$)
5	52
10	50
20	44
32	42
50	38
100	36
200	35
500	22
1000	18
2000	16
4000	15

Table I. MAXIMUM ACCEPTABLE SYSTEM NOISE FOR EACH FREQUENCY BAND.

buoys continuously transmit the last two noise measurements and the current meteorological data. Position information is not recorded on a fixed schedule and is only received during a satellite pass. The large number of ARGOS satellite passes over the Arctic Ocean generally minimizes the gaps in data transmission.

B. PREPARATION OF NOISE DATA

The ANMET noise data were provided by the Naval Oceanographic Office at hourly intervals in units of dB re 1 $\mu Pa^2/Hz$. Following the reasoning of Makris and Dyer (1986),

the decibel values were converted to pressure values for use in the correlation analyses.

The noise records were edited for bad and missing data. Bad data were initially defined as a value below the frequency-dependent system self noise limit, or greater than three standard deviations from the mean of the entire record. The records were then interpolated with a cubic spline to establish an hourly time series. The smoothed record was edited for outliers not yet corrected or inadvertently created by the cubic spline interpolation. The system self-noise limit was used as an absolute floor to define bad data. To remove outliers not deleted by the previous three standard deviation limit, a moving filter was applied. A data point was rejected if it was greater than three standard deviations from the mean of the five points preceding, or succeeding, the point in question. Points were checked both before and after to prevent rejecting data points solely due to a large trend in pressure values. The data were then interpolated linearly to fill gaps created from the previous step.

Two final data quality checks were performed on the data to remove non-physical spikes remaining in the noise records. For low amplitude outliers, caused by the cubic spline interpolation, any values below the system self-noise limit were rejected and the gaps filled by linear interpolation. For high amplitude outliers, if a value was more than 10 dB greater than the average of the values immediately adjacent to it, it was rejected and the gap filled by linear interpolation. A summary of the data statistics is presented in Appendix A.

C. PREPARATION OF METEOROLOGICAL DATA

Although the meteorological data were measured every 15 min, their values were recorded only during satellite passes

and not at regular time intervals. The raw meteorological time series were edited for data values outside the design range of the associated sensor. The time series were then interpolated with a cubic spline routine, decimated to hourly time intervals, and plotted. Data that caused spikes in the plot were edited.

Often, two sets of meteorological data, only a few minutes apart, were received on the satellite passes. Interpolating this unevenly spaced data with a cubic spline caused non-physical irregularities so a cubic spline was not used in the final processing step. The meteorological data were linearly interpolated and decimated to obtain an hourly time series. To remove high frequency noise in the data, a 3 hour boxcar filter was applied. Each data point was replaced by the average of itself and the points immediately adjacent to it. A summary of the data statistics is presented in Appendix A.

D. PREPARATION OF POSITION DATA

Position data were recorded only during satellite passes. The raw position data were interpolated using a cubic spline routine and decimated to obtain hourly time series for latitude and longitude. The resulting time series were plotted and position fixes causing non-physical spikes in the plot were edited. Many passes yielded two fixes which were often of differing qualities. The lower quality fix was removed if it caused a spike in the time series plot. Linear interpolation was used to generate the final hourly time series. A 5 hour boxcar filter was applied after the interpolation to reduce the high frequency noise in the position time series data. A summary of the data statistics is presented in Appendix A.

The separation between Buoys 13 and 19 is fairly constant for the entire experiment until the Buoy 13

hydrophone ran aground; ranges varied between 66 km and 100 km for the entire 471 day period. The initial separation between Buoy 15 and the other buoys was approximately twice the distance between Buoys 13 and 19, 171 km and 185 km versus 99 km. Buoy 15 was installed to the northwest of Buoys 13 and 19, but by the time it sank it had moved about twice as far from its installation point as the other two buoys.

E. CALCULATION OF WIND SPEED DATA

There were no supporting environmental measurements made for the AREA '92 experiment, so it was necessary to calculate wind speed from the buoy position and meteorological data. The surface geostrophic wind speed was calculated using a method suggested by Williams (personal communication, 1994). The position data were transformed onto a polar stereographic map projection where the longitude, latitude and barometric pressure became the x, y, and z Cartesian coordinates. The barometric pressure at each buoy was then represented in three dimensional Cartesian space.

The equation of the plane passing through all three points was then determined. The general equation of a plane is: $Ax + By + Cz + D = 0$, where A, B, C and D are constants. Solving this equation for z (barometric pressure) yields a simple way to determine the partial derivatives necessary to calculate the pressure gradient terms required to estimate the surface geostrophic wind speed. The geostrophic wind speed is defined by the equations:

$$U_g = - (1/\rho f) \partial p/\partial y \qquad (1)$$

$$V_g = (1/\rho f) \partial p/\partial x \qquad (2)$$

where U_g and V_g are the eastward and northward geostrophic components, ρ is the atmospheric density, f is the Coriolis parameter, p is the barometric pressure, and $\partial p/\partial x$ and $\partial p/\partial y$

are the pressure gradients in the eastward and northward directions, respectively.

The U_g and V_g components were then transformed back to spherical coordinates for determination of the magnitude and direction of the geostrophic wind. The resulting wind vector represents the geostrophic wind velocity at the center of the triangle defined by the positions of the three buoys. This method requires that meteorological and positional data be available from all three buoys, so wind speed information is available only during the period when all three buoys were active.

The calculated geostrophic wind was used for all correlation analyses because it was the only wind speed data available at the same hourly sampling rate as the noise measurements. In addition, charts of observed surface winds and the surface pressure field prepared by the National Weather Service were used during the event analysis.

F. CALCULATION OF WIND STRESS

Wind stress was determined from:

$$|\tau| = \rho * C_D * |U_{wind}|^2 \qquad (3)$$

where $|\tau|$ is the magnitude of the wind stress, ρ is the density of the air, C_D is the drag coefficient, and $|U_{wind}|$ is the magnitude of the surface wind velocity. The density was determined using the measured air temperature and pressure. The coefficient of drag used was 0.023, based on the measurements from the CEAREX 1988/89 experiment (Bourke and Parsons, 1993). The CEAREX value was chosen since it was measured with high accuracy from a research ship frozen into the ice, and the region of the CEAREX experiment was reasonably close to the current experimental area. In fact, the buoys from this experiment ended up near where the CEAREX buoys were inserted.

G. CALCULATION OF ICE SPEED DATA

The ice speed time series for each buoy was calculated from the individual buoy trajectory using a centered time difference technique. The first and last hourly ice speeds of the record were calculated using a forward-in-time and backward-in-time differencing scheme, respectively. The buoy latitude and longitude positions were transformed onto a polar stereographic projection. The ice speeds were then calculated, and the velocity components transformed back to spherical coordinates. Any non-physical spikes in the data were removed during the position data preparation.

III. NOISE, METEOROLOGICAL AND POSITION DATA ANALYSIS

A. NOISE ANALYSIS

1. NOISE SPECTRA

The first step in characterizing the observed ambient noise field in the Nansen and Amundsen Basins was to examine the spectral levels measured by the three ANMET buoys. The median spectra were chosen as the measure of central tendency since median spectra are commonly reported in the literature. In addition, the 5^{th} and 95^{th} percentile noise levels were examined to establish the characteristics of the noise field during periods of extremely loud and quiet conditions, respectively. Spectra were calculated for the first year of data to establish the annual noise levels. The spectral levels were also partitioned into winter (November through March) and summer (May through September) seasons to examine the seasonal noise characteristics.

Summary statistics for the annual and seasonal spectra are listed in Tables II, III and IV. In the discussion that follows trends are primarily based on graphical representations. The tables provide a useful summary of absolute noise levels.

The median noise level from Buoys 13, 15 and 19 for the first year of data from 21 April 1992 to 21 April 1993 are illustrated in Figure 5. The three buoys have different median levels below 200 Hz, but all are within 10 dB of each other. The measured spectra for all three buoys are nearly identical for frequencies at or above 200 Hz. The spectral slope shown in Figure 5 is typical of the -6 dB/octave slopes observed in decades of buoy data collected in the central Arctic (Buck and Wilson, 1986).

BUOY	FREQUENCY (Hz)	MEAN (dB // 1μPa²/Hz)	MEDIAN (dB // 1μPa²/Hz)	STANDARD DEVIATION (dB)
BUOY 13	5	95.41	95.50	13.05
	10	90.12	90.90	8.12
	32	83.95	84.80	7.69
	100	74.82	75.20	7.57
	200	64.00	63.40	7.10
	500	57.11	56.10	7.01
	1000	51.84	50.40	4.87
BUOY 15	5	91.14	88.30	13.56
	10	86.64	85.40	9.72
	32	81.21	80.90	8.39
	100	72.81	72.60	8.42
	200	62.71	62.80	7.32
	500	56.14	55.70	6.80
	1000	51.10	49.80	4.96
BUOY 19	5	87.97	85.00	9.94
	10	85.73	85.70	7.93
	32	78.90	79.00	6.05
	100	71.64	71.50	6.89
	200	63.07	62.90	7.20
	500	56.69	56.10	6.60
	1000	51.51	50.40	4.46

Table II. Summary statistics for annual noise records from 21 Apr 92 through 21 Apr 93.

During the first year, the average distance between buoy pairs is shown in Table V. Buoys 13 and 19 drifted

BUOY	FREQUENCY (Hz)	MEAN (dB // 1μPa²/Hz)	MEDIAN (dB // 1μPa²/Hz)	STANDARD DEVIATION (dB)
BUOY 13	5	95.87	94.40	12.11
	10	91.45	91.10	6.42
	32	84.91	85.10	6.68
	100	76.62	76.70	6.40
	200	68.35	68.50	5.93
	500	61.25	61.20	6.07
	1000	54.27	53.90	5.09
BUOY 15	5	94.17	91.10	12.96
	10	90.64	88.40	9.01
	32	85.06	84.00	7.30
	100	76.65	75.30	7.73
	200	67.34	67.20	5.55
	500	60.29	60.20	5.84
	1000	53.99	53.40	5.02
BUOY 19	5	88.87	85.40	8.70
	10	88.59	87.90	6.34
	32	81.82	81.60	4.55
	100	74.71	74.30	5.80
	200	67.31	67.20	6.20
	500	60.48	60.30	6.07
	1000	53.72	53.00	4.82

Table III. Summary statistics for winter 1992/1993 noise records.

close together with a mean separation of only 87 km. Buoy 15 followed a similar drift pattern but remained about 300 km to the west. It was anticipated that Buoys 13 and 19 would exhibit spectra that were quite similar due to their

BUOY	FREQUENCY (Hz)	MEAN (dB // 1μPa²/Hz)	MEDIAN (dB // 1μPa²/Hz)	STANDARD DEVIATION (dB)
BUOY 13 1992	5	95.41	97.20	13.89
	10	88.54	91.00	9.29
	32	82.68	84.70	8.71
	100	72.68	73.40	8.15
	200	58.70	58.10	4.50
	500	51.94	51.20	4.23
	1000	48.83	48.20	2.55
BUOY 13 1992	5	87.17	83.40	13.35
	10	81.58	80.20	8.56
	32	76.25	75.20	7.32
	100	67.95	66.80	7.07
	200	57.17	56.40	5.42
	500	51.12	50.10	4.41
	1000	47.80	47.00	2.45
BUOY 15 1992	5	87.05	84.30	11.31
	10	82.08	81.50	7.92
	32	75.16	75.20	5.67
	100	67.77	67.40	6.25
	200	58.11	57.50	5.13
	500	52.23	51.40	4.32
	1000	49.04	48.20	2.57
BUOY 19 1993	5	93.71	99.10	14.94
	10	91.89	87.80	15.10
	32	83.13	79.10	11.79
	100	72.34	72.30	9.17
	200	55.69	55.00	4.22
	500	50.58	49.80	3.70
	1000	48.10	487.80	2.56

Table IV. Summary statistics for summer 1992 noise records.

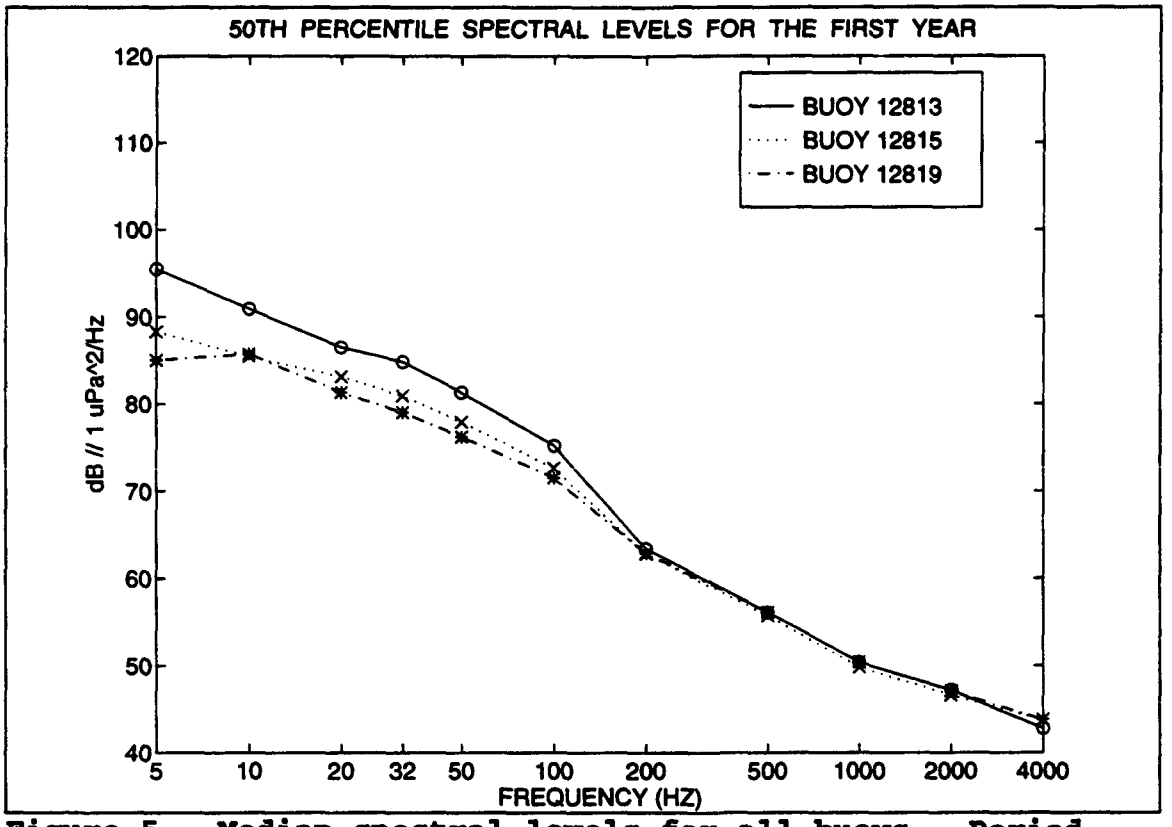

Figure 5. Median spectral levels for all buoys. Period covered is 21 Apr 92 through 21 Apr 93.

relative proximity, but this was not the case. Noise levels for Buoy 13 from 100 Hz and below are louder by about 5 dB than the other buoys, with Buoy 19 being quieter than Buoy 15 by 1-2 dB. All the buoys were in water deeper than 1000 m during the entire first year, though Buoy 15 was closest to land (Svalbard) and farthest south by the end of the year. Buoy 19 was the farthest north with Buoy 13 between the other buoys (but much closer to Buoy 19), so no explanation for Buoy 13's higher spectral levels is apparent.

At higher frequencies local noise generating sources dominate over noise arriving from more distant noise sources. The nearly identical spectral levels above 200 Hz

BUOY PAIR	13/15	13/19	15/19
AVERAGE SEPARATION (KM)	279.3	86.8	322.0

Table V. Average separation distance between buoy pairs from 21 Apr 92 through 21 Apr 93.

indicates that the noise generating mechanisms surrounding the buoy cluster were statistically very similar.

The 95th percentile levels for the first year are shown in Figure 6. The same characteristic spectral shape present in the median spectra was observed. For the lower frequencies (≤ 100 Hz) Buoys 13 and 15 exhibit nearly similar values. As was the case at median levels, Buoy 19 recorded the lowest levels, approximately 5-7 dB less than the other two buoys. At 200 Hz and above, the spectra of all buoys are nearly identical.

Much less difference is noted between the buoys at the 5th percentile as shown in Figure 7; all are within 3-5 dB of each other. Buoy 15 and 19 noise levels were within 1 dB of each other with the notable exception at 50 Hz where Buoys 13 and 19 recorded an anomalous, but identical peak in noise level. This buoy pair is closest together so a unique noise generating source could possibly affect these buoys and not Buoy 15.

Figure 8 shows the median spectra for the summer of 1992. This is the only summer in which all three buoys were active for the entire five month season. As in the year-long spectra, Buoy 13 noise levels at 100 Hz and below were the loudest. The year-long and summer spectra were nearly identical below 100 Hz. The summer median spectra was about

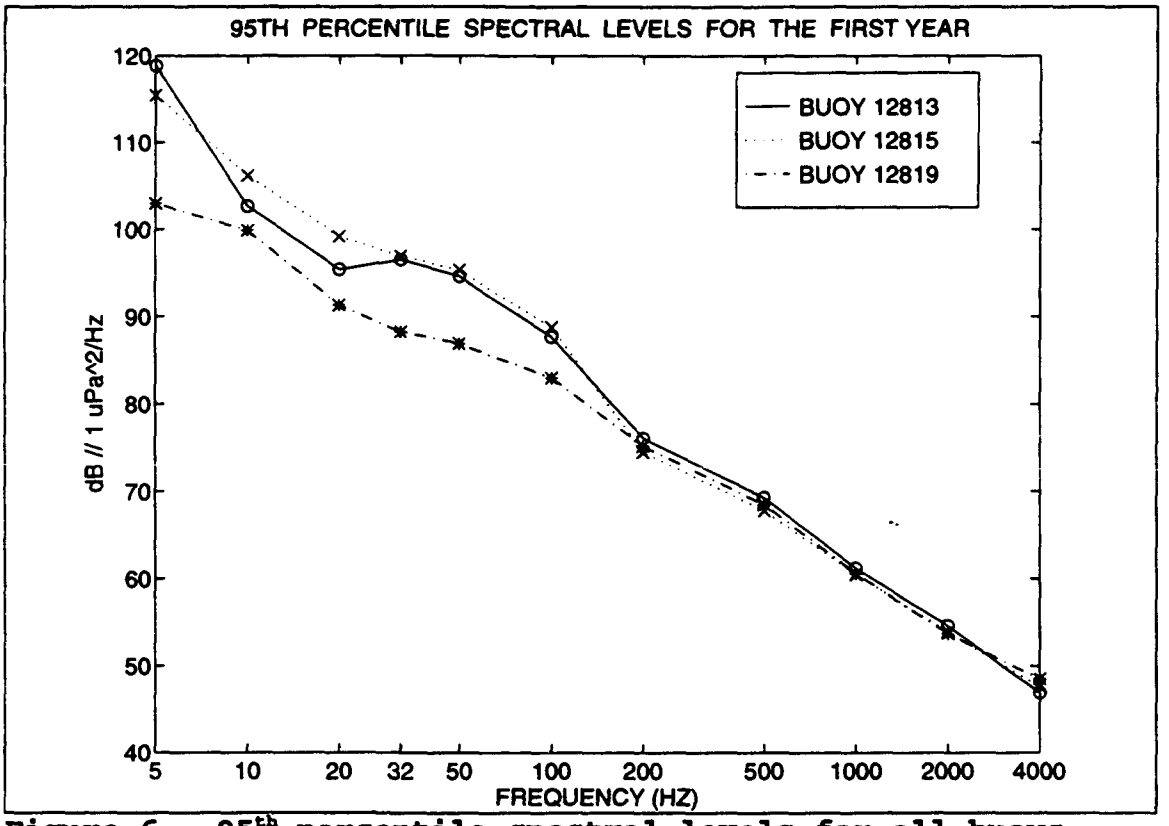

Figure 6. 95th percentile spectral levels for all buoys. Period covered is 21 Apr 92 through 21 Apr 93.

5 dB quieter than the median annual spectra between 100 and 1000 Hz, but were again nearly identical above 1000 Hz.

Buoys 15 and 19 demonstrate nearly identical levels but are lower by about 3-5 dB than the year-long record. This trend towards quieter values in summer has been observed repeatedly within the Arctic basin for many years (Buck and Wilson, 1986). The median spectra in summer for Buoy 13 is virtually identical with its year long spectra below 100 Hz. The reason for the lack of the normal seasonal dependance is unknown.

The spectral shape of the 95th percentile for Buoy 13 at frequencies 100 Hz and below during the summer of 1992 (Figure 9) is similar to the year long spectra. The major

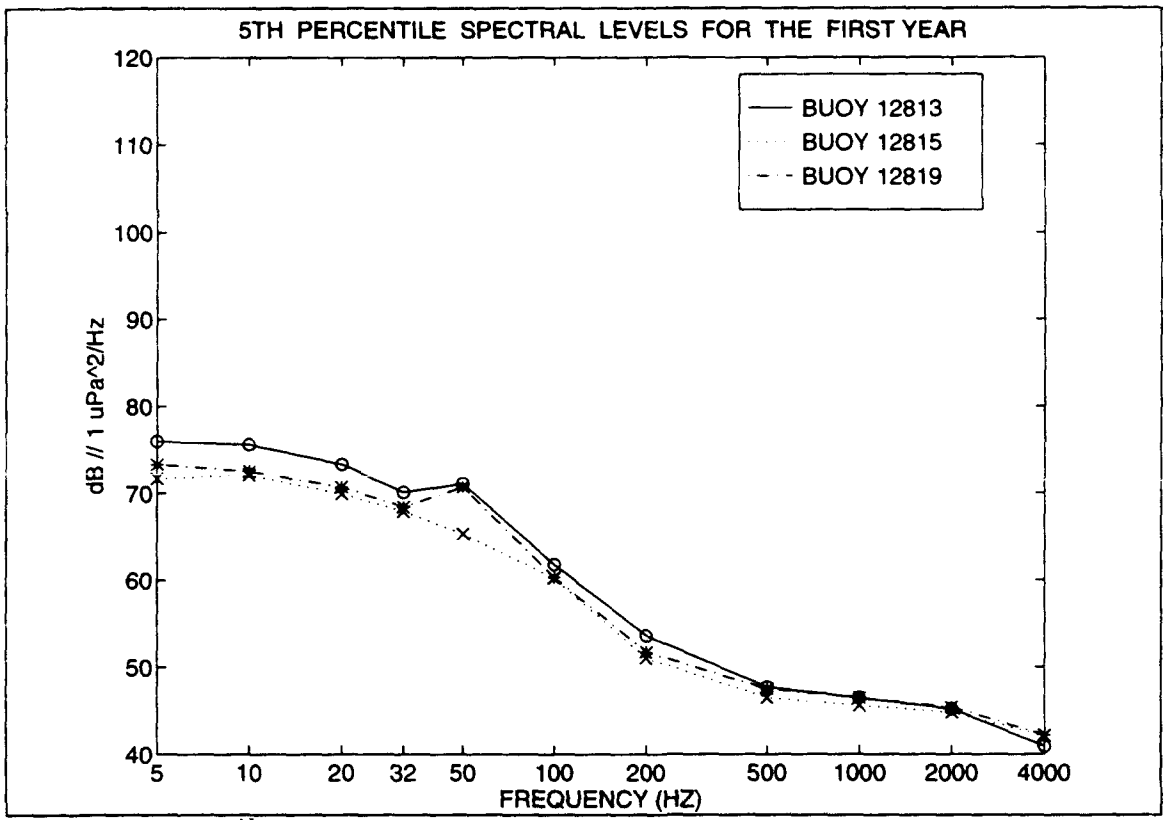

Figure 7. 5th percentile spectral levels for all buoys. Period covered is 21 Apr 92 through 21 Apr 93.

seasonal change is the approximately 10 dB reduction in noise level for Buoy 15 and 5 dB reduction for Buoy 19. Above 200 Hz the loud noise events of summer are relatively quiet, being about 10 dB less than the yearly 95th percentile levels. This decrease in noise level at higher frequencies is especially apparent for Buoy 13 where a 22 db/octave reduction is noted between 100 and 200 Hz.

The summertime and mean annual spectra for times of extreme quiet conditions (5th percentile) exhibit nearly the same shape but with summertime values about 3 dB less (compare Figure 10 with Figure 7). This is not unexpected as Poffenberger et al. (1989) found in the Eurasian Basin that occurrences of extremely quiet conditions were

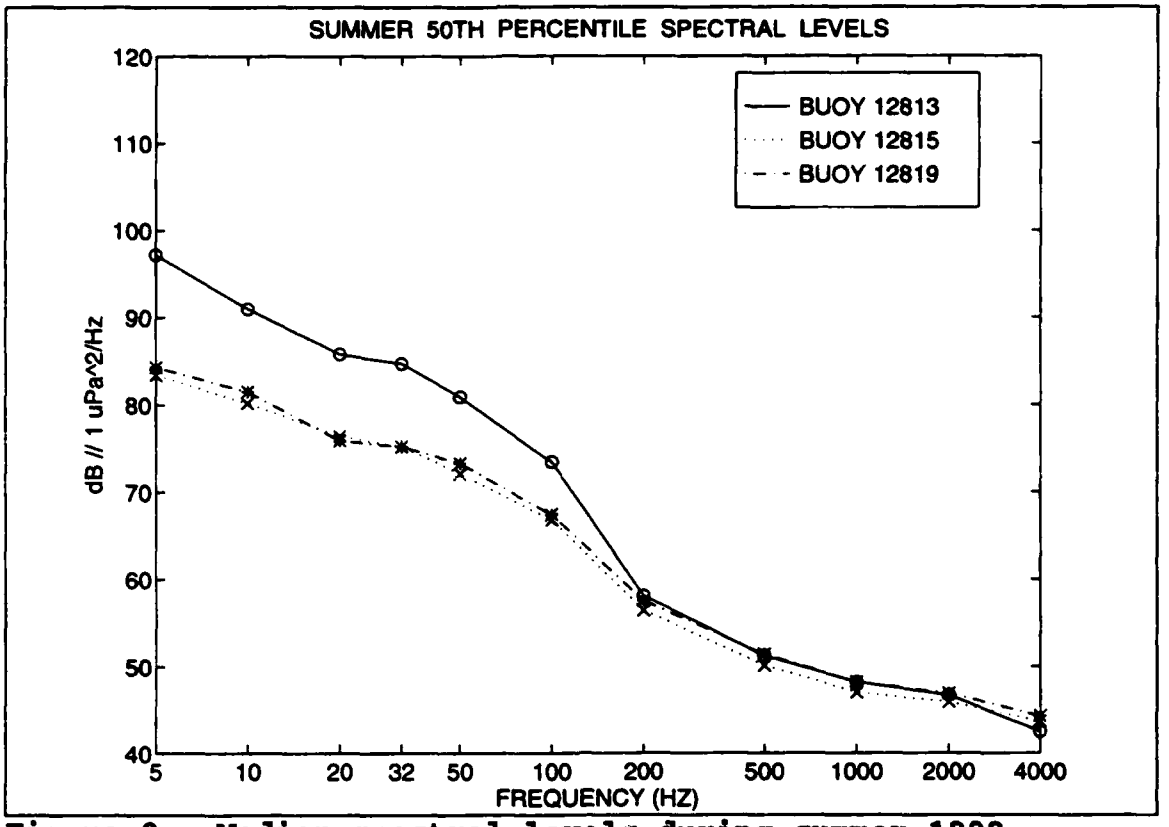

Figure 8. Median spectral levels during summer 1992.

predominantly a summertime phenomena. The relatively small anomalous peak at 50 Hz seen in the median annual spectra is evident as well.

One expects the noise level in winter to be greater than in summer (Buck and Clarke, 1989; Urick, 1983; Poffenberger, 1987; Oard, 1987) due to the increased compactness of the ice pack and the more extensive wind forcing. This is indeed the case for Buoys 15 and 19 which have winter median noise levels more than 10 dB louder than their summer median levels for frequencies of 100 Hz and below (compare Figures 8 and 11). However, little seasonal difference is noted in the Buoy 13 median spectra; winter values are louder than summer values by only 1-2 dB and are almost identical with the annual median levels. A major

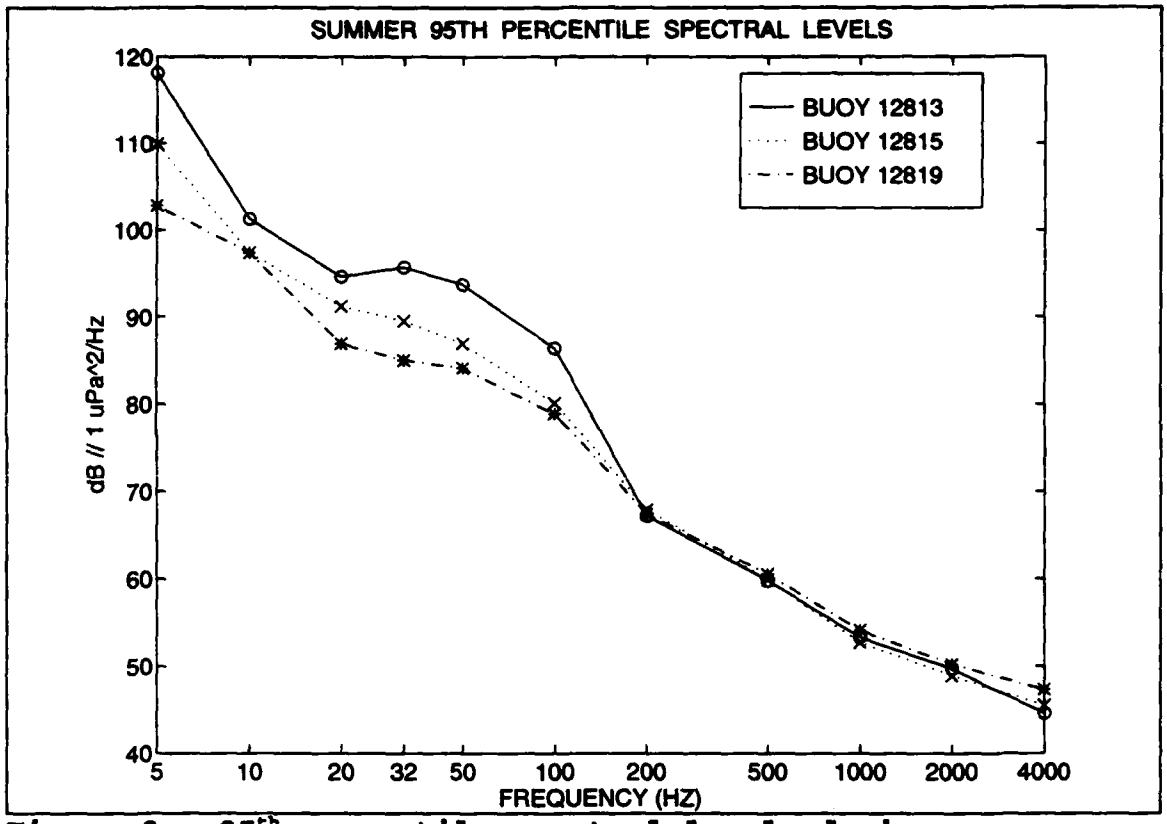

Figure 9. 95th percentile spectral levels during summer 1992.

difference in spectral shape is also observed between the summer and winter median levels for frequencies greater than 100 Hz. The rapid fall off between 100 and 200 Hz previously noted in the summer spectra is absent in winter. Median noise levels at 200 and 500 Hz are more than 10 dB greater in winter than in summertime. The more energetic ice-ice collisions and ice fracturing experienced during the winter extend the range of their high frequency contributions to the noise field at least to 500 Hz.

The winter 95th percentile noise levels (Figure 12) for Buoys 13 and 19 are virtually the same as the annual 95th percentile levels. Poffenberger et al. (1988) have previously indicated that in the Eurasian Basin most extreme

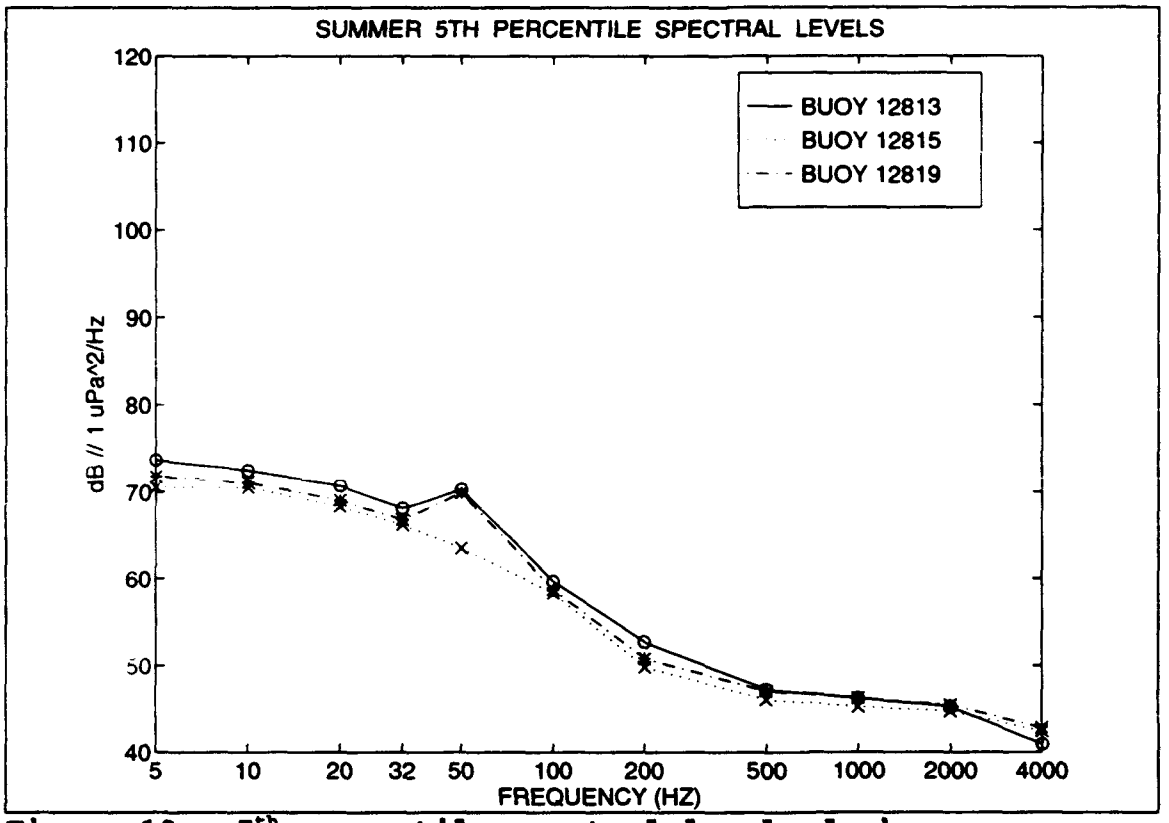

Figure 10. 5th percentile spectral levels during summer 1992.

loud noise events occur during the winter months. Hence, the close association of the annual and winter 95th percentile levels supports this conclusion. The Buoy 15 levels clearly represent a special case. Its winter 95th percentile levels are more than 5 dB greater than the levels of Buoy 13 and are also about 5 dB greater than the annual Buoy 15 95th percentile noise levels. In the case of extreme loud levels in winter the Buoy 15 levels appreciably exceed the other two. In general, the noise levels measured below 200 Hz at Buoy 15 are greater than the noise levels at the other two buoys. Also as seen previously, the spectral levels at 200 Hz and higher are nearly the same for all buoys.

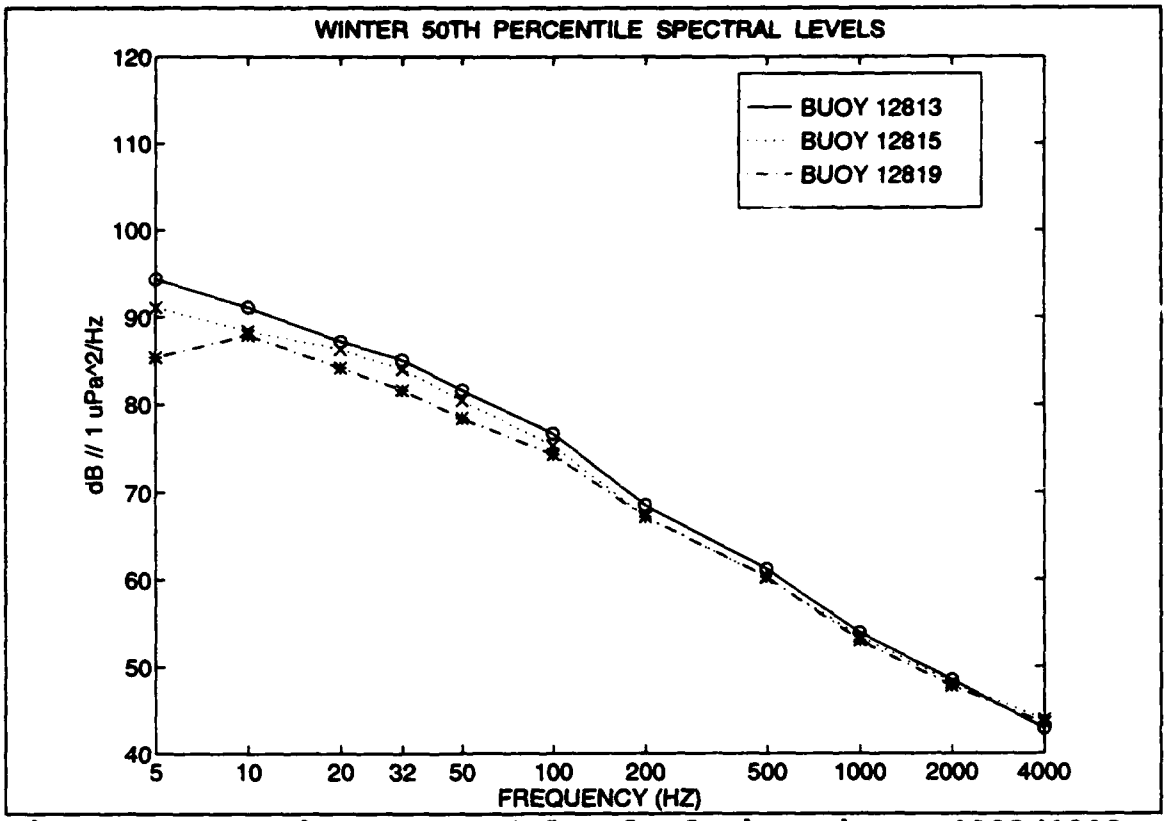

Figure 11. Median spectral levels during winter 1992/1993.

Although louder than their summertime counterparts, quiet periods (5% threshold level) are present in the winter as well (Figure 13). All buoys indicate nearly identical levels with one another in winter across the spectrum. These are about 10 dB less than wintertime median values. However, the quiet periods of winter are still noisy relative to summer quiet periods by about 10 dB. Note also that the small noise peak at 50 Hz seen in both the annual and summer 5th percentile spectra of Buoys 13 and 19 is absent in the winter 5th percentile spectra for these buoys. The reason for this noise peak, observed only at 50 Hz, during quiet periods is unknown. Examination of the raw data suggested no artifacts, data drop outs, etc. that may

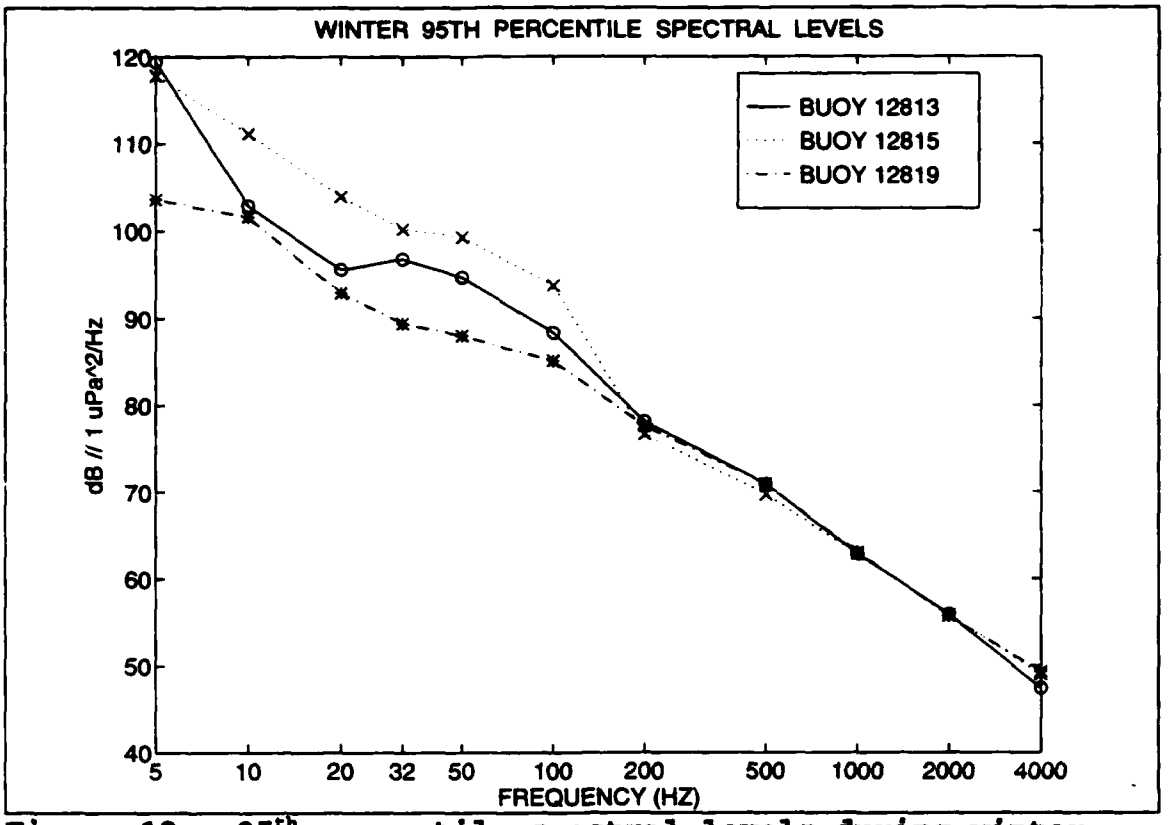

Figure 12. 95th percentile spectral levels during winter 1992/1993.

have artificially raised the noise floor. An interesting, but speculative, possibility for its cause may be from 50 Hz electrical power generation from an ice camp, or fishing or research vessels operating near the ice margin in the summer. The lack of such a signal at the Buoy 15, site more than 200 km to the west, may be a result of excessive propagation loss over the longer transmission path or bathymetric blockage along the transmission path between the two locations.

The median and standard deviation decrease as frequency increases for all three buoys for the year-long record and the seasonal records. This is the same trend observed in the data collected in the northwest Barents Sea during the

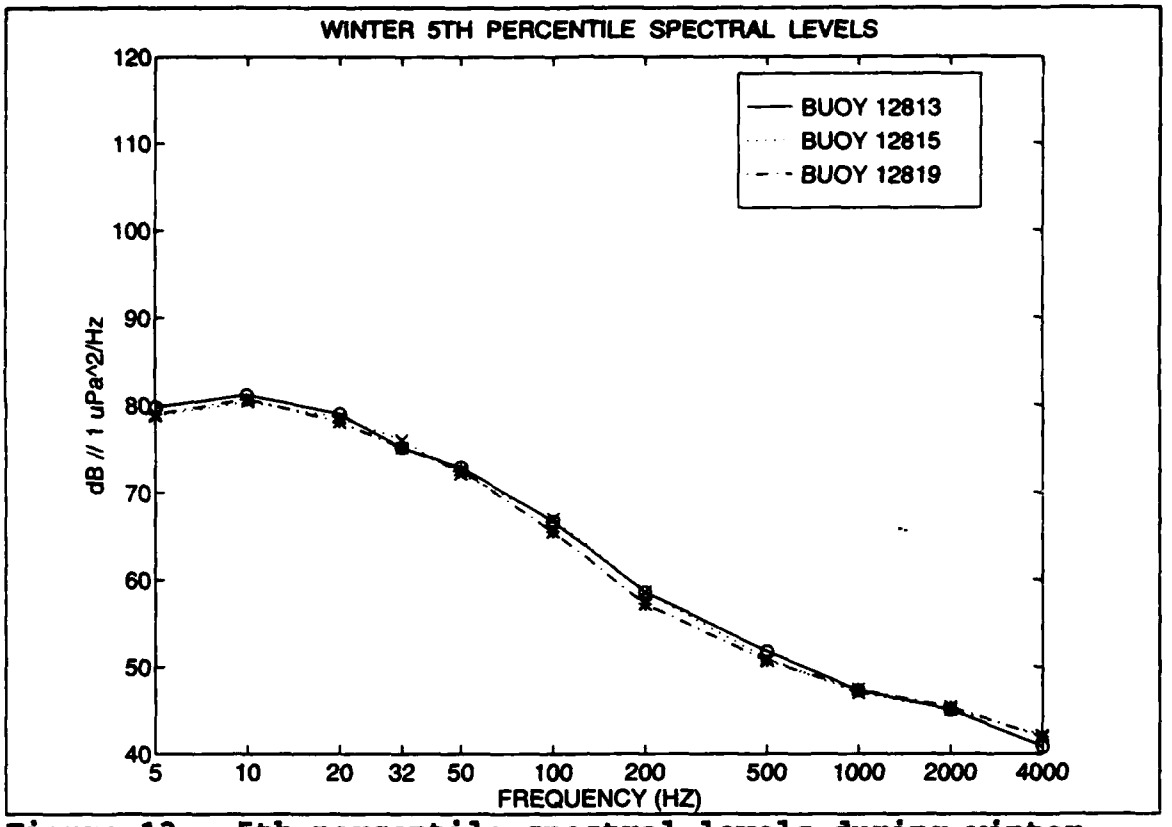

Figure 13. 5th percentile spectral levels during winter 1992/1993.

CEAREX (Coordinated Eastern Arctic Experiment) 1988-89 experiment (Parsons, 1992; Cousins, 1991). The CEAREX data were collected in the northwest Barents Sea. Though not exactly the same region as the AREA '92 experiment, it is nearby and in fact there is a small region of overlapping coverage northeast of Svalbard.

The major ambient noise source mechanisms at the lower frequencies (below 200 Hz) are ridging, lead formation, and rafting (Buck and Wilson, 1986). These phenomena are expected to exhibit intermittent high source levels and relatively low propagation loss. The intermittent occurrence of these events would be expected to cause the large fluctuations observed at these frequencies, with

significant contributions to the measured noise levels from both local and distant ridging events. The major ambient noise source mechanisms at the higher frequencies (above 200 Hz) are associated with local noise events since propagation loss is relatively high at frequencies greater than 200 Hz. The source levels for noise events above 200 Hz are not well known. Smaller noise level fluctuations are consistent with local noise events that are caused by mechanisms such as thermal cracking and blowing snow that are less intermittent in time than the low frequency storm-related mechanisms.

The noise characteristics from this relatively unsampled region of the Arctic can be placed in perspective by comparing these noise levels with those measured at other places under similar or differing conditions (Figure 14). The median winter and annual spectra for Buoy 19 were chosen for comparison (curves #3 and #4, respectively).

Curve #1 in Figure 14 represents a snapshot of the spectra recorded in the marginal ice zone during the MIZEX 1984 experiment, measured on 23 June 1984 (Buckingham and Chen, 1988). Since this was an instantaneous measurement and not time averaged, it may not be representative of median values. Due to the action of wind and wave forcing on the ice edge the marginal ice zone (MIZ) is known to be a high ambient noise region (Diachok and Winokur, 1974)(Makris and Dyer, 1991), so it is not unexpected that MIZ levels are considerably louder than Buoy 19 levels which were measured under polar pack ice conditions.

Curve #2 is taken from the Fram IV expedition manned ice camp in the Fram Strait and represents an average spectra over a 24 day span in April 1982 (Makris and Dyer, 1986). The Fram data are louder than the Buoy 19 annual median but are within 3 dB of the Buoy 19 winter median for frequencies below 500 Hz. The ice cover and wind forcing in

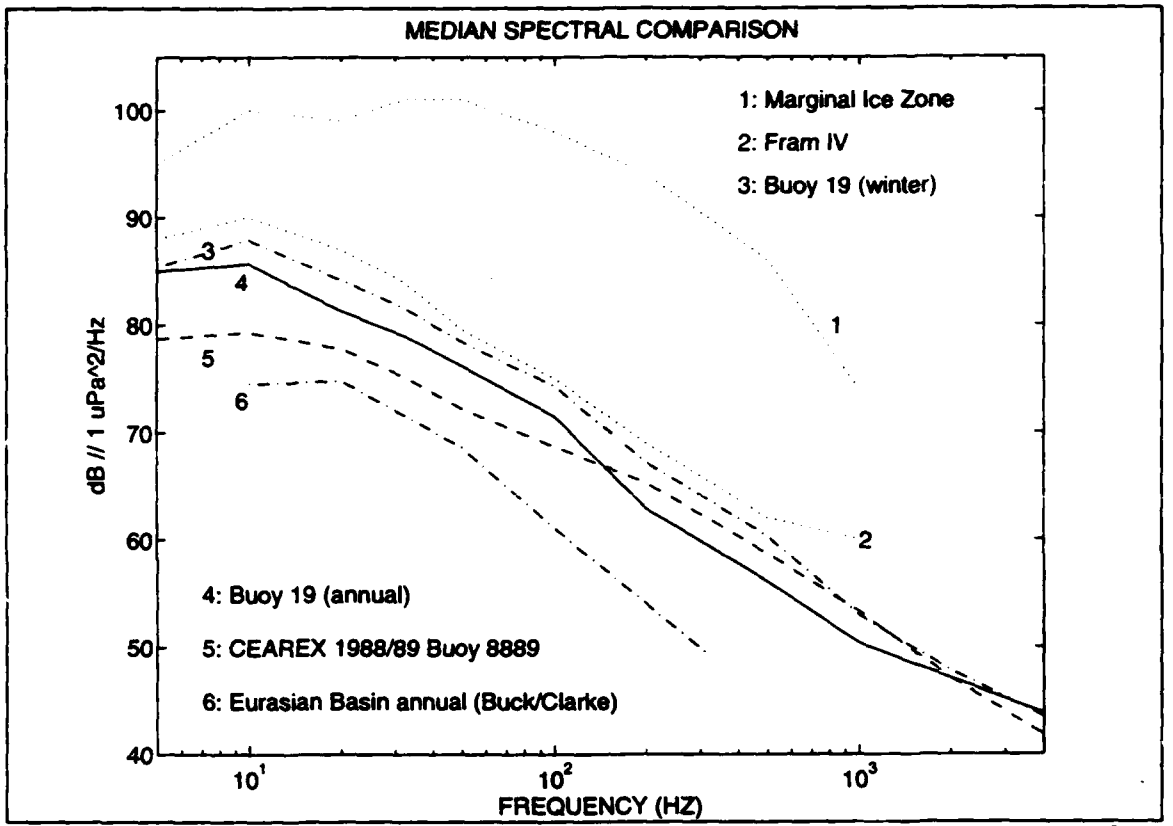

Figure 14. Comparison of Buoy 19 spectra with other Arctic data sets.

winter are similar in these two regions thus leading to the close similarity of the two winter spectra.

Curve #5 is the median spectra measured at Buoy 8889 over 55 days during the CEAREX 1988 experiment. This buoy was chosen for comparison because its hydrophone was at the same depth as the AREA 1992 buoys (305 m) and because it was the farthest north of the CEAREX buoys and therefore closest to the tracks of the AREA 1992 buoys.

The CEAREX buoy drifted in shallow water near the northeast coast of Svalbard over the entire record and the CEAREX noise levels were quieter than the Buoy 19 annual median below 200 Hz. The lower noise levels at low frequencies may be explained by the relatively poor sound

propagation in shallow water decreasing the noise contributions from remote sources.

Curve #6 is the annual median spectra calculated from the records of 13 ambient noise buoys in the Eurasian Basin during the period 1975-1985 (Buck and Clarke, 1986). This curve may be considered representative of mean annual conditions throughout the Eurasian Basin.

The annual basin-wide spectra determined by Buck and Clarke is about 10 dB lower than the Buoy 19 annual spectra at all frequencies. This may be because Buoy 19 represents a single buoy during a noisy year in contrast to a long term average, or because Buoy 19 (as well as the other two buoys) drifted through an area not well sampled by the Buck and Clarke data and is inherently noisier than the central Eurasian Basin.

2. AUTOCORRELATIONS OF AMBIENT NOISE DATA

Autocorrelation analyses were performed to measure the temporal coherency of the noise field. Temporal coherence is a measure of statistical independence over time, or the time over which measurements of the noise field will be valid statistically. A standard measure of temporal coherence is the *e-folding* time. This is the time required for the autocorrelation coefficient to decay by a factor of e^{-1} (0.368). Tables VI, VII and VIII present *e-folding* times in hours for selected frequencies for the annual, summer and winter, respectively.

The *e-folding* times shown for the annual record for all three buoys indicate a fair degree of similarity. Because of their close proximity to each other, the *e-folding* times for Buoys 13 and 19 are nearly the same; Buoy 15 values are slightly (3-5 hours) longer. There is a trend for the temporal coherence at higher frequencies ($\geq$ 200 Hz) to be slightly shorter than at lower frequencies. Buoy 19

BUOY	5 Hz	10 Hz	32 Hz	100 Hz	200 Hz	500 Hz	1 KHz
BUOY 13	16	17	18	16	14	13	14
BUOY 15	23	20	23	19	21	18	15
BUOY 19	15	17	18	22	14	13	12

Table VI. *e-folding* times (hours) determined from the autocorrelation functions for 21 Apr 92 to 21 Apr 93.

BUOY	5 Hz	10 Hz	32 Hz	100 Hz	200 Hz	500 Hz	1 KHz
BUOY 13 1992	14	14	14	14	18	22	13
BUOY 15 1992	7	15	15	15	31	20	13
BUOY 19 1992	5	14	7	14	15	13	11
BUOY 19 1993	190	257	14	11	15	18	9

Table VII. *e-folding times* (hours) calculated from the autocorrelation functions for summer 1992 and 1993.

exhibited anomalously long *e-folding* times at 5 and 10 Hz during the 1993 summer season. The cause for these extended times is unknown. The annual and seasonal *e-folding* times are similar to those reported by Bourke and Parsons (1993) and Lewis and Denner (1987), suggesting that the ice response to wind forcing over the polar ice pack is fairly consistent throughout the Arctic basin.

BUOY	5 Hz	10 Hz	32 Hz	100 Hz	200 Hz	500 Hz	1 KHz
BUOY 13 92/93	18	18	23	17	13	11	13
BUOY 15 92/93	27	26	26	22	19	16	13
BUOY 19 92/93	17	19	21	23	13	12	11

Table VIII. *e-folding times* (hours) calculated from the autocorrelation functions for winter 1992/1993.

3. ENERGY DENSITY SPECTRA

Energy density spectra were calculated using a Fast Fourier Transform for the 32 Hz time series to establish representative significant periodicities for the low frequency noise records. Spectra were computed for the annual and seasonal noise records to determine the strongest frequency components in the data; the area under the curve is proportional to the energy in the system. Significant periods are shown with their associated magnitudes for each buoy and season in Table IX.

Several interesting results are noted. Based on the study of Bourke and Parsons (1993), the semi-diurnal (M-2) tidal period of 12.4 hours and the inertial period (about 12.1 hours at these latitudes) were expected to exhibit significant energy peaks. No energy peaks at exactly those periods are present, but significant energy is present at periods sufficiently near them to suggest that energy from these sources does contribute to the noise field.

Statistically significant energy peaks are also found at periods ranging from 60 hours up to 147 hours that are assumed to derive from a periodic synoptic forcing.

FREQUENCY = 32 Hz		BUOY 13		BUOY 15		BUOY 19	
		PERIOD (HOURS)	MAGNITUDE (dB^2/Hz) or (mb^2/Hz)	PERIOD (HOURS)	MAGNITUDE (dB^2/Hz) or (mb^2/Hz)	PERIOD (HOURS)	MAGNITUDE (dB^2/Hz) or (mb^2/Hz)
FIRST YEAR	AMBIENT NOISE	146.7 18.3 11.9	1.8 E10 1.0 E 9 1.4 E 9	146.7 16.3 11.6	5.1 E10 9.9 E 8 1.6 E 9	146.7 11.9 10.2	4.9 E 9 2.8 E 8 1.1 E 8
	AIR PRESSURE	11.6 5.6	1.7 E 0 5.5 E-2	11.6 9.4	1.2 E 0 1.1 E-1	11.6 9.0	1.8 E 0 1.2 E-1
SUMMER 1992	AMBIENT NOISE	61.3 10.8 7.7	7.9 E 9 1.5 E 9 2.6 E 8	3.5	1.5 E 7	61.3 13.1 11.5	6.6 E 8 1.0 E 8 2.8 E 8
	AIR PRESSURE	11.5	1.0 E 0	6.8	2.1 E-2	11.5 5.9	1.2 E 0 2.5 E-2
SUMMER 1993	AMBIENT NOISE	NO DATA	NO DATA	NO DATA	NO DATA	10.2 9.2	2.2 E 9 9.2 E 9
	AIR PRESSURE	NO DATA	NO DATA	NO DATA	NO DATA	11.5	7.1 E 0
WINTER 1992/93	AMBIENT NOISE	60.7 18.2 10.7	8.5 E 9 9.8 E 8 4.9 E 8	60.7 7.0	3.3 E10 1.7 E 9	11.4	1.1 E 8
	AIR PRESSURE	11.4 7.3	9.3 E-1 8.8 E-2	11.4 5.9	8.2 E-1 4.8 E-2	11.4 5.9	1.0 E 0 4.9 E-2

Table IX Significant periods (hours) from ambient noise and atmospheric pressure energy density spectra by buoy and season at 32 Hz.

Statistically significant energy peaks also exist at periods shorter than 10 hours but these peaks are small compared to the periods of maximum energy (less than 5% in most cases). Since the main focus of this research is related to synoptic scale forcing, these short period peaks are not listed in Table IX and will not be considered further.

Within each analysis period in Table IX, two and sometimes three buoys always exhibit exactly the same significant period (or within 0.5 hours of each other). This indicates that at 32 Hz, the same forcing mechanisms contribute to the noise field measured by the buoy cluster. This association of a common forcing mechanism (e.g., a synoptic event) and a uniform response by all three buoys will be examined in greater detail in the next chapter where the response of the ice generated noise to individual storms is discussed.

Energy density spectra were calculated for the air pressure time series for the same time periods. Significant periodicities and their associated magnitudes are shown for each buoy in Table IX. A period of about 11.5 hours is present in each record except for Buoy 15 during the summer of 1992. This suggests forcing near inertial periods. No significant energy peaks were found with periods longer than about 11.5 hours. As with the noise spectra, the significant peaks with periods shorter than 11.5 will not be considered further.

4. AMBIENT NOISE CROSS CORRELATIONS

To determine the spatial coherency of the noise field, cross correlations were computed between each pair of buoys at each frequency measured. Results from the analysis are shown in Table X. A positive lag time means the second listed buoy lagged the first.

The cross correlation between Buoys 13 and 19 was the highest at all frequencies as expected because this pair had the smallest separation (i.e., approximately 100 km apart). Both buoys were about 300 km from Buoy 15.

FREQ (HZ)	BUOYS 13/15		BUOYS 13/19		BUOYS 15/19	
	COEFF (MAX)	LAG (HR)	COEFF (MAX)	LAG (HR)	COEFF (MAX)	LAG (HR)
5	0.561	-5	0.667	-1	0.511	9
10	0.594	-5	0.650	-2	0.560	5
32	0.669	-4	0.791	-1	0.692	5
100	0.635	-5	0.777	-2	0.663	5
200	0.776	-3	0.839	-4	0.754	1
500	0.745	-7	0.820	-4	0.751	5
1000	0.799	-6	0.840	-5	0.785	5

Table X. Cross correlation coefficients for the period 21 Apr 92 through 21 Apr 93 between buoys at the same frequency. A positive lag time indicates the second listed buoy lags the first.

There is strong trend for the coefficients to be higher at higher frequencies. The buoy separations were smaller than a synoptic scale meteorological system. Analysis of the weather charts during the experiment showed that the three buoys usually were experiencing similar meteorological forcing. At higher frequencies local noise generating effects become more important than distant effects, so higher correlations are expected.

The same trends were observed in the seasonal data (not shown). The seasonal correlations were somewhat higher than

the annual correlations with the summer correlations generally slightly higher than in winter.

The lag times for maximum correlation between Buoys 13 and 19 were small and at low frequencies ($\leq$ 100 Hz) were near the minimum resolution of the calculations (one hour). These buoys responded nearly simultaneously to synoptic events with Buoy 13 lagging slightly. Buoy 15 led both Buoys 13 and 19 by approximately five hours at most frequencies. These lag times are consistent with storms propagating from west to east through the region, at a speed of about 17 m/s.

These cross correlation results are consistent with the mean and standard deviation data shown in Tables II, III and IV. At low frequencies the noise field at any single buoy is the sum of contributions from local and distant noise events. When distant noise is significant at a buoy, the propagation effects from numerous distant noise events (e.g., ridging) is both complex and unique to that buoy. For low frequencies the cross correlation of noise records between buoys is expected to be relatively low. On the other hand, for high frequencies where local noise events dominate, the passage of a synoptic noise event will show relatively higher correlation at the appropriate lag times for the travel time from buoy to buoy for the synoptic event.

To see how the local noise fields varied between frequencies, cross correlations were performed between each pair of frequencies as measured by the same buoy. The correlation between frequencies measured by the same buoy (not shown) demonstrated results similar to those obtained by Bourke and Parsons (1993). The highest frequencies correlate with each other best since they are forced primarily by local events. The second best correlations

are between the lowest frequencies. The lowest correlations are between the mid-range frequencies and any other frequencies. These trends hold for the full record as well as for each season.

5. ENVIRONMENTAL CROSS CORRELATIONS

Cross correlations of the noise field were performed with three environmental parameters: wind speed, wind stress and ice speed. The methods used to calculate these parameters were discussed in Chapter II.

Surface winds do not directly generate ambient noise at low frequencies under the ice cover (Oard, 1987). The *effects* of the wind, such as ice pellets blowing onto the ice surface or the resulting motion of the ice sheet, are actually high frequency noise sources (Dyer, 1983). Wind stress is the means by which the wind energy is transferred into ice motion. The overall ice motion and ice/ice interactions are the main mechanisms for the generation of low frequency noise in the Arctic.

Table XI shows the environmental cross correlations for Buoy 19 based on the year long record. The correlations of the other buoys and the seasonal length records demonstrate similar trends. Peak coefficients are higher at low frequencies (below 200 Hz) in winter and higher at high frequencies in summer.

All three correlates demonstrate relatively high correlation (most are 0.7 to 0.8) with ambient noise, with ice speed being the best for 5 Hz and 10 Hz. Wind speed showed the highest correlation at 32 Hz and 100 Hz. At or above 200 Hz wind stress was the best correlate. One expects wind and ice speed to be similarly correlated with ice-generated noise as the cross correlation between wind speed and ice speed was very high (0.872) with a short

FREQ (HZ)	WIND SPEED		WIND STRESS		ICE SPEED	
	COEFF (MAX)	LAG (HR)	COEFF (MAX)	LAG (HR)	COEFF (MAX)	LAG (HR)
5	0.700	-2	0.592	-25	0.754	-1
10	0.590	-4	0.455	-38	0.612	-1
32	0.826	-1	0.769	-19	0.811	0
100	0.782	-1	0.709	-35	0.779	0
200	0.738	6	0.742	-11	0.686	7
500	0.746	6	0.756	-10	0.690	7
1000	0.806	2	0.831	-11	0.760	5

Table XI. Maximum cross correlation coefficients between ambient noise and environmental parameters for Buoy 19 from 21 Apr 92 to 21 Apr 93. Negative lag times indicate the noise lagged the forcing.

response (lag) time of two hours, close to the minimum lag time resolution of 1 hr.

Table XI indicates that at low frequencies (≤ 100 Hz) the ambient noise fluctuations lagged the fluctuations in ice speed by about one hour, similar to that reported by Bourke and Parsons (1993), Poffenberger et al. (1988), and Lewis and Denner (1988). The noise field was slower in responding to fluctuations in wind speed (4 hr) implying about a 2-3 hour time delay for the wind forcing to overcome the inertia of the moving ice pack. The fact that the wind speed calculation is a composite of data from all three buoys while the ice speed is unique to each buoy may also affect the response time between wind forcing and ice motion.

6. ICE SPEED

The speeds of the ice floes in which each buoy was embedded were calculated from irregularly spaced position data of varying quality and are shown in Table XII. Buoy 15 sank on 28 August 1993, so its data for summer 1993 represents just under four months of data rather than the full five month season.

PERIOD	BUOY 13	BUOY 15	BUOY 19
21 APR 92 TO 21 APR 93	9.2	9.6	9.3
SUMMER 1992	9.9	9.6	10.1
SUMMER 1993	8.7	9.1	8.3
WINTER 1992/3	8.3	9.7	8.3

Table XII. Mean scalar ice drift speeds (cm/s) of ANMET buoys by season.

The buoy drift speeds are significantly slower than seen during the CEAREX experiment, where the mean ice speeds varied between 14.2 and 28.6 cm/sec (Parsons, 1992). There are probably two major reasons for the ice speed differences. The CEAREX buoys drifted through shallow water past the east coast of Svalbard and were influenced by the relatively fast tidally influenced inshore currents compared to the open ocean currents experienced by the AREA 1992 buoys. Second, the CEAREX buoys were also much closer to the storms spawned by the Icelandic low and thus subject to stronger winds. The AREA 1992 buoys were farther to the north and away from the typical storm tracks. The combination of stronger winds and stronger currents, which

are the major contributors to ice motion, resulted in faster drift speeds for the CEAREX buoys.

During its last 69 days of life from 1 Nov 93 through 9 Jan 94, Buoy 13 drifted along the northern coast of Svalbard near the region where the CEAREX experiment began. The average scalar drift speed for Buoy 13 during this period was 22.7 cm/s, in the center of the range of drift speeds determined from the CEAREX data. This suggests that location has a great effect on the forcing responsible for ice motion.

B. MESOSCALE ANALYSIS OF WIND FORCING AND AMBIENT NOISE

The tracks for the three buoys show an interesting pattern. For almost the entire experiment the buoys move approximately in unison. Minor deviations exist, but the general direction of motion is the same for each buoy. The overall tracks can be divided into five legs as shown in Figures 2, 3 and 4. During the first four legs the dominant motion of the buoys is relatively straight translation. The fifth leg (only for Buoys 13 and 19) deviates from this pattern becoming more rotational and random. In anticipation that the buoy drift pattern of each leg was in response to a change in long term wind forcing, a stick plot (Figure 15) of the calculated geostrophic wind velocity and the three buoy drift velocities was created. The vertical bars represent the boundaries between each leg. A close examination of the wind and ice vectors for each leg indicates that each leg was the result of a significant change in wind forcing.

Table XIII contains the period covered by each leg, the general direction of motion, the distance covered between the endpoints of each leg, and the magnitude of the average velocity during each leg. The average velocity was

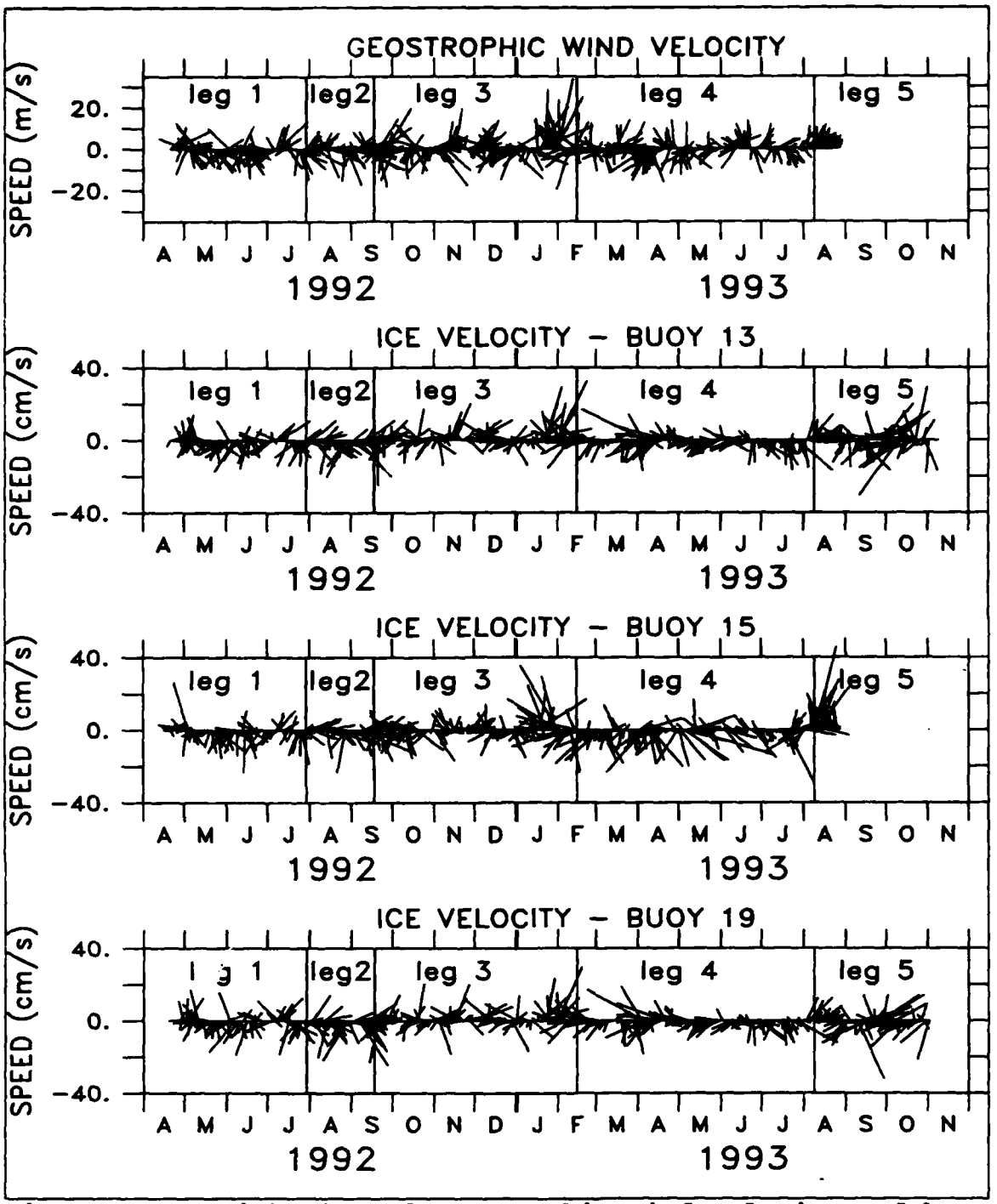

Figure 15. Stick plot of geostrophic wind velocity and buoy drift velocities. Vertical bars represent boundaries between drift legs. All vectors point in the direction of motion to facilitate comparison.

calculated by measuring the distance between the endpoints of each leg and dividing by the elapsed time. The drift regime during leg #4 extends to julian date 93/221, the start of leg #5, but was truncated to julian date 93/122 to coincide with the end of life of Buoy 15 to facilitate comparing noise records.

The endpoints of the legs were easy to choose because the buoy drift tracks underwent large direction changes. As an example, the wind and buoy drift vectors for leg #2 are shown in Figure 16 along with the 10 days before and after the leg. The vector averaged wind and ice speeds for the 10 day periods before and after the start and end of leg #2 are shown in Table XIV.

The winds and ice are moving just east of due south for the last 10 days of leg #1. During the first 10 days of leg #2 the mean wind shifted about 65° to the left, and slowed from 9.3 to 6.8 m/s. All three buoy drift patterns exhibited this same near 65° direction change to the left with corresponding reductions in speed. The 10 day periods before and after the end of leg #2 show the wind shifted 26° to the right and reduced speed by two thirds. The buoys responded by turning to the right and slowing, but the response varied more than it did at the beginning of leg #2. The less uniform response was due to weaker wind forcing at the beginning of leg #3 which was less able to force uniform ice motion over the buoy region. This leg demonstrates clearly how the ice motion responded to the wind forcing.

The most striking comparison in the data is the difference in speeds between legs #2 and #3. These two legs have roughly reciprocal tracks. The eastward drift speeds in leg #2 are roughly three to five times faster than the westward drift speeds in leg #3. This is a direct result of the nearly six-fold increase in wind speed during leg #2

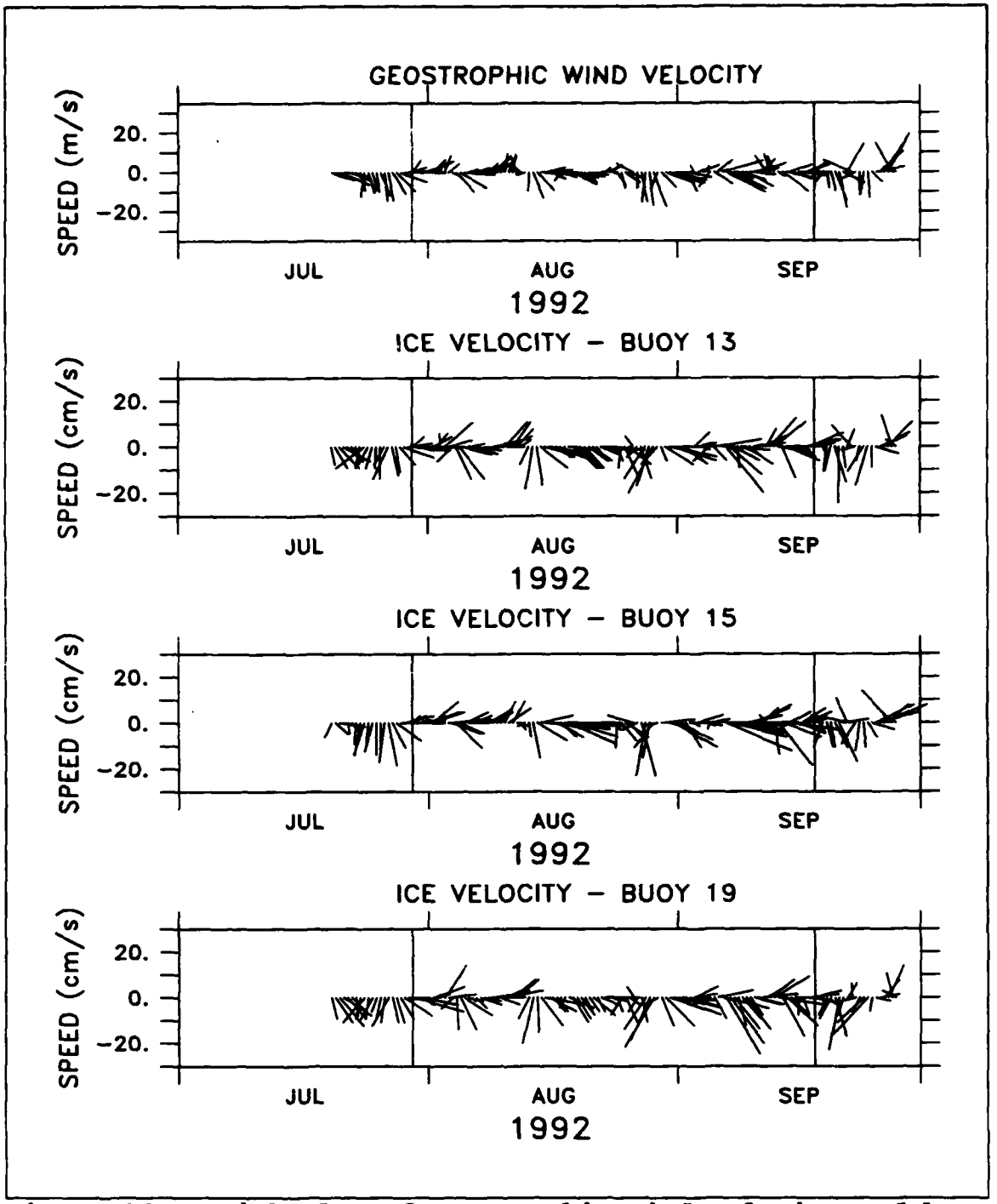

Figure 16. Stick plot of geostrophic wind velocity and buoy drift velocities for leg #2. Vertical bars represent the leg endpoints. All vectors point in the direction of motion to facilitate comparison.

compared to leg #3. The faster and steadier wind velocity during leg #2 resulted in a relatively linear trajectory for the buoy cluster. The more circuitous path of leg #3 is in direct response to the strong northward wind shifts embedded in an overall westward pattern.

LEG		1	2	3	4	5
START DATE		92/112	92/212	92/262	93/046	93/221
END DATE		92/212	92/262	92/046	93/122	93/305
GENERAL DIRECTION		SOUTH	SOUTH EAST	NORTH WEST	SOUTH WEST	WEST/ RANDOM
DISTANCE (KM)	13	228.6	315.6	201.5	305.1	199.3
	15	328.7	278.0	301.1	399.9	NO DATA
	19	230.2	314.0	236.5	311.8	155.1
AVERAGE BUOY SPEED (CM/S)	13	2.7	7.3	1.6	4.7	2.7
	15	3.8	6.4	2.3	6.1	NO DATA
	19	2.7	7.3	1.8	4.8	2.1
AVERAGE WIND SPEED (M/S)		2.8	6.3	1.1	2.6	5.8

Table XIII. Net buoy displacements and magnitudes of the average velocities for the five identified legs of the buoy tracks. Dates are Julian dates.

The noise record at 32 Hz from Buoy 19 was chosen for inter-leg noise comparisons. Table XV summarizes the noise field for each leg. During leg #1 the buoys drifted slowly and nearly unidirectionally. The minimal convergence caused by this drift regime resulted in low noise levels. Leg #2 had the fastest drift speeds, but again experienced nearly

		BEFORE/AFTER LEG #2 BEGINNING		BEFORE/AFTER LEG #2 ENDING	
START DATE		202	212	252	262
STOP DATE		212	222	262	272
BUOY 13	ICE SPEED (CM/S)	8.6	7.5	10.5	2.5
	DIRECTION	167.8°	102.1°	91.0°	156.0°
BUOY 15	ICE SPEED (CM/S)	8.9	7.5	8.7	2.8
	DIRECTION	164.3°	82.6°	89.8°	103.9°
BUOY 19	ICE SPEED (CM/S)	9.0	7.0	11.0	2.4
	DIRECTION	171.5°	109.6°	101.3°	185.1°
WIND	WIND SPEED (M/S)	9.3	6.8	7.5	2.4
	DIRECTION	137.9°	73.6°	87.0°	113.4°

Table XIV. Comparison of net vector speeds and directions for 10 day periods before and after the beginning and end of leg #2. Dates are julian dates.

unidirectional drift. The low noise levels imply that limited convergence was present. Leg #3 had low drift speeds but higher noise levels than the first two legs. The higher noise levels may be due to torquing of the ice pack due to four strong wind shifts, which caused ice shear and convergence as the ice motion underwent large directional changes. Leg #4 displayed moderately fast buoy drift speeds and loud noise levels. The wind pattern during leg #4 shows repeated strong wind shifts, which resulted in shearing and torquing of the ice cover and hence increased ice stress with its resultant fracturing. Leg #5 exhibited highly

LEG	MEAN (dB // 1 $\mu Pa^2/Hz$)	MEDIAN (dB // 1 $\mu Pa^2/Hz$)	STANDARD DEVIATION (dB)
1	74.8	75.1	5.3
2	75.7	74.7	6.5
3	81.4	81.0	4.7
4	81.8	81.8	4.7
5	96.1	97.0	3.3

Table XV. Summary noise statistics by leg for Buoy 19 at 32 Hz.

irregular motion including eddy-like drift periods. The result were periods of strong convergence causing the highest noise levels of any leg.

IV. SYNOPTIC EVENT ANALYSIS

The second goal of this research was to examine the correlation between observed environmental parameters and the ambient noise measured under the ice pack. The previous chapter addressed correlation analyses to examine relationships between noise levels observed at seasonal and annual time scales and for several types of environmental forcing. This chapter will adopt a more synoptic viewpoint in the effort to identify causal relationships between weather patterns, particularly synoptic-scale disturbances, and significant events in the noise record. Significant events are defined as periods where the noise level remained greater than the 95th percentile, or less than the 5th percentile, for at least one day. The percentiles were based on seasonal record lengths and calculated over the appropriate summer (May through September) or winter (November through March) season.

One may consider two basic approaches when attempting to model ambient noise. Most efforts in the past involved attempting characterizations of the noise field in terms of local noise events and basing predictions only on local environmental parameters (Dyer, 1988; Lewis and Denner, 1988). The present study abandoned that approach since these efforts have not been successful in producing an accurate Arctic noise model. In addition, the spectra of the many forcing mechanisms are not well known due to the lack of accurate source level measurements. Instead, significant loud and quiet noise events were identified in the noise record. Synoptic surface weather charts were then examined to determine if the observed changes in the noise field could be related to the presence or absence of synoptic features. Numerous significant events in the noise record

were examined to determine if any relationship could be discovered. Three of these events are described in the sections that follow. The frequencies examined for these events are 50 Hz, 100 Hz, and 500 Hz.

A. SYNOPTIC EVENT OF 29 JANUARY - 5 FEBRUARY 1993

The first event studied was a loud event that persisted for about 7 days. This event occurred between 29 January 1993 (julian date 29) and 1200Z 5 February 1993 (day 36.5) of the AREA 1992 experiment, which was during drift leg #3. It will be referred to as synoptic event #1. During the event, Buoy 15 was north of Franz Josef Land and Buoys 13 and 19 were north of Severnaya Zemlya as shown in Figures 2 through 4.

1. DESCRIPTION OF THE NOISE RECORD

The 50 Hz noise time series for Buoy 13 (Figure 17) indicates that noise conditions were extremely quiet for approximately 12 hours during julian day 29, i.e., noise levels were near the 5 percent threshold with a minimum of 70.5 dB. Over the next 30 hours the noise level made two nearly step increases to exceed its 95th percentile level (maximum of 97.4 dB), a total increase of nearly 27 dB. The 50 Hz noise record for Buoy 15 shows a gradual ramp increase of over 37 dB from its 5 percent level (minimum of 69.0 dB) to above its 95 percent level (maximum of 107.3 dB) over approximately two days, day 29.5 to day 31.5. Buoy 19 shows the same trend as Buoy 15, although the increase of over 23 dB from the 5th to the 95th percentiles (minimum of 69.6 to a maximum of 93.0 dB) is more gradual and begins about 12 hours sooner. The noise level at 50 Hz for all buoys remained near or above the 95th percentile for the next five days, except for Buoy 13 which experienced a short term decrease to about 5 dB above the median for about one day centered on day 34. The maximum noise level occurred near

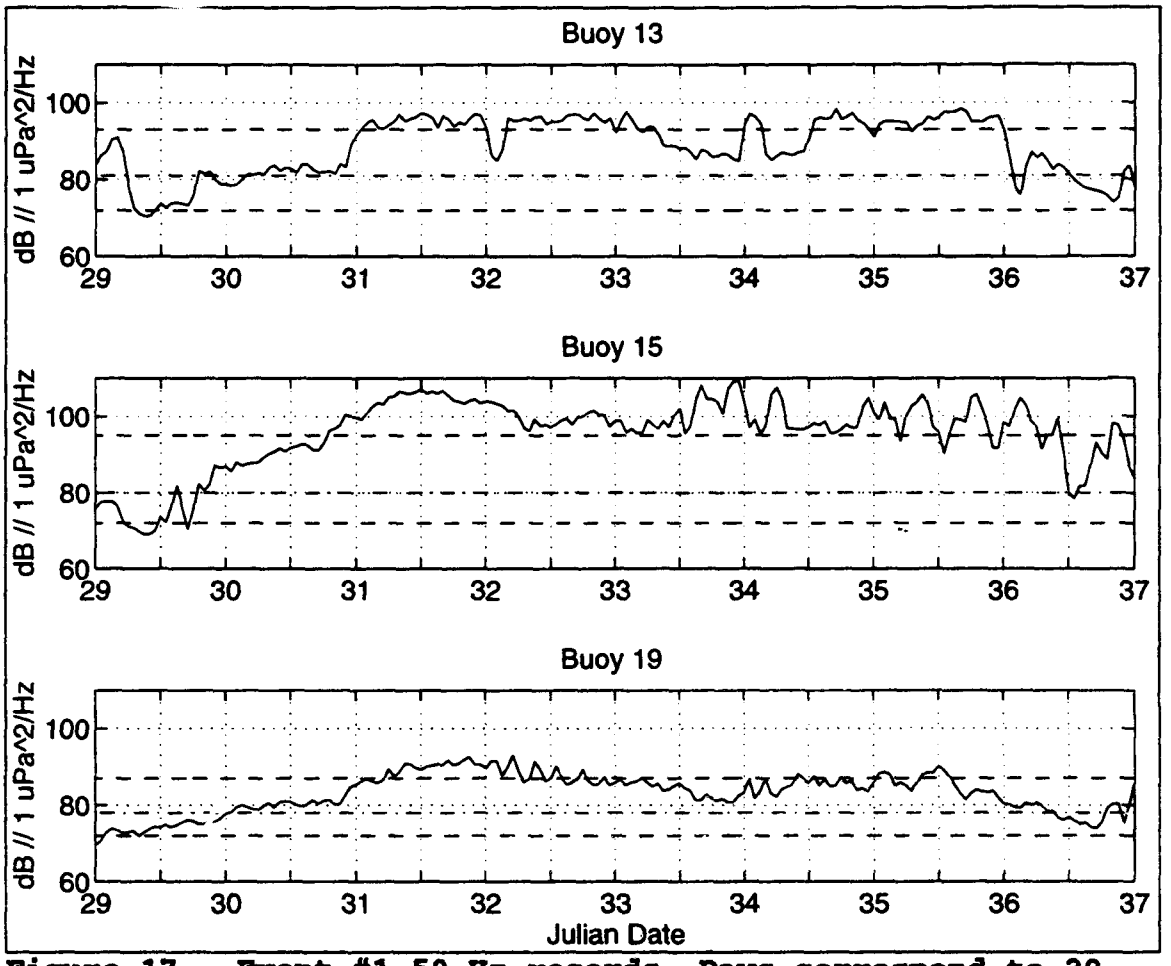

Figure 17. Event #1 50 Hz records. Days correspond to 29 Jan - 6 Feb 1993 at 0000Z. Dashed lines and dash-dot line are the seasonal 95th, 5th and median percentiles, respectively.

day 31.5 for Buoy 15 and near day 32 for Buoy 19. Buoy 13 does not have a single discernable peak during this time; rather the maximum noise level holds steady throughout days 31 and 32.

The 50 Hz noise level dropped rapidly below the median at all buoys as the event ended on or about day 36. The Buoy 19 noise level decreased first, followed by Buoy 13 and then Buoy 15. As will be described later, this order coincides with the relative distance of each buoy from the

core of maximum winds; Buoy 19 was farthest away and Buoy 15 was closest.

The 100 Hz noise record is shown in Figure 18. This record exhibits nearly identical features to the 50 Hz record. The relative increase in noise level at 100 Hz due to the passage of the storm is, on average, about 5 dB greater than at 50 Hz. Buoy 13 increased 28 dB from 63.7 to 91.9 dB, Buoy 15 increased 41 dB from 61.2 to 102.0 dB, and Buoy 19 increased 31 dB from 62.6 to 93.6 dB. These large increases (30 - 40 dB) occurred over about a 48 hour period.

The 500 Hz noise record is shown in Figure 19. The impact of the storm at this frequency is less well defined than at the lower frequencies, but the same trend is present. A large increase (about 32 dB) in noise level is present in the Buoy 15 record with smaller increases in the other buoy records (26 dB at Buoy 13, 28 dB at Buoy 19).

Table XVI summarizes the noise level increases by buoy and frequency. The dynamic range at 100 Hz is slightly larger than at 50 Hz mainly due to the relatively low noise level at 100 Hz prior to the arrival of the storm.

2. ENVIRONMENTAL CORRELATIONS

Having identified and characterized this eight day loud noise event, an attempt was made to determine its cause. Initially, cross correlations of the noise field with wind speed, wind stress and ice speed were run for the duration of event #1 and compared with their seasonal counterparts (Table XVII). The correlations were calculated using vector magnitudes only; the vector directions were not included. Wind speeds and wind stresses were calculated from geostrophic parameters since no in-situ measurements were made. Buoy 19 was chosen for this analysis.

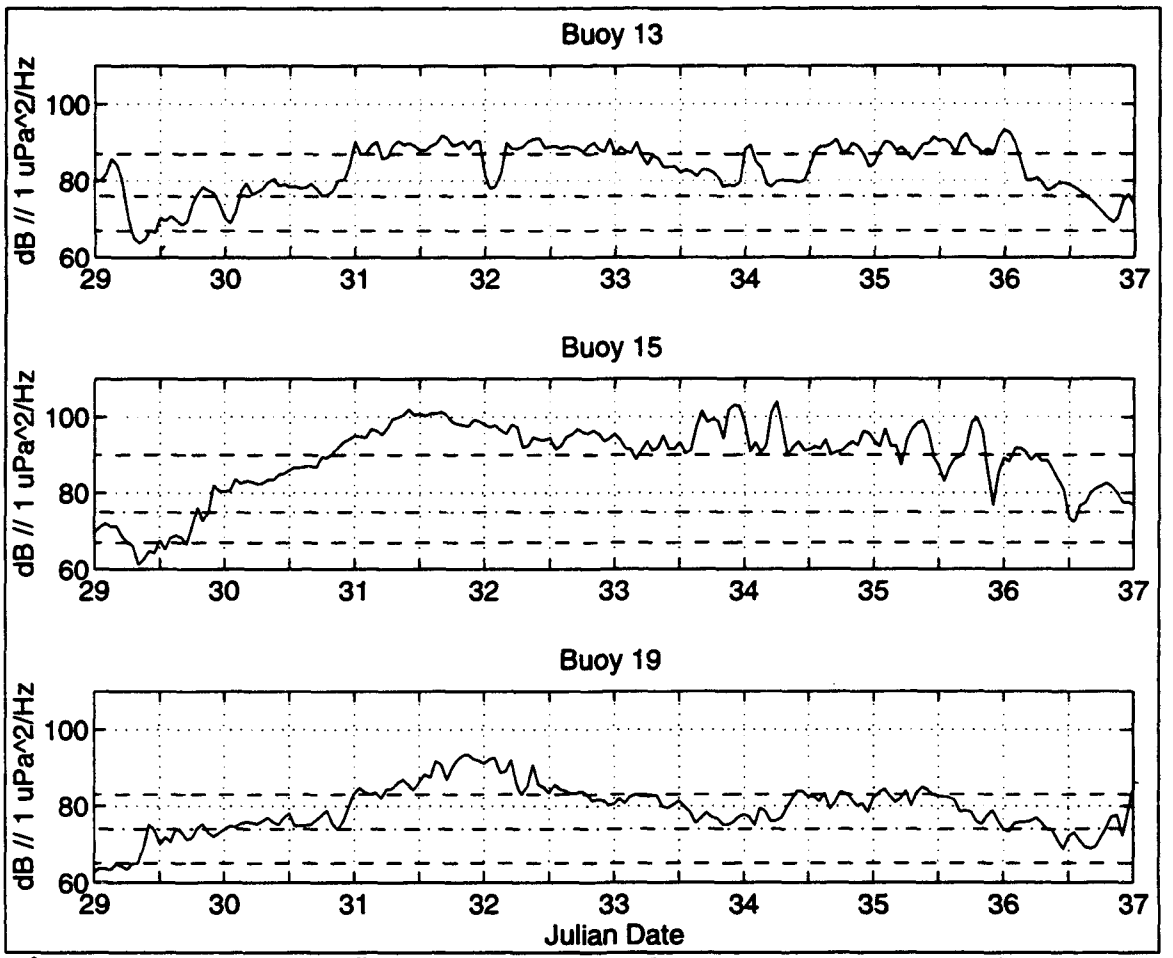

Figure 18. Event #1 100 Hz records. Days correspond to 29 Jan - 6 Feb 1993 at 0000Z. Dashed lines and dash-dot line are the seasonal 95th, 5th and median percentiles, respectively.

Table XVII demonstrates that during the time period of this extreme noise event, the noise field correlation with these environmental forcing mechanisms is much greater than during the season as a whole. The largest improvements in the cross correlation coefficients are generally at 500 Hz. As a strong synoptic event passes nearby, the local vice distant environmental forcing functions will be dominant at higher frequencies. Propagation under the ice at higher frequencies is much poorer than at lower frequencies so the

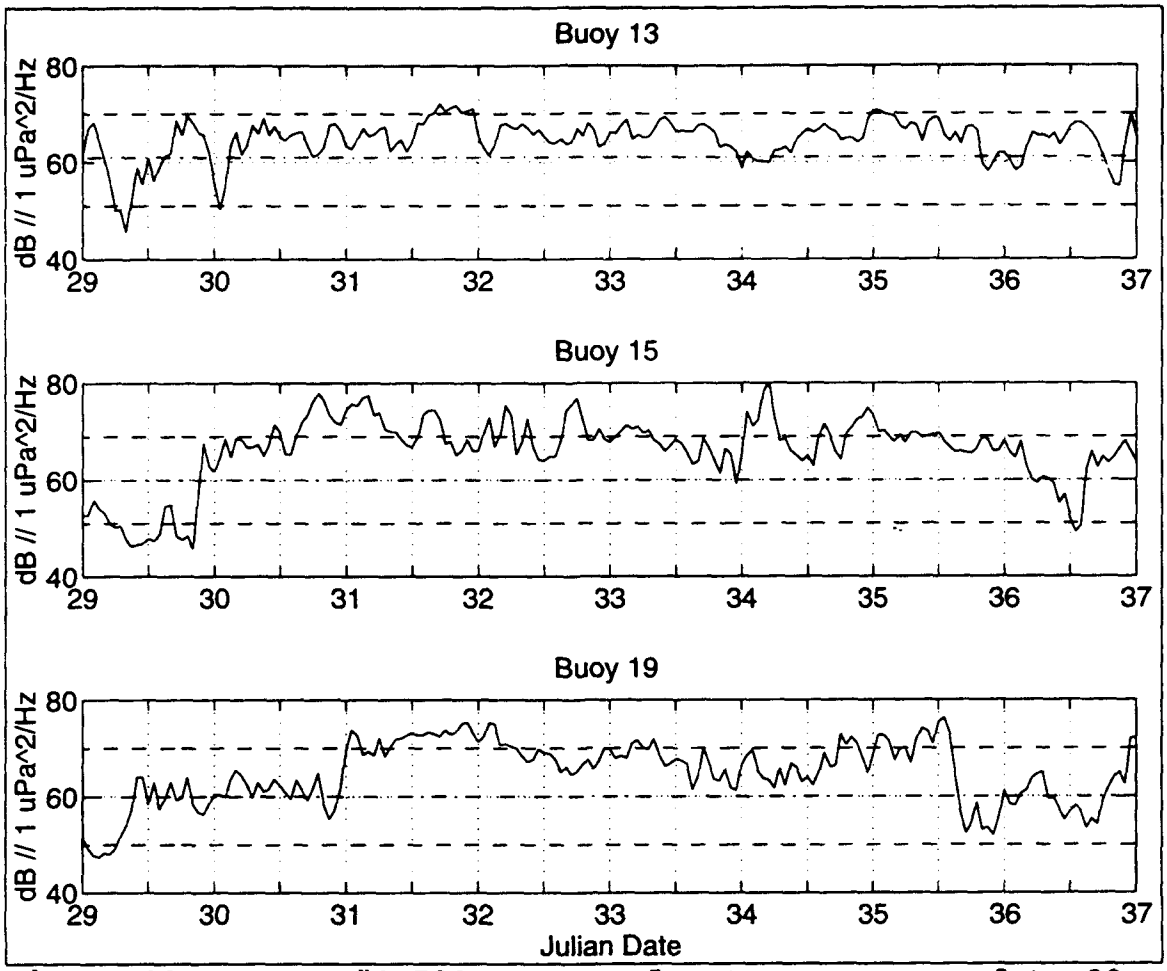

Figure 19. Event #1 500 Hz records. Days correspond to 29 Jan - 6 Feb 1993 at 0000Z. Dashed lines and dash-dot line are the seasonal 95th, 5th and median percentiles, respectively.

high frequency noise field at a given location will be more dependent on local events than the low frequency noise field, which may be contaminated by the propagation of low frequency noise from distant areas.

The maximum cross correlation coefficients are uniformly high during the event, implying a strong relationship between the noise field and the various environmental forcing parameters, especially wind speed and ice speed. Both are in excess of 0.9 at all frequencies.

BUOY	50 HZ (dB re 1 $\mu Pa^2/Hz$)	100 HZ (dB re 1 $\mu Pa^2/Hz$)	500 HZ (dB re 1 $\mu Pa^2/Hz$)
13	26.9	28.2	25.9
15	38.3	40.8	32.1
19	23.4	31.0	28.1

Table XVI. Summary of noise level increases due to event #1. Increases are calculated from before the event began to the first large peak in the noise level.

Ice speed is observed to be the best correlate at all frequencies with wind stress the worst, but only about 10 percent poorer. This is significantly different from the CEAREX 1988/89 experiment, which found wind stress to be the best correlate at all frequencies (Bourke and Parsons, 1993). This difference may be ascribed to the relative accuracy of the wind and ice speeds calculated during the two experiments. During CEAREX local meteorological observations were available from a ship frozen into the ice. Calculations of wind speed and stress were more exact and of finer temporal resolution than ice speed. The reverse was true for the present study. Therefore, the more accurately described fluctuations in ice speed are better correlated with the noise field fluctuations than the less certain wind speed/stress fluctuations.

The lag times for wind speed are relatively long compared to the other two environmental mechanisms during the event. The negative lag times indicate that peak winds occur 7 - 10 hours *before* the corresponding noise peaks. Peak winds occurring before the peak noise are reasonable as

BUOY 19		SEASON		EVENT	
FREQ (HZ)	ENVIRONMENTAL PARAMETER	COEFF (MAX)	LAG (HRS)	COEFF (MAX)	LAG (HRS)
50	WIND SPEED	0.868	-1	0.946	-10
	WIND STRESS	0.808	-20	0.877	0
	ICE SPEED	0.871	0	0.978	2
100	WIND SPEED	0.833	-2	0.911	-7
	WIND STRESS	0.756	-31	0.783	0
	ICE SPEED	0.842	0	0.947	1
500	WIND SPEED	0.803	4	0.902	-9
	WIND STRESS	0.797	-7	0.840	0
	ICE SPEED	0.759	6	0.926	4

Table XVII. Comparison of maximum environmental cross correlation coefficients for the winter season 1992/1993 and for synoptic event #1 for selected frequencies at Buoy 19.

it should take the ice time to react to the changing environmental forcing, but the lag times for the maximum cross correlations are larger than expected. One explanation is the width of the peak of the cross correlation curve. The coefficient varies less than two percent over a ±7 hour spread from the maximum (±10 hours for Buoy 19) which could make the lag times for event #1 consistent with lag times for the winter season.

The lag times for the ice speed correlation are positive, indicating that the fluctuations in ice speed occur *after* fluctuations in the noise level. The lag times for the ice speed correlation at 50 and 100 Hz are 2 hours and 1 hour, respectively, which is near the minimum resolution of the calculation. Thus the near zero lag times imply that noise and ice speed changes occur nearly simultaneously. The ice speed lag time at 500 Hz is 4 hours. Ice speed near the measurement site is expected to correlate well at high frequencies at zero lag time. A possible cause of this positive ice speed lag time is the relative width of the peak in the cross correlation curve. The cross correlation coefficient varies less than one percent between zero hours lag time and plus seven hours lag time, so the actual maximum and its associated lag time could be closer to zero.

3. SURFACE WEATHER CHART ANALYSIS

The next step was to try to determine if a synoptic scale disturbance could cause the observed response in the noise field by its strengthening and subsequent dissipation at it moved through the region surrounding the buoy cluster. Since upper air meteorological features have little direct correspondence to surface features, synoptic events were defined during this period by surface weather charts. These charts were produced by the National Meteorological Center of the National Weather Service, and were obtained from Brian Wallace of the Naval Oceanography Command Detachment, Asheville, NC. The charts were generally available at 0000Z and 1200Z every day, although data from a few time periods were missing. The surface analyses on these charts consisted of an analyzed pressure field, with frontal locations displayed. In addition, charts of 1000 mb isotachs (observed, not geostrophic) from the National

Meteorological Center Global Spectral Model were used to examine the regional wind field, rather than the single point calculation used to determine the geostrophic wind associated with the buoy cluster. The 1000 mb winds were assumed to be representative of the actual surface winds. Charts of the surface wind and pressure fields during event #1 are shown in Appendix B.

Prior to the event, the general drift of Buoy 15 was to the west. Buoys 13 and 19 drifted more to the northwest. The mean speed for all buoys was about 3-5 cm/s. This pattern is consistent with the general direction of drift previously discussed for this leg (leg #3) and only slightly faster than the average speeds (1.5-2.3 cm/s) during this leg. With the arrival of the storm, the buoy drift directions rotated anticyclonically an average of 108 degrees. The maximum directional change was reached 36 hours later at day 30.5, when Buoy 15 drifted nearly to the north and Buoys 13 and 19 drifted to the northeast. During this 36 hour period the wind speed steadily increased. After the passage of the low pressure system the buoys slowly turned towards the direction of their pre-event drift tracks in response to the shifting wind pattern. Buoy 13 ended up drifting to the southwest, Buoy 15 to the south-southwest, and Buoy 19 toward the west-southwest. These final directions correlate well with the winds at the end of the event. This large change in direction of the ice floe trajectories caused strong ice/ice interactions and shearing which are postulated to cause the large changes in ambient noise levels at low frequency shown in Figures 17 through 19.

Prior to the start of the event (day 29, 0000Z), the average winds in the region of Buoy 15 were 12-15 m/s to the northwest, with a component blowing offshore from Severnaya

Zemlya and Franz Josef Land. These were moderate winds, so wind-forced noise generating mechanisms were not expected to be very strong. The offshore component resulted in divergence of the ice pack which has been shown (Lewis and Denner, 1988) to be related with lower noise levels. The noise record from Buoy 15 shows noise levels at all three frequencies to be near the 5th percentile.

The winds at Buoys 13 and 19 were similar to those in the vicinity of Buoy 15. The low wind speeds and non-convergence of the ice pack along the coast are believed to explain the low noise levels at Buoy 19 (near the 5th percentile) prior to the storm. Buoy 13 was only 82 km away from Buoy 19 when the noise event began. Its noise level was above the median and about 10-15 dB greater than that at Buoy 19 for all three frequencies. Since Buoy 13 was closer to the region of strongest winds, this difference is attributed to propagation loss effects over the difference in distances between the buoys and the maximum wind speed region.

The situation is similar 12 hours later at 1200Z, though the winds are lower (10 m/s). Noise levels at 500 Hz have increased to near median levels for all buoys. Higher winds are beginning to move in from the east as a low pressure center moves slowly westward toward the three buoys.

At 0000Z, day 30, the low pressure center is about 700 km southwest of Svalbard, but the northeastern edge of the system has run into the high pressure system northeast of Severnaya Zemlya, causing the winds over the buoy cluster to increase in speed and shift toward the northwest. Wind speeds near the three buoys are 18 m/s at Buoy 15 and 14 m/s at Buoys 13 and 19. By 1200Z, the core of maximum winds of about 21 m/s is located north of the buoy cluster, with the

winds directed to the north-northeast. The noise level had risen 8-17 dB at 50 Hz, 7-19 dB at 100 Hz, and 10-15 dB at 500 Hz from the minimum level before the event began.

At 0000Z, day 31, the low pressure center was just southeast of Svalbard. The core of maximum winds was about 26 m/s, and just west of Buoy 15. The noise level at Buoy 15 at all three frequencies has risen above the 95th percentile. Noise levels at Buoys 13 and 19 experienced a rapid rise of about 10 dB in one or two hours and are at or above the 95th percentile.

Twelve hours later the core of maximum winds is centered just south of Buoy 15, and the Buoy 15 noise level has reached its peak at all frequencies. During the period from day 29.3 through 31.6, the noise level at Buoy 15 at all frequencies rose from levels below the 5th percentile to levels above the 95th percentile. During this period the ice speed increased from 2.7 cm/s to 49.7 cm/s and the ice drift veered almost 60 degrees clockwise (from 270° to 360°). The combination of the large speed increase and the torquing of the ice field due to the large directional change were enough to cause sufficient ice pack convergence to elevate the noise levels at all frequencies from below the 5th percentile to levels above the 95th percentile.

The noise level at Buoy 19 reached its peak about 12 hours later. This delay is correlated with the westward migration of the high-wind regions towards Buoys 13 and 19. Buoy 13 does not have a well-defined peak; rather the noise level stays fairly constant during most of event #1.

Peak noise levels are achieved during day 31. Buoy 15 is just north of the region of maximum winds and its noise level is consequently the loudest of the three. Buoy 13 is closer to the maximum wind region than Buoy 19, but its noise level is louder only at 50 Hz. This difference may be

due to local ice/ice interaction effects and varying propagation loss effects.

The 12 hour period with the second-largest wind direction change occurred from day 30.96 (2300 Z) through 31.46 (1100 Z). The wind field rotated cyclonically about 15° but, importantly, with wind speeds (about 20-25 m/s) at a maximum immediately surrounding the buoys. This time period corresponded to the period of greatest noise level increase, although its exact time varied slightly with buoy and frequency. In contrast, this can be compared to a period of large change in wind direction but only moderate wind speed. The period with the largest direction change was at the start of the event, days 29 through 29.3, when the noise levels remained low. During this time the regional wind speed was less than 15 m/s. These two periods demonstrate that it is the combination of large direction changes combined with high wind speeds that results in sufficient torque on the ice field to raise the noise level above the 95th percentile.

By day 33 the wind speeds have slowed below 20 m/s and the noise levels start to decrease. On day 35 the core of maximum winds reached 30 m/s due to cyclogenesis but is located farther to the northeast than the earlier area of maximum winds. The speed gradient is also greater during day 33. The greater distance from the area of strongest winds and a stronger gradient result in lower wind speeds near the buoys. Both effects (more distant maximum speeds and lower local speeds) are believed to be responsible for the small peak seen in the noise record at this time. This peak is most pronounced at 50 Hz and 100 Hz for Buoys 13 and 19.

By day 36 the low and high pressure systems have separated. The maximum wind speed within 300 km of the buoy

cluster is about 18 m/s with an average speed about 10 m/s. The noise levels responded to this reduced forcing by decreasing to near-median levels.

The low pressure system crossing through the buoy region from west to east was directly responsible for the high surface winds observed during this event. The peaks in the noise record correspond almost exactly in time to the peaks in the regional, or distant, wind speed, but do not occur at the same time as the peaks in the local wind fields. The wind speed maxima do not occur directly over the buoys, but several hundred kilometers from the buoy cluster. The local wind field also increased in speed due to the presence of the synoptic system propagating through the region. This seems to indicate that peak levels in the ambient noise field, especially at low frequencies, are associated with peak periods in the regional or distant wind field and not the local wind speed alone.

The evidence presented supports the theory that the most important environmental correlate to extremely loud (greater than the 95th percentile) noise events is the build up of ice stress (ridging) due to convergence of the ice at times of high regional wind speeds.

4. SUMMARY

The noise field started near the 5th percentile level, then increased to above the 95th percentile level when the regional winds changed direction enough to cause the direction of the ice motion to rotate more than 90°. This large direction change apparently induced enough convergence to increase the internal stress in the ice field sufficiently to generate extremely high noise levels. The regional surface wind speed increased during the event causing a related increase in ice speed. The noise levels remained near the 95th percentile level for several days.

The noise levels declined to the 5th percentile levels when the ice speed abated and the distant storm subsided.

B. SYNOPTIC EVENT OF 4 - 6 JULY 1992

This event was chosen as an example of a period where the noise levels remained near the 5th percentile level for longer than one day. A small noise peak is present in the center of the time period on 5 July, which will be discussed, but the major focus of this event was to determine the environmental forcing responsible for an extended period of low noise levels. This event occurred during the period 4-6 July 1992 (julian dates 186-189) of the AREA 1992 experiment and will be referred to as event #2. During this event the buoys were drifting southward as part of leg #1. Buoys 13 and 19 were approximately 400 km north of Franz Josef Land. Buoy 15 was about 200 km west of the other two buoys. The buoy positions are shown in Figures 2 through 4.

1. DESCRIPTION OF THE NOISE RECORD

The 50 Hz noise record is shown in Figure 20. At 0000Z on day 186, the noise levels at Buoys 13 and 15 were slightly below the median level (77 dB). Over the next 10 hours the noise level fell to about the 5th percentile and commenced oscillating about this level for the next 2.5 days. During this period Buoy 13 experienced a temporary increase in noise level centered on day 187.7. This noise peak was not present in the record of either of the other two buoys. The noise level at Buoy 19 began just below the median at 72 dB and varied between the 5th and 50th percentiles for the balance of the event. However, the difference between the 5th and 50th percentiles for this buoy was less than 5 dB during this summer season.

The 100 Hz noise record is shown in Figure 21 and all three buoy records exhibit the same general characteristics.

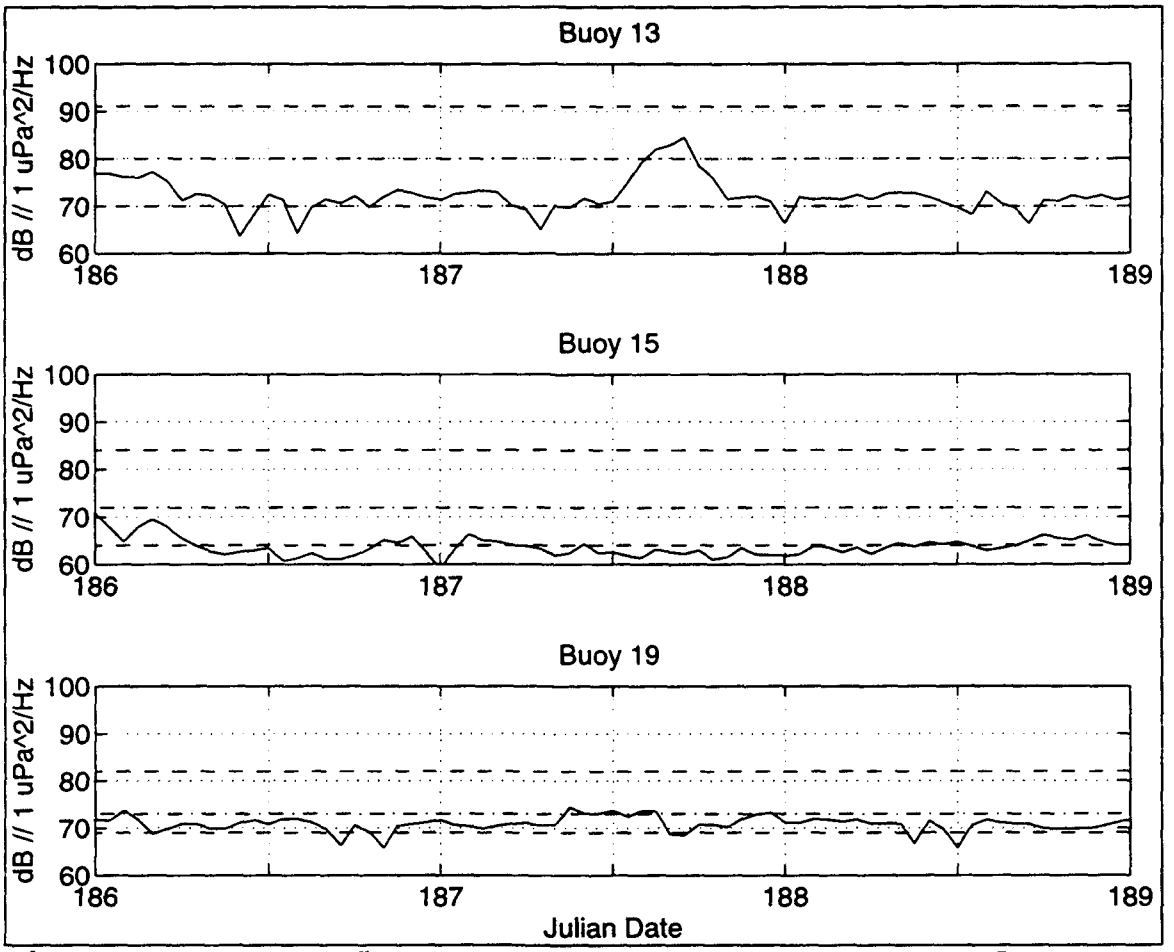

Figure 20. Event #2 50 Hz records. Days correspond to 4-7 July 1992 at 0000Z. Dashed lines and dash-dot line are the seasonal 95th, 5th and median percentiles, respectively.

They started just below their median levels then decreased over the next 12 hours to commence oscillating about their 5th percentile levels. The noise peak seen at Buoy 13 at 50 Hz is also seen at 100 Hz. There is a hint of increased noise levels at Buoy 15 about 12 hours earlier. The noise level at Buoy 15 increased at the end of event #2 and hovered just below the median for about seven hours at the end of the record. The other buoys did not exhibit this rise in noise levels at the end of event #2.

The 500 Hz noise field was fairly constant during this entire three day period with no significant features (Figure 22). All three records begin near the median. They vary predominantly between the 5th and 50th percentiles throughout event #2 with an occasional excursion beyond those limits. The sharp noise peak seen near day 187.7 in the low frequency records is not discernible at 500 Hz, but the tendency towards higher noise levels is present.

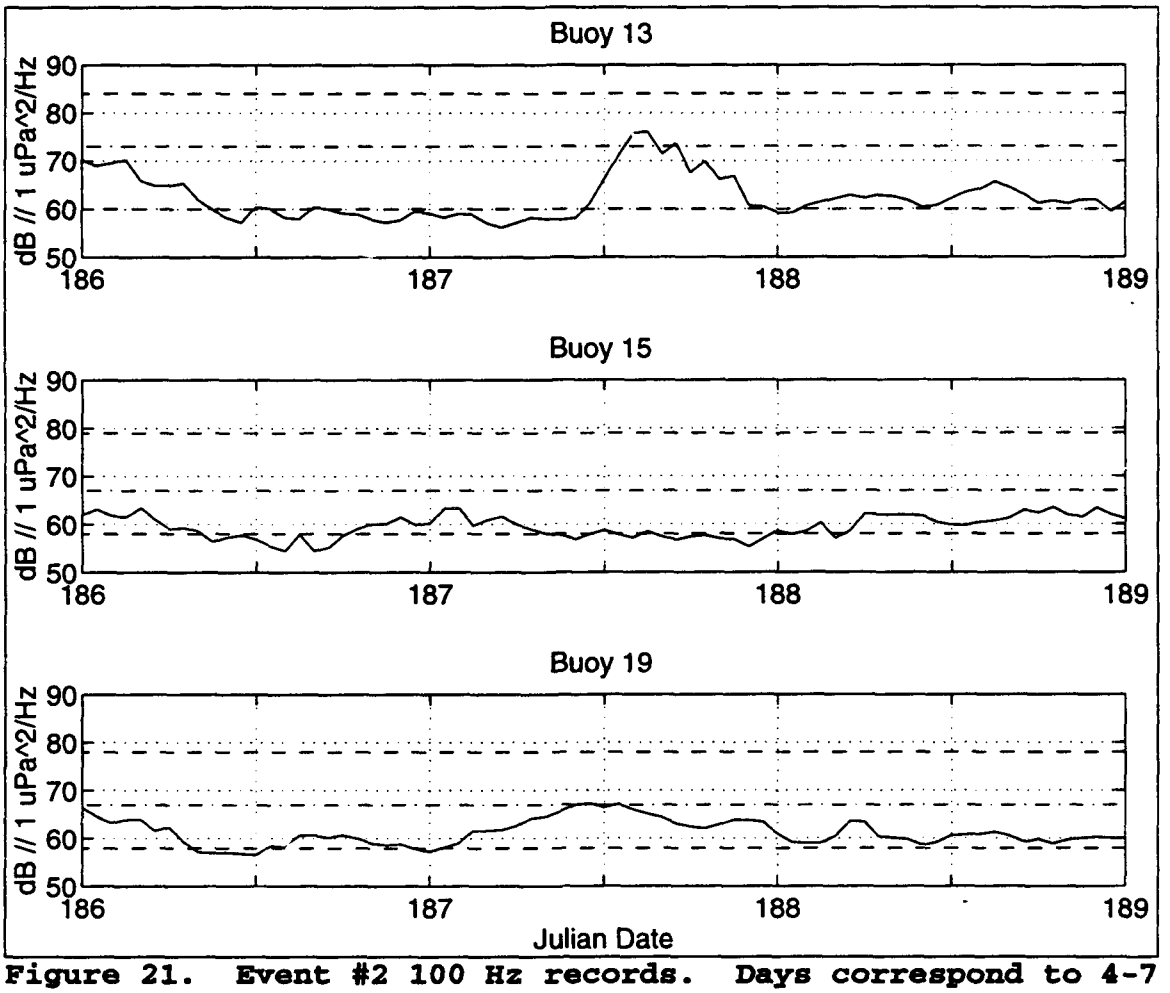

Figure 21. Event #2 100 Hz records. Days correspond to 4-7 July 1992 at 0000Z. Dashed lines and dash-dot line are the seasonal 95th, 5th and median percentiles, respectively.

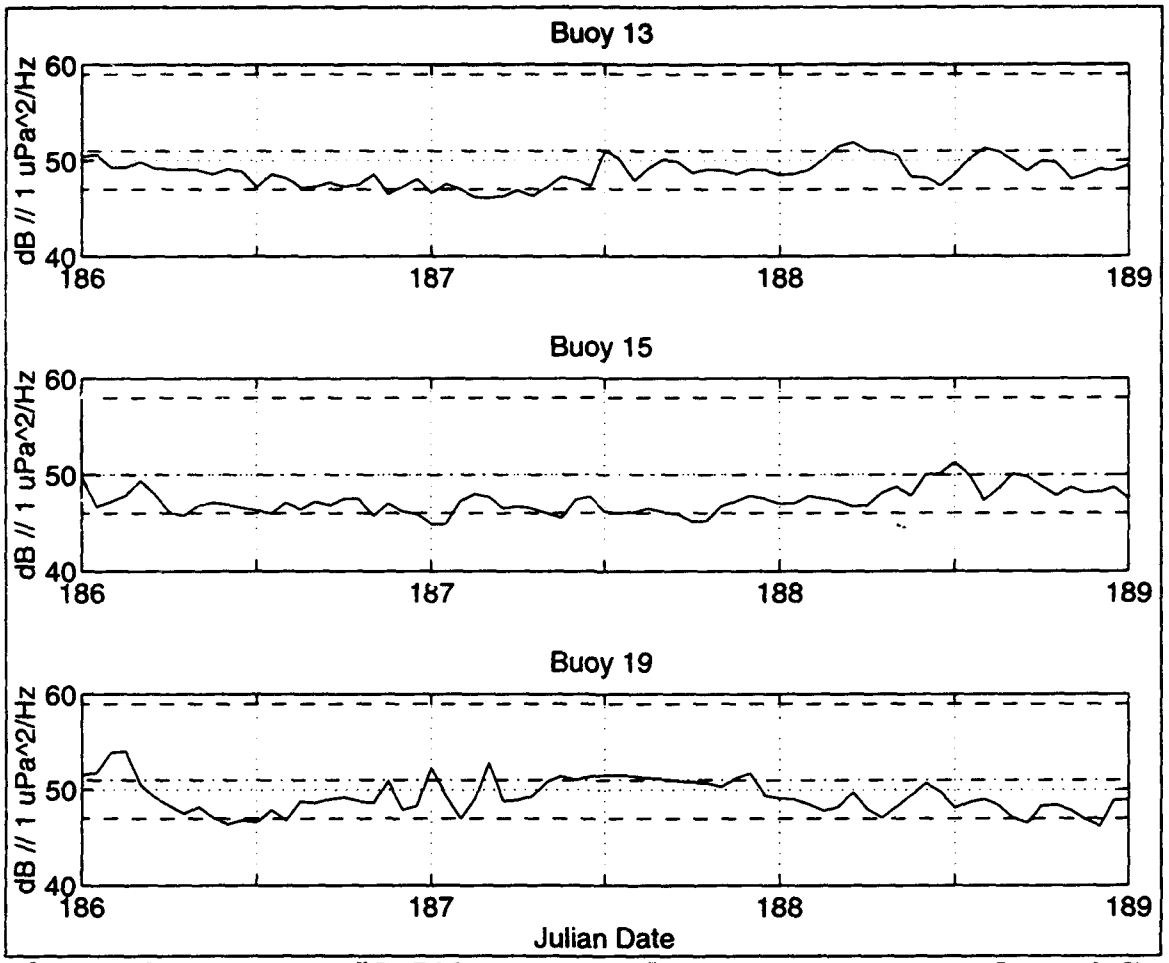

Figure 22. Event #2 500 Hz records. Days correspond to 4-7 July 1992 at 0000Z. Dashed lines and dash-dot line are the seasonal 95th, 5th and median percentiles, respectively.

2. ENVIRONMENTAL CORRELATIONS

Environmental cross correlations were performed as was done for event #1 to determine how well the noise field responded to environmental forcing during this quiet period. Table XVIII shows a comparison between the maximum environmental cross-correlation coefficients during event #2 and those for the entire summer 1992 season for selected frequencies. The correlations were performed as described

for event #1. Buoy 19 was again chosen to illustrate the correlation results for this event.

BUOY 19		SEASON		EVENT	
FREQ (HZ)	ENVIRONMENTAL PARAMETER	COEFF (MAX)	LAG (HRS)	COEFF (MAX)	LAG (HRS)
50	WIND SPEED	0.814	0	0.958	0
	WIND STRESS	0.781	0	0.985	0
	ICE SPEED	0.858	-1	0.919	0
100	WIND SPEED	0.769	-1	0.961	0
	WIND STRESS	0.704	0	0.948	0
	ICE SPEED	0.816	-1	0.940	0
500	WIND SPEED	0.824	0	0.972	0
	WIND STRESS	0.835	0	0.977	0
	ICE SPEED	0.802	1	0.933	0

Table XVIII. Comparison of maximum environmental cross correlation coefficients for the winter season 1992/1993 and synoptic event #2 for selected frequencies at Buoy 19.

As was the case for the short (several days) duration loud event in winter (event #1), the correlations are significantly greater during the limited duration of event #2 than during the entire season. The maximum cross correlation coefficients are all well above 0.9 implying a

strong relationship between the noise field and the three environmental forcing mechanisms.

The wind stress and wind speed are only slightly better correlated with the noise field than the ice speed at all frequencies. This is directly opposite the finding from event #1, where ice speed was the best correlate at all frequencies. This is probably due to the fact that ice speeds were much greater during event #1 and therefore had a stronger effect on the noise field. The lag times in Table XVIII are all one hour or less. Since the minimum resolvable time is one hour, the peaks in the noise field and the environmental forcing may be considered to occur simultaneously.

3. SURFACE WEATHER CHART ANALYSIS

The observed surface wind charts during event #2 were studied next, and are shown in Appendix C. Over the 24 hour period prior to 4 July the winds were blowing towards the south with steadily decreasing speed. The ice floes that carried the buoys were forced towards Franz Josef Land, but as the winds slowed the forcing abated, reducing the convergence of the ice field and resulting in low noise levels.

Prior to this quiet period Buoy 13 was drifting south-southwest (about 230°) at a speed of about 10 cm/s. At 0300Z on day 187 the buoy began a 16 hour clockwise change in direction that ultimately reached a heading of 034° before turning back towards its final heading of 157°. During the most rapid part of the direction change the buoy drift speed had slowed to below 6 cm/s. The noise peak of day 187 began as the direction of ice motion turned through 345°. At this time a velocity component was directed opposite to the initial direction of motion, which evidently

caused a convergence in the ice field that generated the moderate noise peak seen at 50 Hz and 100 Hz.

Buoy 15 drifted nearly south (about 205°) prior to the start of event #2 at about 8 cm/s. During day 187 the speed slowed to about 4 cm/s and the buoy drift veered anticyclonically with a maximum directional change of about 100° before returning to its original heading. This direction change coupled with the speed reduction did not generate sufficient convergence to cause the noise peak seen at the other two buoys.

Buoy 19 drifted west-southwest (about 240°) prior to the start of event #2 at about 10 cm/s. The buoy speed slowed to about 4-6 cm/s four hours after the event began. The drift direction began rotating clockwise about day 186.9 and a speed increase began at day 187.2. The maximum heading and speed changes occurred simultaneously at day 187.6, correlating well with the period of increased noise. After this peak period the drift direction rotated cyclonically and at the end of the event was southeast. The speed dropped below 4 cm/s within 12 hours of the peak speed and rarely exceeded 4 cm/s throughout the rest of event #2.

Throughout day 186 the regional wind speeds were everywhere below 12 m/s. The winds just north of Franz Josef Land had a small and decreasing southward velocity (less than 8 m/s) and the resulting decreasing convergence was responsible for the decreases seen in the noise record at all frequencies.

During the first half of day 187, the winds began to rotate clockwise and by noon almost the entire regional wind field had reversed direction and was then blowing to the north. This is the period of maximum noise levels at all frequencies. The evidence strongly suggests that the reversal of the surface winds, and the resulting convergence

of the ice field, was directly responsible for the well defined peak in the noise record. However, the low wind speeds were of insufficient force to greatly increase the internal ice stress and hence only a moderate increase in the noise level resulted.

During day 188 the regional wind field was comprised entirely of fairly steady, but weak, surface winds. The ice field had adjusted to the new wind field and was no longer subject to the convergence that caused the noise level peak. As a result, the noise levels at all frequencies hovered near the 5th percentile levels.

No atmospheric surface fronts passed near the buoy cluster during event #2. One small low pressure center passed over the buoy cluster, but was too weak to generate strong winds. This event lacked the strong, dynamic winds characteristic of event #1, resulting in the predominantly low noise levels measured during this event.

4. SUMMARY

Event #2 was predominantly a quiet event, with noise levels remaining near the 5th percentile for most of the three days. The regional wind field was comprised generally of slow speed winds without onshore components near Svalbard, Franz Josef Land and Severnaya Zemlya. This wind pattern resulted in reduced or limited convergence of the ice field, resulting in low noise levels.

During event #2 the noise levels at Buoys 13 and 19 increased for a short time to near the seasonal median. This noise peak occurred shortly after the regional wind field near the buoy cluster reversed its direction. The wind reversal caused the ice motion to reverse and resulted in convergence of the ice field. The regional wind speeds remained low and therefore the ice convergence caused louder

noise levels but was not sufficient to reach the 95th percentile plateau.

C. SYNOPTIC EVENT OF 27 - 29 AUGUST 1992

This was a loud event that occurred during 27-29 August 1992 (julian days 240 and 243) of the Area 1992 experiment while in drift leg #2 and it will be referred to as synoptic event #3. Buoys 13 and 19 were about 300 km north-northeast of Franz Josef Land and Buoy 15 was about 350 km north of Franz Josef Land.

1. DESCRIPTION OF THE NOISE RECORD

The noise level at 50 Hz (Figure 23) for Buoy 13 at the beginning of the event was 70.9 dB, just above the 5th percentile level, where it had been for the previous 18 hours. Over the next three hours the noise level increased 13 dB, and after a further 12 hours the noise level had increased to the 95th percentile level (93.7 dB), a 23 dB gain in 15 hours. The noise level remained near the 95th percentile level for almost two days before it returned to the 5th percentile level, which it reached on day 242.6. Buoy 15 recorded a similar rapid (23 dB) rise in noise level but approximately 12 hours later. This buoy then experienced a series of large oscillations of approximately 15 dB with a periodicity of 12-13 hours, suggesting they were of tidal and/or inertial origin. The Buoy 15 noise level began its final drop three hours after Buoy 13. Buoy 19 did not experience the sudden rise in noise level but instead showed a steady but slow rise extending over two days, ultimately reaching its 95th percentile on day 241.3 and reached its maximum of 84.9 dB (for a total increase of nearly 14 dB) on day 242. All three buoys show a dramatic decline in noise level after the passage of the storm (day 242), returning to values well below the median in about 6

hours. The reduction was experienced first at Buoy 13, followed 2-3 hours later by the other two buoys.

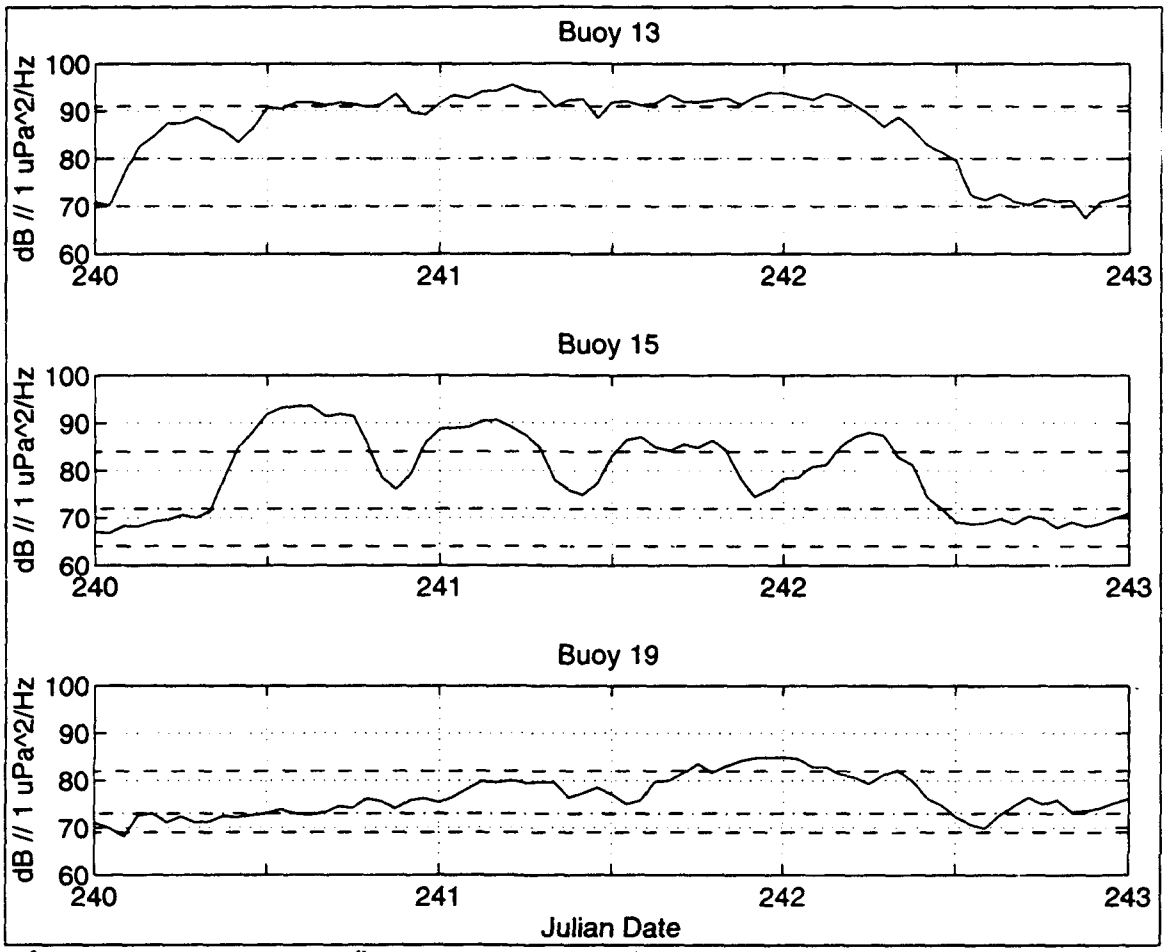

Figure 23. Event #3 50 Hz records. Days correspond to 27-31 August 1992 at 0000Z. Dashed lines and dash-dot line are the seasonal 95th, 5th and median percentiles, respectively.

The 100 Hz noise records for all three buoys (Figure 24) are very similar to their respective 50 Hz noise records. Buoy 13 experienced a noise gain of 20 dB in 7 hours, then gradually increased to the 95th percentile level where it remained for almost two days before decreasing to the 5th percentile level. The Buoy 15 noise level at 100 Hz began at 63.6 dB, then rose slowly for 9 hours until the

large (15 dB) 12-13 hour oscillations commenced, dominating the next two days. The Buoy 15 noise levels then decreased to the median level by day 243. Buoy 19 displayed the same slow ramp up to a noise peak on day 242 as observed in the 50 Hz record. The drop off in noise level near 0600Z on day 242 at all three buoys was similar to that at 50 Hz, with Buoy 13 preceding the other two buoys by 2-3 hours.

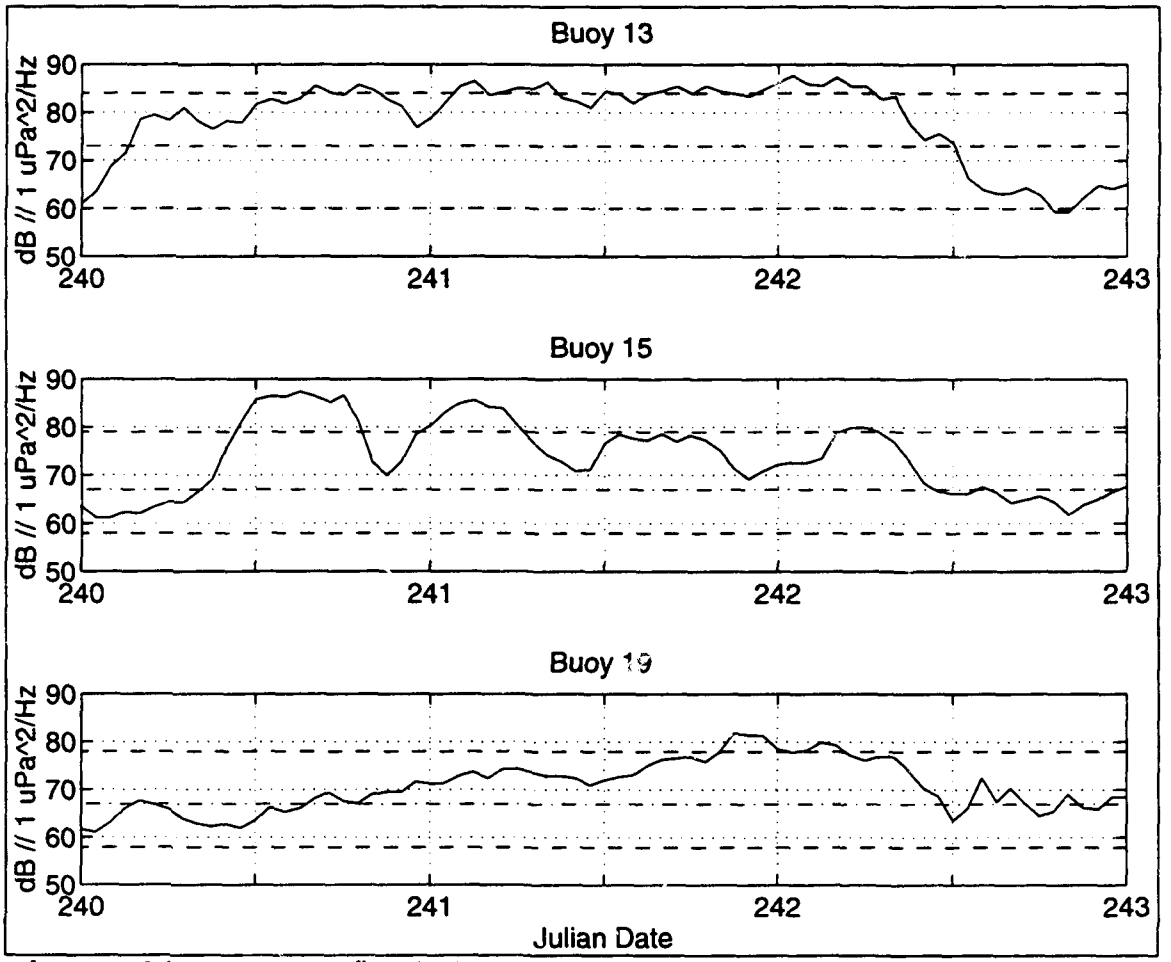

Figure 24. Event #3 100 Hz records. Days correspond to 27-31 August 1992 at 0000Z. Dashed lines and dash-dot line are the seasonal 95th, 5th and median percentiles, respectively.

The 500 Hz noise records (Figure 25) bear little resemblance to the 50 Hz and 100 Hz records and are probably

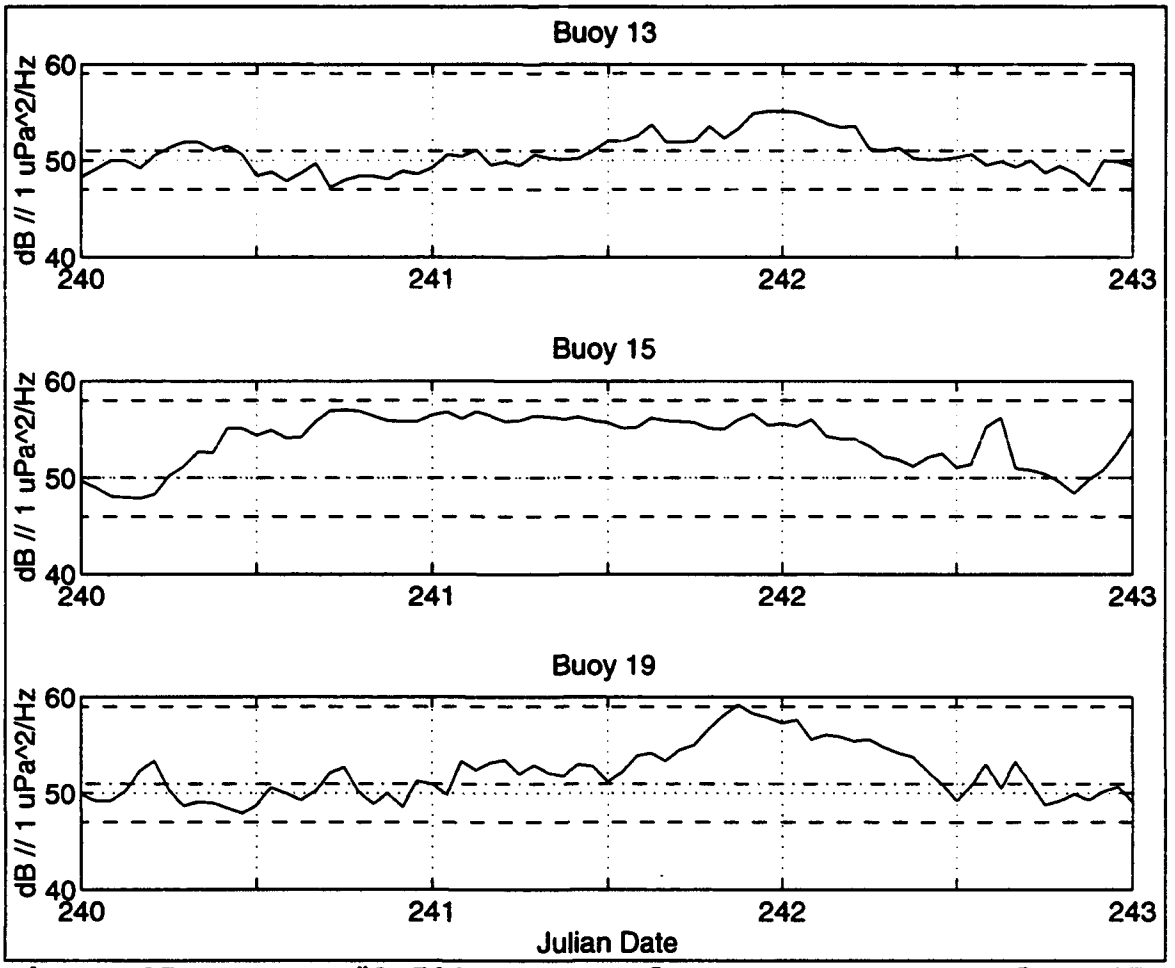

Figure 25. Event #3 500 Hz records. Days correspond to 27-31 August 1992 at 0000Z. Dashed lines and dash-dot line are the seasonal 95th, 5th and median percentiles, respectively.

dominated by local wind and ice speed conditions. The 500 Hz noise record for Buoy 13 was constant for all of day 239 and then fluctuated slowly within 4 dB for the first 17 hours of day 240. The Buoy 13 noise level then reached its minimum value of 47.2 dB before increasing to its maximum value of 55.1 dB at day 242. The noise level then decreased slowly throughout day 242 as event #3 ended. The Buoy 15 noise record increased 10 dB over 12 hours before remaining steady just below the 95th percentile level for about 36

hours. Buoy 15 reached its plateau about 36 hours before the other buoy noise levels peaked. Buoy 19 exhibited behavior similar to that of Buoy 13, except it reached its 95th percentile while Buoy 13's maximum was 3 dB below this threshold, and peaked about 4 hours before Buoy 13.

Table XIX summarizes the noise level increases by buoy and frequency. The dynamic range of the 100 Hz noise is greater than that of the 50 Hz noise due to the relatively low levels at 100 Hz prior to the event. Buoys 13 and 15 exhibited similar behavior. Buoy 19 had a much smaller response to the environmental forcing, with a larger response at higher frequencies.

Several potential explanations were investigated to explain the unusual behavior of the noise records from Buoys

BUOY	50 HZ (db re 1 $\mu Pa^2/Hz$)	100 HZ (db re 1 $\mu Pa^2/Hz$)	500 HZ (db re 1 $\mu Pa^2/Hz$)
13	22.8	26.8	16.8
15	24.8	26.2	20.8
19	6.8	9.1	10.0

Table XIX. Summary of noise level increases due to event #3. Increases are calculated from before the event began to the first large peak in the noise level.

15 and 19. The 12-13 hour periodicity measured at 50 Hz and 100 Hz by Buoy 15 suggested a tidal or inertial forcing. All three buoys were in water too deep (greater than 3000 m) for the tidal signal to cause the large (15 db) observed fluctuations. The Buoy 15 track was examined for evidence

of inertial forcing, but the track did not contain any oscillations at this period. Thermal cracking is associated with a diurnal period with louder noise levels at night while the ice is cooling. The Buoy 15 data showed a semidiurnal period with maximum levels in the afternoon, so thermal cracking was ruled out as a potential cause. With the likely causes ruled out, the fluctuations in the Buoy 15 noise record remain unexplained.

The Buoy 19 noise levels ramped up 7-10 dB slowly over a two day period while those at Buoy 13 increased 17-27 dB over 12 hours. This buoy pair was closest together (about 90 km apart) and the noise records were expected to be more similar, as they were during events #1 and #2. All three buoys were moving in unison during the event. The mean scalar ice speeds ranged from 13.7 cm/s (Buoy 15) to 14.9 cm/s (Buoys 13 and 19), so a slower ice speed at Buoy 19 could not explain its anomalous behavior. The drift speeds and directions for all three buoys changed together at the same rates in response to the changing wind forcing. Buoy 19 noise levels tracked well with Buoy 13 levels before and after this event as well. No cause could be found to explain the measured behavior.

2. ENVIRONMENTAL CORRELATIONS

Table XX shows the maximum environmental cross correlation coefficients and their associated lag times for Buoy 19. As seen in the events #1 and #2, the noise field correlation with the environmental forcing increases during the event.

As was seen during event #1, the maximum correlation coefficients showed the largest increase from seasonal values at 500 Hz. The high correlation coefficients show that the noise field was highly correlated with the environmental forcing, though the correlations quite were

not as high as they were during event #1, where a more severe storm occurred.

BUOY 19		SEASON		EVENT	
FREQ (HZ)	ENVIRONMENTAL PARAMETER	COEFF (MAX)	LAG (HRS)	COEFF (MAX)	LAG (HRS)
50	WIND SPEED	0.814	0	0.924	0
	WIND STRESS	0.781	0	0.886	0
	ICE SPEED	0.858	-1	0.969	0
100	WIND SPEED	0.769	-1	0.888	-2
	WIND STRESS	0.704	0	0.837	0
	ICE SPEED	0.816	-1	0.946	0
500	WIND SPEED	0.824	0	0.952	0
	WIND STRESS	0.835	0	0.940	0
	ICE SPEED	0.802	1	0.975	0

Table XX. Comparison of maximum environmental cross correlation coefficients for the summer 1992 season and synoptic event #3 for selected frequencies at Buoy 19.

Table XX shows that ice speed was the best correlate at all frequencies and wind stress was the worst correlate at all frequencies, as was the case for event #1. There was no synoptic front within 900 km of the buoy cluster during this event. The meteorological forcing was entirely due to low

and high pressure synoptic systems migrating through the Arctic Basin.

Negative lag times indicate that the noise field lagged the forcing. All lag times during event #3 are zero except for wind speed at 100 Hz, which is -2 hours. Since the minimum resolution of the analyses is 1 hour, the noise field responded nearly simultaneously with the environmental forcing during event #3, as it did throughout the entire summer season.

3. SURFACE WEATHER CHART ANALYSIS

The observed surface wind charts were studied to determine the environmental forcing, and are shown in Appendix D. Throughout day 239 the winds near the buoy cluster slowly increased in speed. At 1200Z on day 239, the core of maximum winds was about 250 km north of the buoys with a core speed about 21 m/s. The wind direction near the core of maximum winds had not changed appreciably. The wind direction near the buoy cluster rotated cyclonically approximately 90° and the buoy drift tracks began to rotate in response to the wind shift over the previous 12 hours, but due to the low wind speeds (less than 8 m/s at the buoys) no component of the ice velocity was directed opposite to the initial ice motion, thus no significant ice convergence was experienced. As a result, the noise levels at 0000Z on day 240 were below the median values at all frequencies and near the 5^{th} percentile level at 50 Hz and 100 Hz.

At the same time, the wind field just north of Franz Josef Land was directed to the east, so there was no onshore component to cause ice field convergence against the islands. There were onshore components of the wind vector north of Svalbard and Severnaya Zemlya. The wind speeds were below 7 m/s in both regions, which was evidently too weak to

cause sufficient ice field convergence near those islands (due to the onshore components). As a result, there were low noise levels at the buoy cluster.

At 0000Z on day 240, the core of maximum winds reached 28 m/s and wind speeds near the buoys were 10-15 m/s to the southwest. The winds just north of Svalbard, Franz Josef Land and Severnaya Zemlya were predominantly to the south but the wind speeds were still below 7 m/s. The onshore forcing was not sufficient to generate high noise levels at the buoy cluster.

By 1200Z on day 240 the core of maximum winds had dissipated. Winds in the buoy cluster region were generally to the south at speeds below 10 m/s. The noise field had by this time begun to increase toward the 95th percentile levels, and had reached that plateau on several records, without having the ice or wind directions shift in excess of 90° as seen in events #1 and #2. The convergence in this case and the resulting increase in the noise field is attributed to the steady, if slow, onshore ice motion, rather than a direction change of greater than 90°. The buoy drift speeds increased from about 8 cm/s to the south to about 25 cm/s to the south for Buoy 15 (Buoys 13 and 19 reached about 15 cm/s) over the first half of day 240. This acceleration in the onshore direction caused a convergence of the ice against the island land masses resulting in the high noise levels at low frequencies seen in Figures 23 and 24.

Throughout day 241 the winds remained below 15 m/s near the buoys and the islands, though a strong core developed that reached 24 m/s at 1200Z. The wind and ice directions remained within 40° of due south with ice speeds ranging from 14-25 cm/s. This constant southward drift caused

continuing convergence and thus the noise level remained high.

At 0000Z on day 242 the regional wind speeds were everywhere below 12 m/s, with the highest wind speeds between the buoy cluster and Franz Josef Land. The wind direction was still to the south over most of the region. Over the next 12 hours the winds slowed further and the ice speeds responded by slowing, reducing the convergence of the ice field against the islands. The resulting noise field decreased as well, decreasing to the 5th percentile for most frequencies. By 1200Z the winds near the islands had shifted away from straight onshore and were no longer acting to cause ice field convergence against the islands.

4. SUMMARY

The noise levels began near the 5th percentile levels due to low speed cross-shore winds near the islands. The noise levels increased in spite of 12-24 hours of mostly slow wind speed since the southward wind direction had converged the ice pack against the three island groups of Svalbard, Franz Josef Land and Severnaya Zemlya. The wind direction and the resulting ice motion varied little from due south over the next day and a half, causing the continued ice convergence that resulted in the noise levels remaining near the 95th percentile level. The noise levels decreased after the wind stopped forcing the ice pack onshore.

D. EVENT ANALYSIS SUMMARY

The three events analyzed in this chapter, while all different, had several common factors. The noise levels were lowest (near the 5th percentile) when the regional surface wind speeds were low (below about 10 m/s) and the regional surface wind direction was steady over at least several hours. The low wind speeds resulted in low ice

speeds and thus low ice motion related noise. The steady wind direction over several hours gave the regional ice field motion time to stabilize in one direction, minimizing the convergence known to generate high source levels.

The noise levels were highest (at or above the 95th percentile) when a synoptic low pressure system (storm) was moving through the vicinity. Two main factors contributed to the high noise levels. The large wind direction changes associated with a storm passage caused associated ice motion changes that resulted in a component of the ice motion reversing. Reversal of the ice motion caused wide area convergence of the ice field. In addition, the high wind speeds caused large ice speeds, increasing the ice motion-generated noise as well as enhancing the convergence caused by the changes in ice drift direction.

High ice speeds or large directional changes in the ice motion alone were not sufficient to maintain noise levels near the 95th percentile for periods longer than one day. A strong, persistent storm such as event #1 was able to maintain extremely high noise levels for five days. Slow and steady winds in the absence of a strong storm (event #2) caused noise levels to increase by forcing the ice field up against land, in this case three island chains. This mechanism caused convergence of the ice field and raised the noise level, but was not able to reach the 95th percentile. One can postulate that stronger onshore winds for a longer time period would have resulted in noise levels reaching the 95th percentile.

V. CONCLUSIONS AND RECOMMENDATIONS

A. CONCLUSIONS

During the AREA 1992 experiment three ANMET buoys were inserted on separate ice floes about 600 km north of Franz Josef Land. The initial pattern was roughly an isosceles triangle with two long sides approximately 175 km and the short side approximately 100 km. The buoy drift patterns included five distinct regimes wherein the direction of ice motion was generally constant. The overall drift direction was to the southwest and all buoys sank when their respective floes broke up near the northern coast of Svalbard after periods ranging from 13-21 months. Two buoys eventually had their hydrophones run aground which limited the usable noise records to 12-19 months. The buoys provided hourly measurements of ambient noise in 11 frequency bands centered between 5 Hz and 4000 Hz. Limited meteorological measurements were also obtained. No other supporting atmospheric measurements were available during the experiment.

The buoys exhibited nearly identical annual median spectra at or above 200 Hz. Below 200 Hz the spectra diverged, but were always within 10 dB of each other. Buoys 13 and 19, which were closest together, unexpectedly had the largest differences in spectral levels (approximately 6 dB) below 200 Hz. This trend of divergent levels at low frequencies and similar levels at high frequencies was also exhibited in the annual 95^{th} and 5^{th} percentile levels, and in the winter and summer data at the median and 95^{th} percentile levels.

The measured annual median spectra was about 10 dB greater than the Eurasian Basin annual median reported by Buck and Clarke (1986) at all frequencies. The annual

median spectra was 6-7 dB louder than the median reported for the CEAREX 1988/89 experiment at low frequencies, but above 100 Hz was quieter than the CEAREX data. The winter median spectra was within 3 dB of the late winter Fram IV median spectra at all frequencies below 1000 Hz.

The three extreme ambient noise events studied in detail (two loud, one quiet) showed that persistent ambient noise levels above the 95th percentile or below the 5th percentile could extend over periods of several days. Sustained levels above the 95th percentile were directly related to the passage of large synoptic weather systems. These systems caused large ice motion direction changes and high sustained ice speeds due to strong winds, which resulted in large amounts of convergence in the ice field. The release of the large levels of internal stress built up through convergence is responsible for the extremely loud noise levels. Sustained noise levels near the 5th percentile were caused by long periods of low speed winds without significant variation in the wind direction. Noise levels near the 95th percentile were also sustained for longer than a day when the regional wind field caused the ice pack to pile up against a land mass.

Temporal coherency for the annual noise record was between 12 and 23 hours at all frequencies, comparable to other data reported in the literature. The temporal coherency in winter was similar to the annual record, but was generally slightly shorter (although wider ranging) in the summer, ranging from 5-31 hours. Unexplained anomalous values were found in the Buoy 19 data at 5 Hz and 10 Hz.

Significant periodicities were found at synoptic time scales from 16-148 hours, and at tidal/inertial time scales from 10-12 hours, though these contained less than 15 percent of the energy of the synoptic periods. Significant

periodicities were also found at periods shorter than the tidal/inertial periods with energy levels less than 10 percent of the tidal/inertial energy. The three buoys exhibited identical periodicities in many cases at .32 Hz, implying that the three buoys were subject to the same forcing mechanisms despite separation distances of up to 300 km during the first year of the experiment.

The spatial coherency between the three buoys showed that the buoy pair closest together (Buoys 13 and 19), as expected, had the highest correlations. The difference in the correlation coefficients between this buoy pair and the other pairs was smaller at higher frequencies due to local effects being more important in the generation of the high frequency noise field.

Three environmental correlates of the noise field were determined and found to be frequency dependent. Ice speed was the best correlate with ambient noise from 5-10 Hz, wind speed was best from 32-100 Hz, and wind stress was best above 100 Hz.

The drift pattern for the three buoys showed that the buoys moved in unison throughout most of the experiment. In addition, the drift tracks divided themselves into five legs where the buoys drifted along generally persistent tracks. A comparison of the wind vectors and the buoy drift vectors showed that these legs were each in response to the wind direction remaining relatively steady for long periods. During each leg there were occasional large short term wind shifts that caused sufficient ice field convergence to generate unusually high noise levels.

B. RECOMMENDATIONS

Based on the results presented in this study, the following recommendations are made for improvements in subsequent research.

- More frequent and more accurate position data are needed for the ice speed and wind speed calculations. Future ANMET buoys should be equipped with the Global Positioning System rather than relying on the irregular time intervals of ARGOS fixes.
- The ANMET buoys should be modified to store the last few meteorological measurements, as they do with the noise measurements, to ensure more regular sampling intervals. Meteorological data should be recorded at the same time interval as the noise data.
- Larger clusters of buoys capable of sensing wind speed and direction would enable more accurate determination of the local wind field than the rough calculations required in this research. This would enable more precise determination of the factors affecting ice motion, and better document the effects of synoptic events propagating through the region.

APPENDIX A

DATA STATISTICS

Table XXI NOISE DATA SUMMARY FOR ANMET 12813

FREQUENCY (Hz)	RECORD LENGTH (DAYS)	RECORD LENGTH (HOURS)	MISSING OR BAD DATA (HOURS)	MISSING OR BAD DATA (PERCENT)
5	471	11281	767	6.8
10	471	11281	790	7.0
20	471	11281	778	6.9
32	471	11281	778	6.9
50	471	11281	778	6.9
100	471	11281	778	6.9
200	471	11281	778	6.9
500	471	11281	790	7.0
1000	471	11281	880	7.8
2000	471	11281	948	8.4
4000	471	11281	948	8.4

Table XXII NOISE DATA SUMMARY FOR ANMET 12815

FREQUENCY (Hz)	RECORD LENGTH (DAYS)	RECORD LENGTH (HOURS)	MISSING OR BAD DATA (HOURS)	MISSING OR BAD DATA (PERCENT)
5	376	9025	397	4.4
10	376	9025	469	5.2
20	376	9025	433	4.8
32	376	9025	415	4.6
50	376	9025	442	4.9
100	376	9025	451	5.0
200	37	9025	388	4.3
500	376	9025	379	4.2
1000	376	9025	433	4.8
2000	376	9025	542	6.0
4000	376	9025	523	5.8

Table XXIII NOISE DATA SUMMARY FOR ANMET 12819

FREQUENCY (Hz)	RECORD LENGTH (DAYS)	RECORD LENGTH (HOURS)	MISSING OR BAD DATA (HOURS)	MISSING OR BAD DATA (PERCENT)
5	592	14209	564	4.0
10	592	14209	567	4.0
20	592	14209	583	4.1
32	592	14209	575	4.1
50	592	14209	570	4.0
100	592	14209	605	4.3
200	592	14209	622	4.4
500	592	14209	635	4.5
1000	580	13921	635	4.5
2000	580	13921	792	5.7
4000	560	13441	511	3.8

Table XXIV MISSING NOISE DATA STATISTICS FOR ANMET 12813

GAP SIZE (HOURS)	NUMBER OF GAPS
1	178
2	37
3	37
4	10
5	12
6	6
7	7
8	3
9	2
10	2
12	1
14	1
19	1
20	1
24	1
64	1

Table XXV MISSING NOISE DATA STATISTICS FOR ANMET 12815

GAP SIZE (HOURS)	NUMBER OF GAPS
1	79
2	29
3	14
4	3
5	5
6	1
15	1
17	1
19	1
24	2
38	1

Table XXVI MISSING NOISE DATA STATISTICS FOR ANMET 12819

GAP SIZE (HOURS)	NUMBER OF GAPS
1	155
2	45
3	26
4	10
5	6
6	6
7	4
8	3
10	3
11	1
12	1
15	4
16	1
19	1
21	1
24	3
90	1
133	1

Table XXVII METEOROLOGICAL AND POSITION DATA GAP STATISTICS FOR BUOY 12813

METEOROLOGICAL DATA		POSITION DATA	
DATA INTERVAL (HOURS)	OCCURRENCES	DATA INTERVAL (HOURS)	OCCURRENCES
0 - 1	3110	0 - 1	6475
1 - 2	6493	1 - 2	6628
2 - 3	379	2 - 3	159
3 - 4	308	3 - 4	238
4 - 5	58	4 - 5	52
5 - 6	52	5 - 6	41
6 - 7	18	6 - 7	22
7 - 8	5	7 - 8	3
8 - 9	2	8 - 9	2
9 - 10	2	9 - 10	3
10 - 11	3	10 - 11	1
11 - 12	2	11 - 12	2
15 - 16	1	15 - 16	1
16 - 17	3	16 - 17	3
20 - 21	1	22 - 23	1
25 - 26	3	25 - 26	1
26 - 27	1	26 - 27	1
28 - 29	1	27 - 28	2
		28 - 29	2
RECORD LENGTH : 15,025 HOURS		RECORD LENGTH : 15,025 HOURS	
AVERAGE DATA RATE: 16.7 POINTS PER DAY		AVERAGE DATA RATE: 21.8 POINTS PER DAY	

Table XXVIII METEOROLOGICAL AND POSITION DATA GAP STATISTICS FOR BUOY 12815

METEOROLOGICAL DATA		POSITION DATA	
DATA INTERVAL (HOURS)	OCCURRENCES	DATA INTERVAL (HOURS)	OCCURRENCES
0 - 1	2470	0 - 1	5273
1 - 2	5129	1 - 2	5177
2 - 3	238	2 - 3	96
3 - 4	212	3 - 4	144
4 - 5	46	4 - 5	33
5 - 6	50	5 - 6	48
6 - 7	38	6 - 7	38
7 - 8	13	7 - 8	10
8 - 9	9	8 - 9	7
10 - 11	2	9 - 10	21
15 - 16	1	10 - 11	11
17 - 18	1	15 - 16	11
18 - 19	1	16 - 17	1
20 - 21	1	18 - 19	1
25 - 26	2	22 - 23	1
28 - 29	1	25 - 26	2
		27 - 28	1
		28 - 29	1
RECORD LENGTH : 11857 HOURS		RECORD LENGTH : 11857 HOURS	
AVERAGE DATA RATE: 16.6 POINTS PER DAY		AVERAGE DATA RATE: 21.9 POINTS PER DAY	

Table XXIX METEOROLOGICAL AND POSITION DATA GAP STATISTICS FOR BUOY 12819

METEOROLOGICAL DATA		POSITION DATA	
DATA INTERVAL (HOURS)	OCCURRENCES	DATA INTERVAL (HOURS)	OCCURRENCES
0 - 1	3372	0 - 1	7004
1 - 2	6518	1 - 2	6613
2 - 3	316	2 - 3	102
3 - 4	221	3 - 4	138
4 - 5	26	4 - 5	15
5 - 6	27	5 - 6	32
6 - 7	8	6 - 7	8
7 - 8	4	7 - 8	4
8 - 9	5	8 - 9	6
9 - 10	1	9 - 10	2
10 - 11	4	10 - 11	3
11 - 12	2	11 - 12	3
12 - 13	1	13 - 14	1
13 - 14	1	14 - 15	1
14 - 15	1	15 - 16	1
15 - 16	1	16 - 17	4
16 - 17	4	17 - 18	1
17 - 18	1	21 - 22	1
21 - 22	1	25 - 26	4
25 - 26	3	113 - 114	1
113 - 114	1	135 - 136	1
135 - 136	1		
RECORD LENGTH : 14,641 HOURS		RECORD LENGTH : 14,641 HOURS	
AVERAGE DATA RATE: 17.2 POINTS PER DAY		AVERAGE DATA RATE: 22.9 POINTS PER DAY	

APPENDIX B

EVENT #1 WEATHER CHARTS

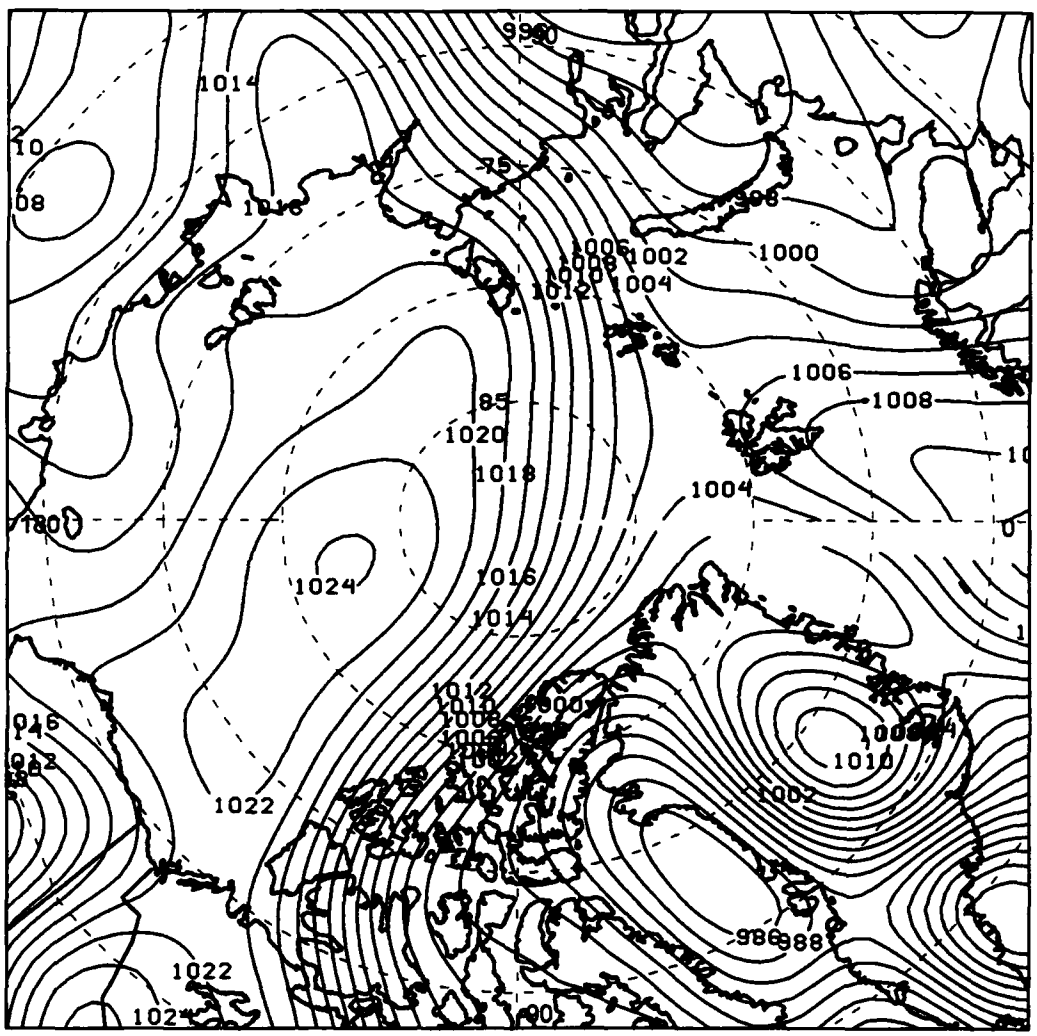

Figure 26. 1000 mb pressure field and fronts for 28 January 1993, 0000Z.

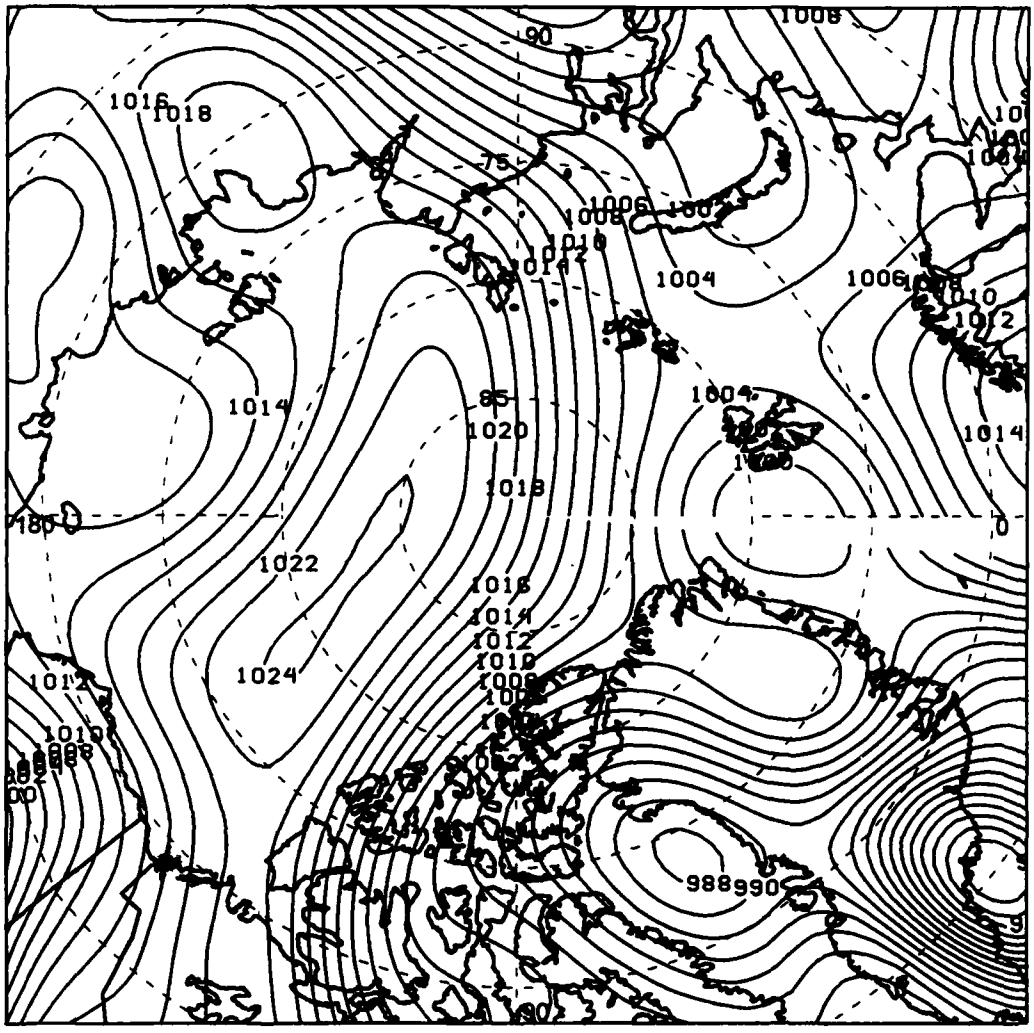

Figure 27. 1000 mb pressure field and fronts for 28 January 1993, 1200Z.

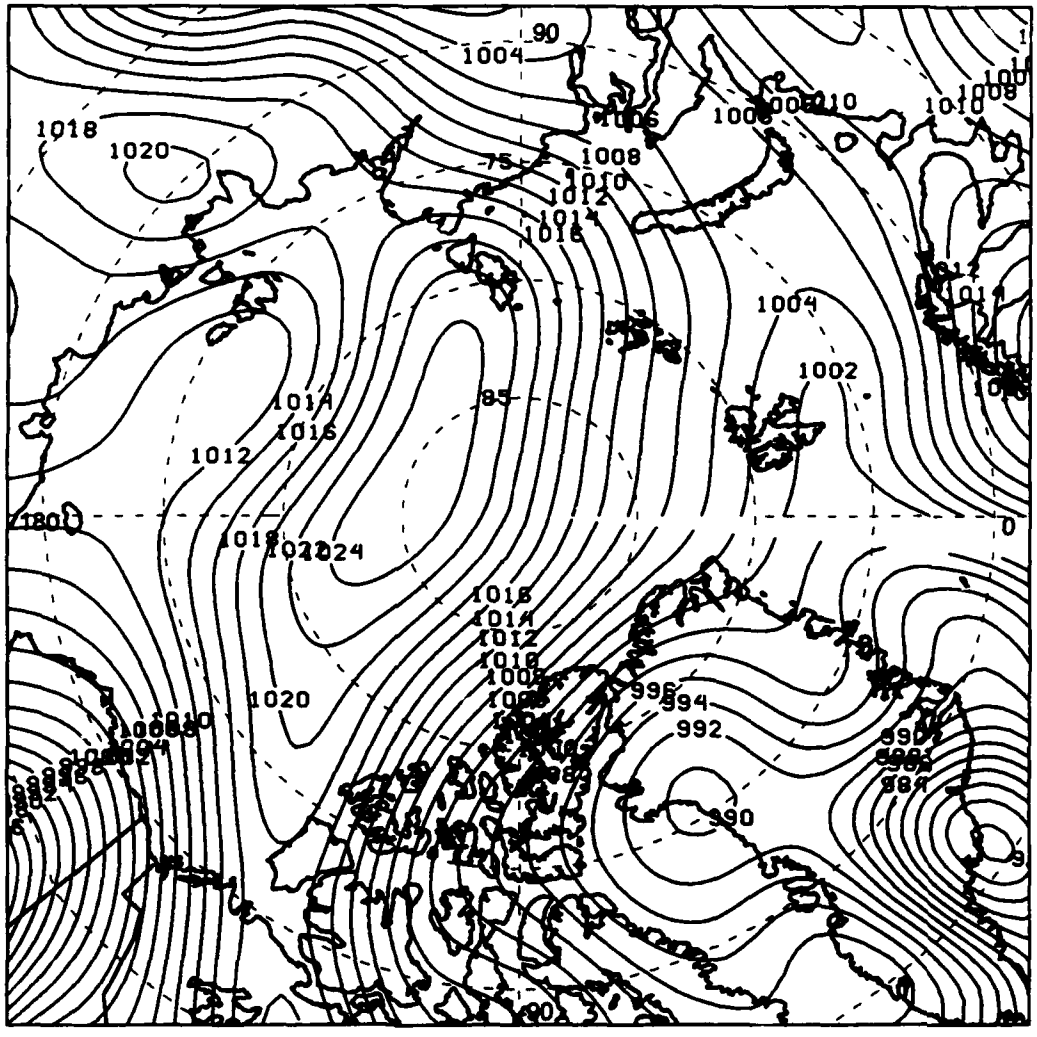

Figure 28. 1000 mb pressure field and fronts for 29 January 1993, 0000Z.

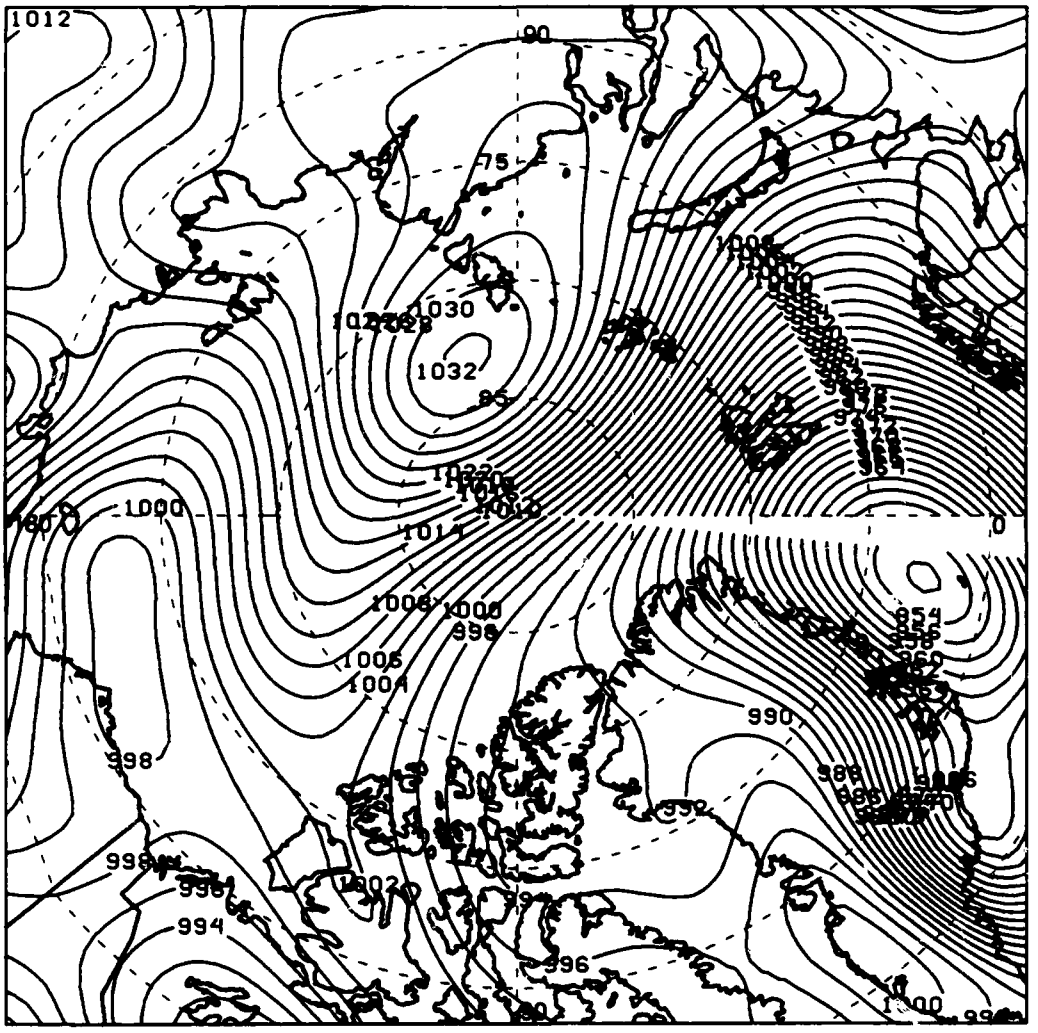

Figure 29. 1000 mb pressure field and fronts for 29 January 1993, 1200Z.

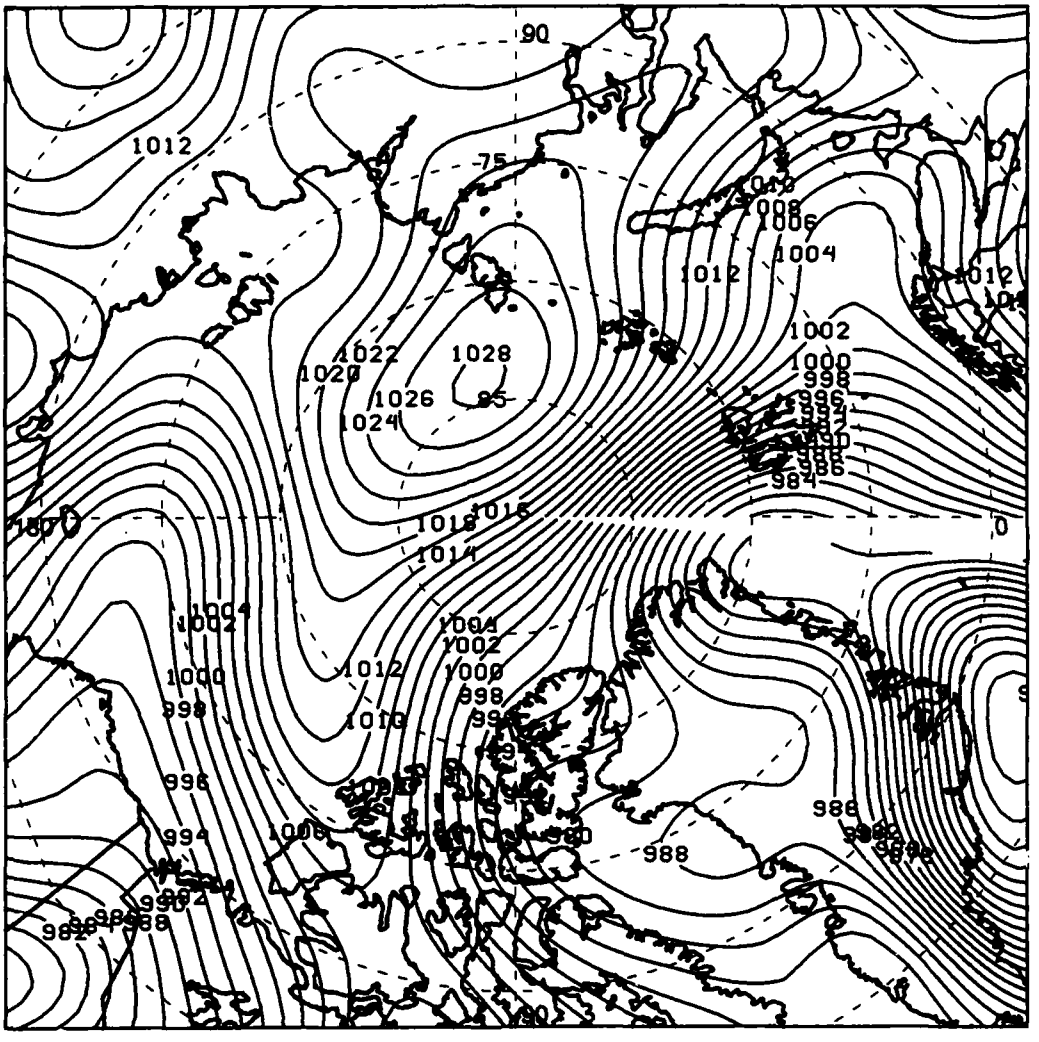

Figure 30. 1000 mb pressure field and fronts for 30 January 1993, 0000Z.

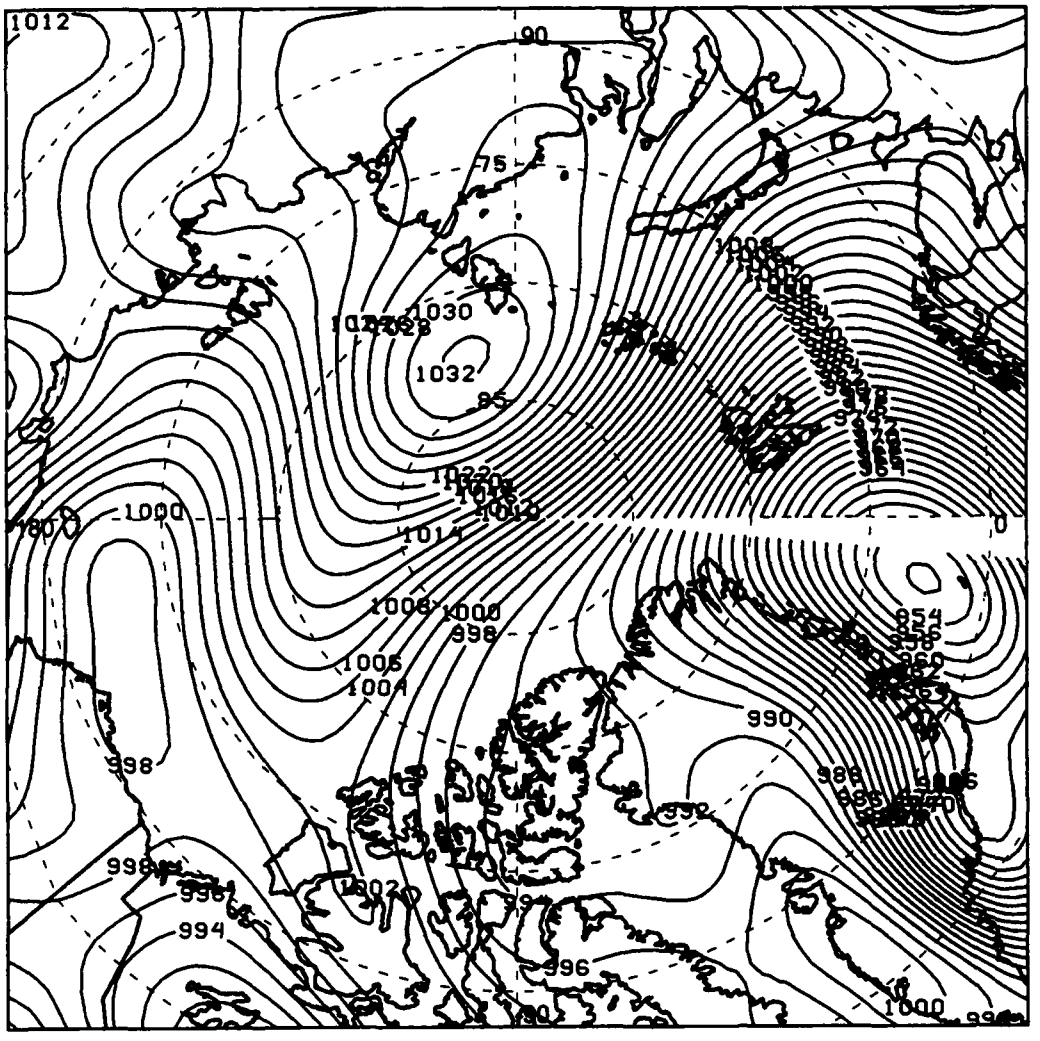

Figure 31. 1000 mb pressure field and fronts for 30 January 1993, 1200Z.

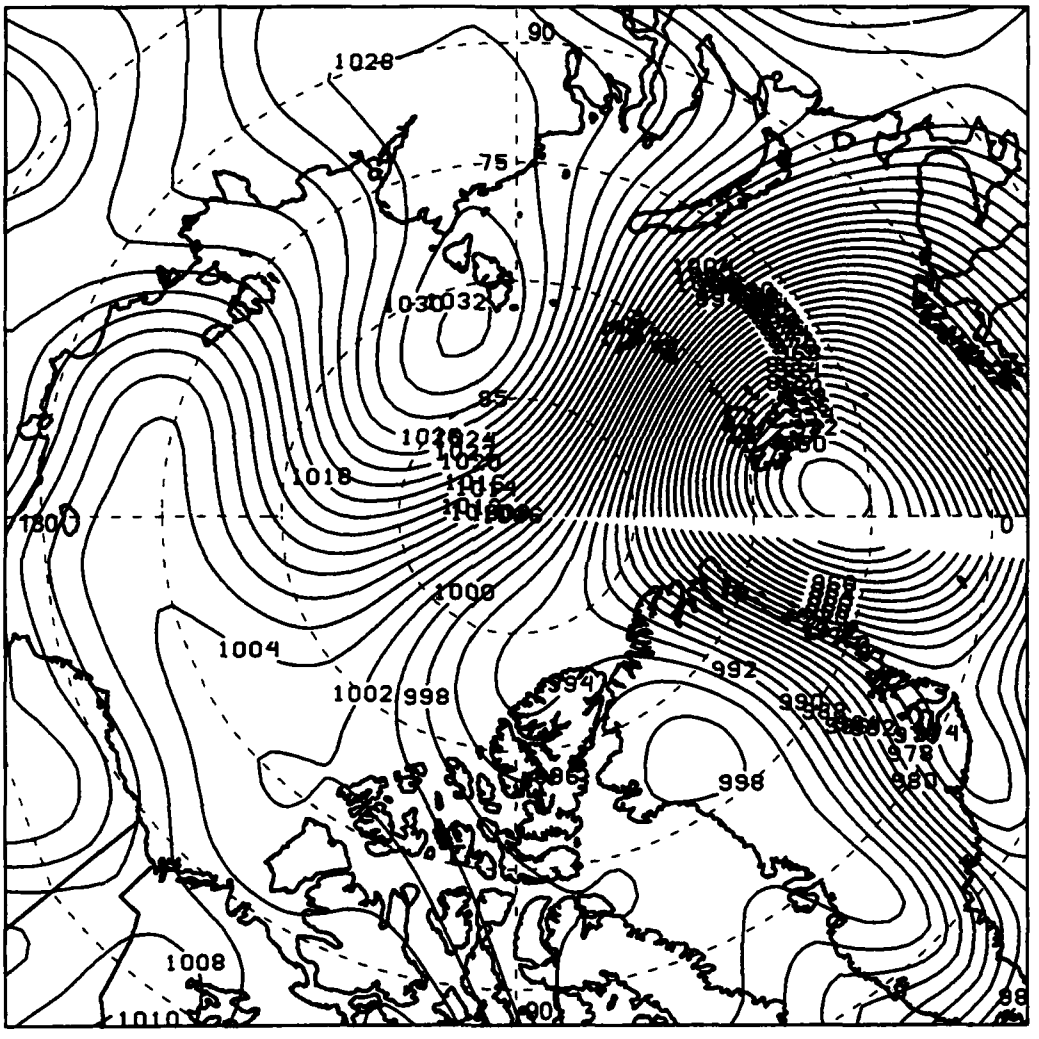

Figure 32. 1000 mb pressure field and fronts for 31 January 1993, 0000Z.

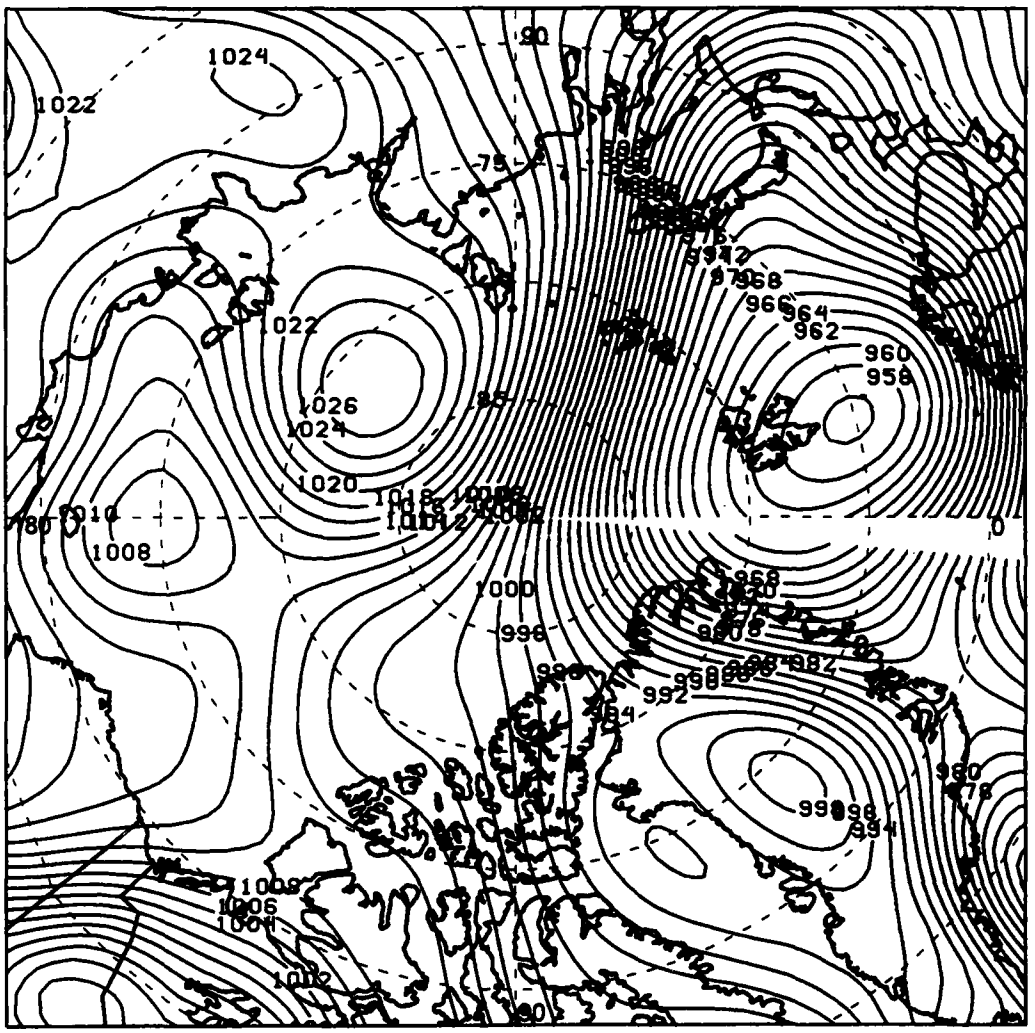

Figure 33. 1000 mb pressure field and fronts for 31 January 1993, 1200Z.

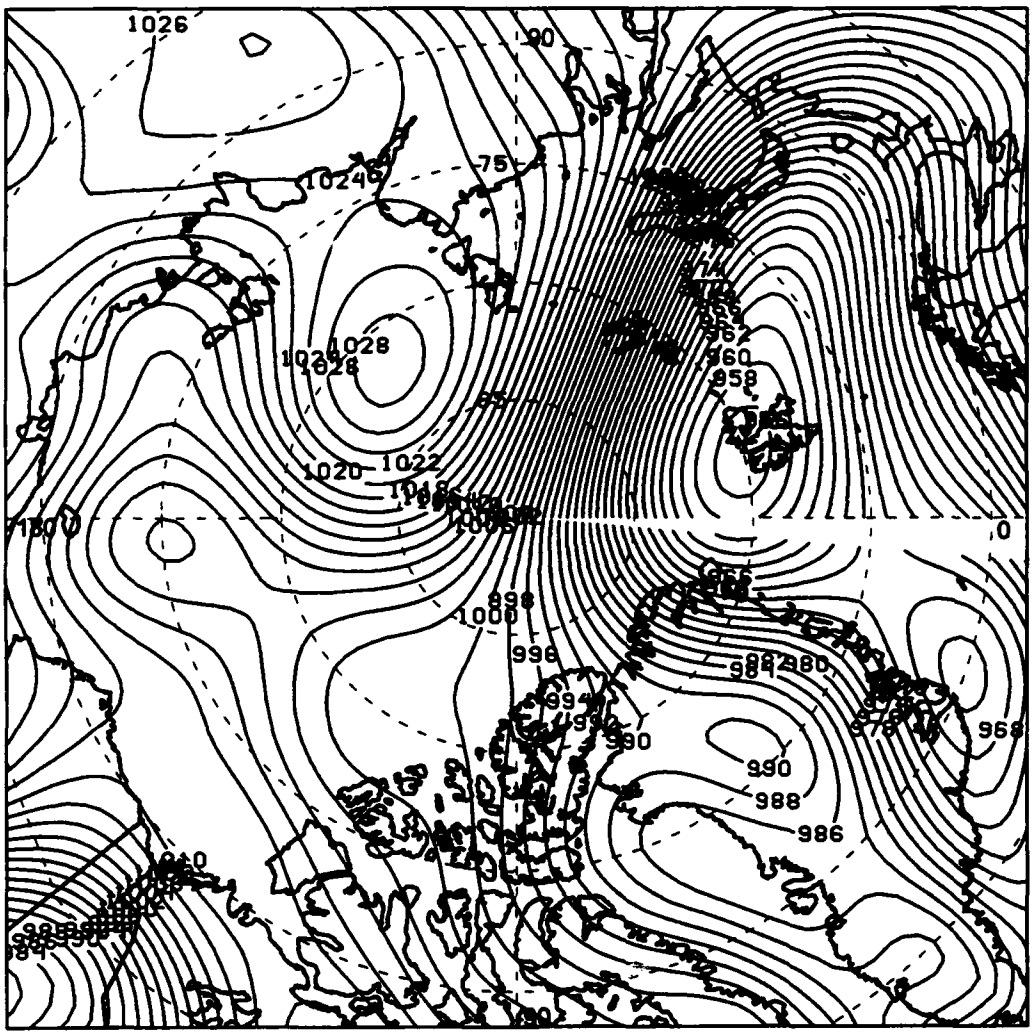

Figure 34. 1000 mb pressure field and fronts for 1 February 1993, 0000Z.

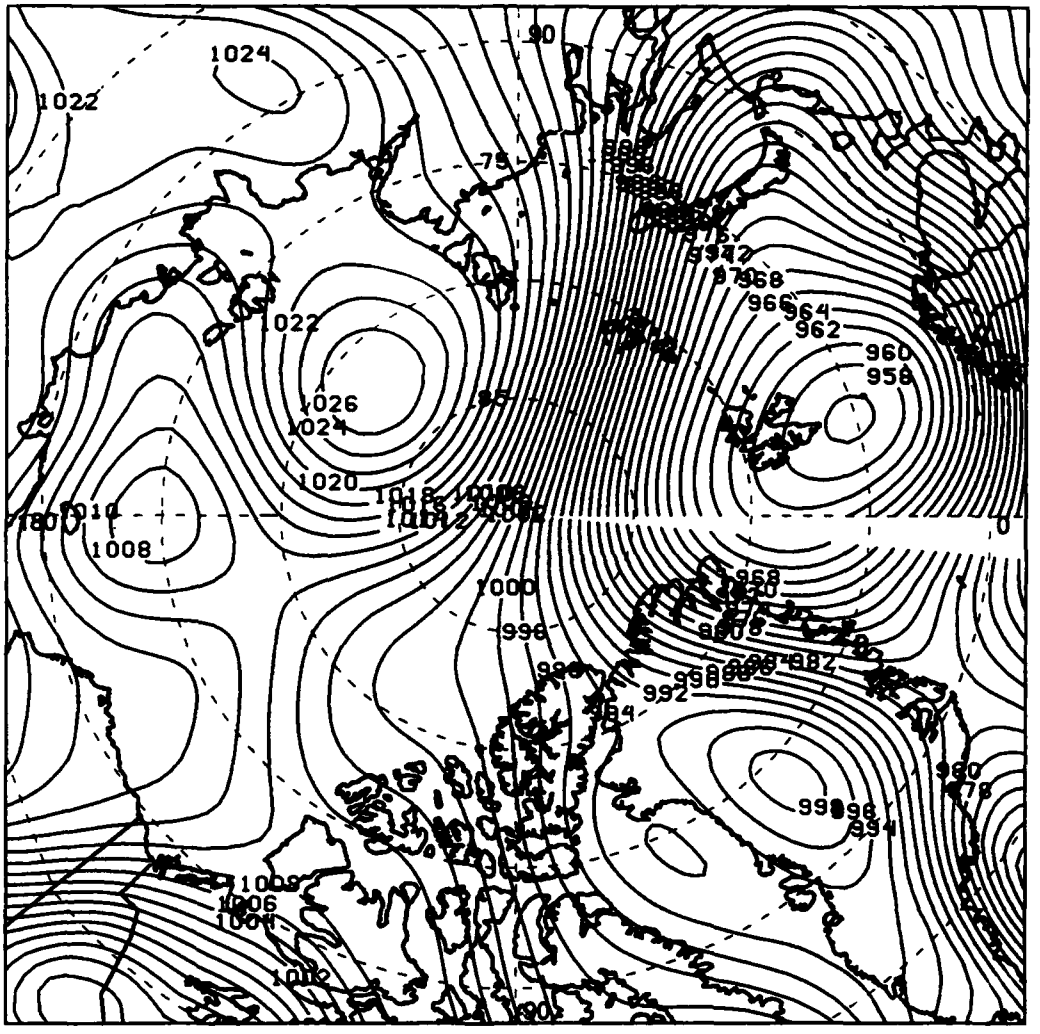

Figure 35. 1000 mb pressure field and fronts for 1 February 1993, 1200Z.

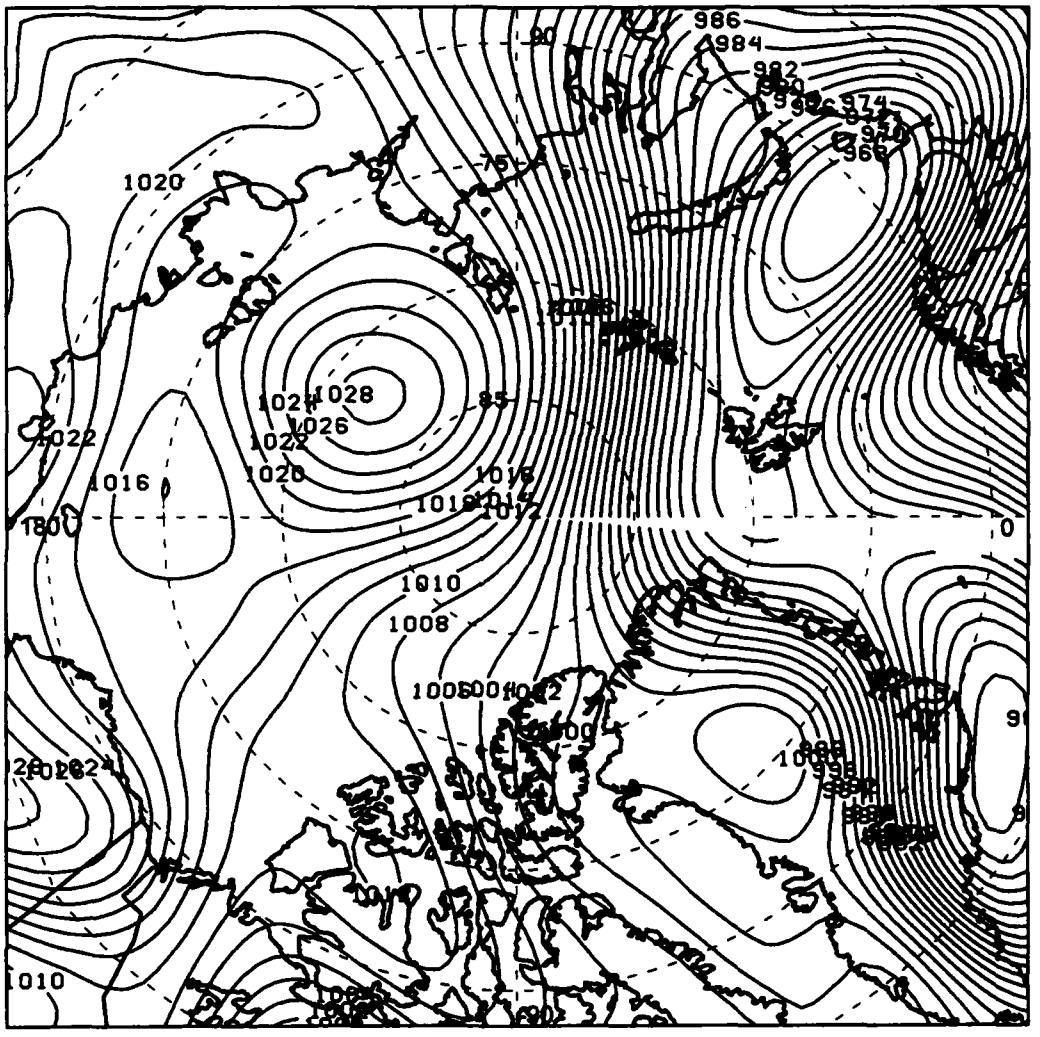

Figure 36. 1000 mb pressure field and fronts for 2 February 1993, 0000Z.

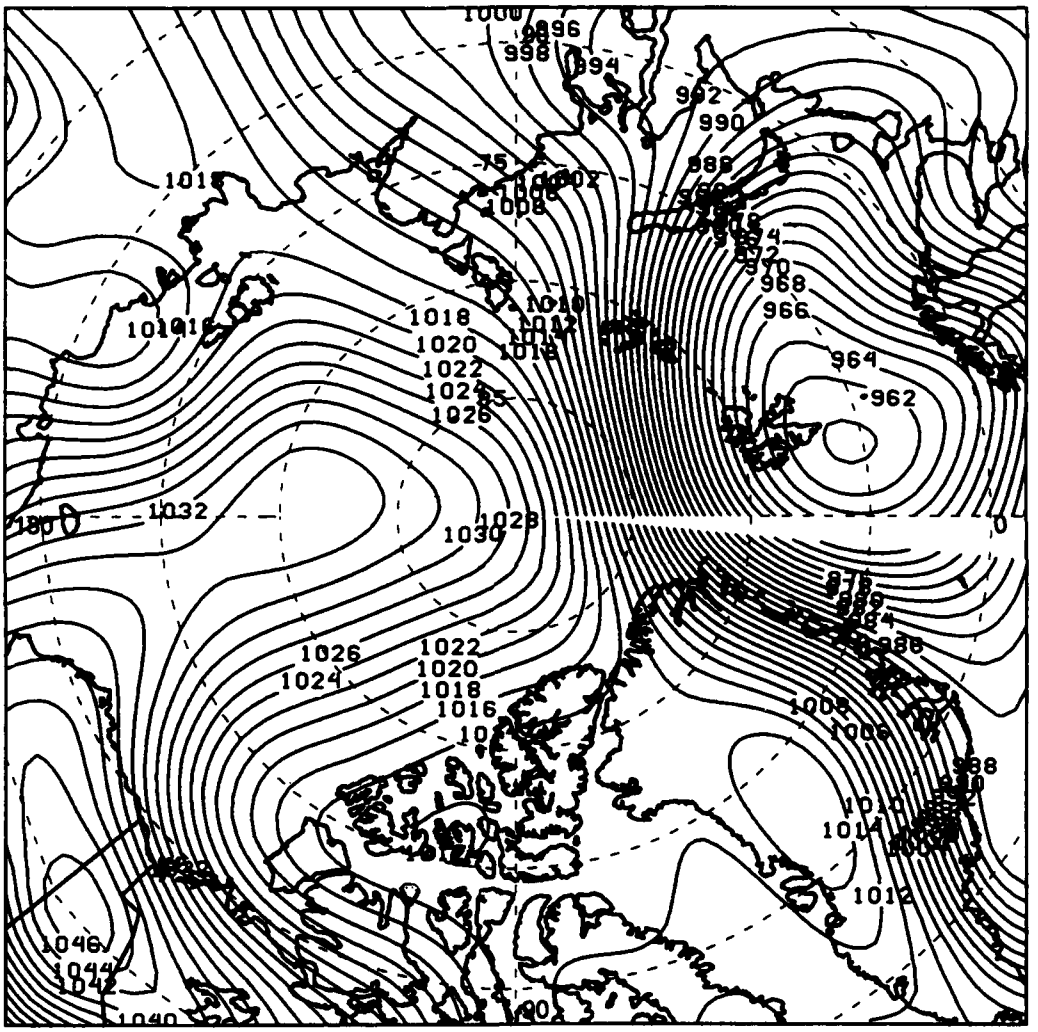

Figure 37. 1000 mb pressure field and fronts for 2 February 1993, 1200Z.

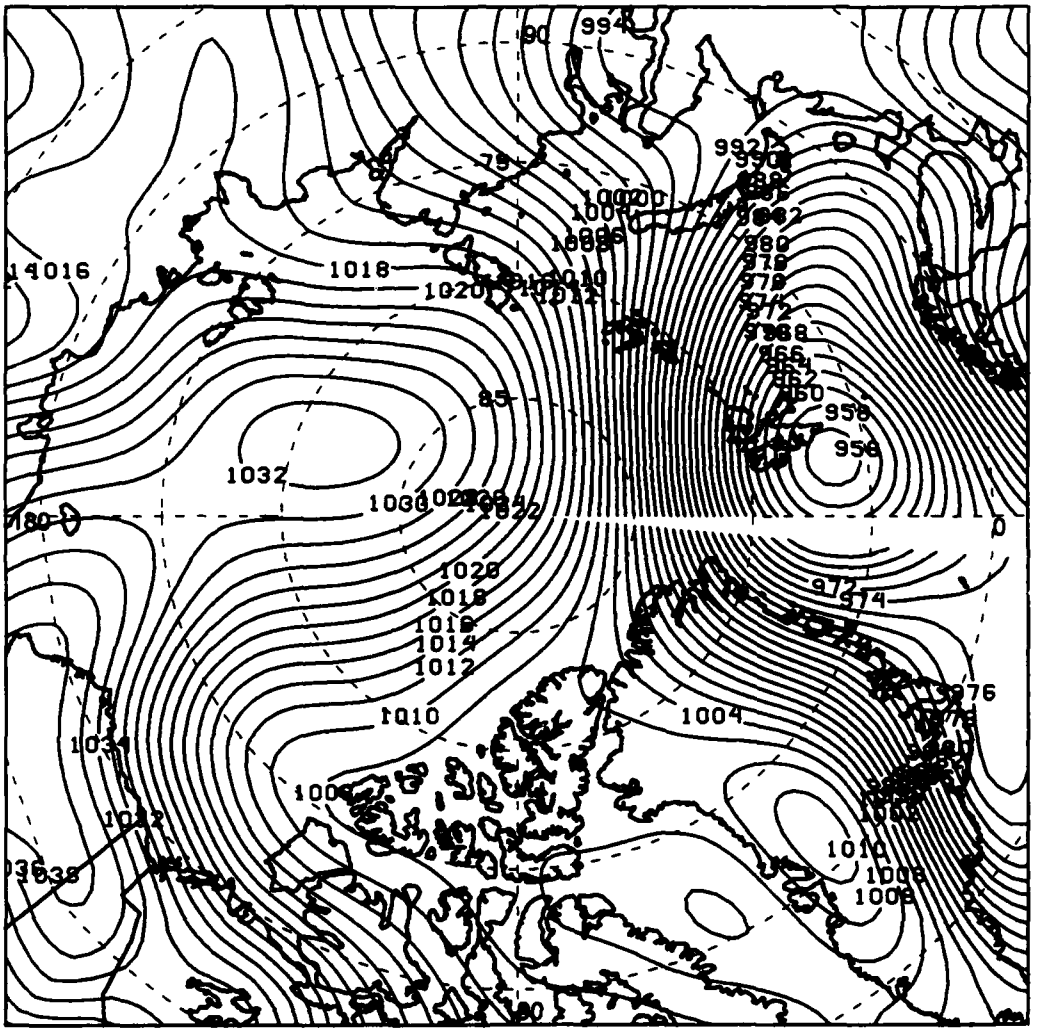

Figure 38. 1000 mb pressure field and fronts for 3 February 1993, 0000Z.

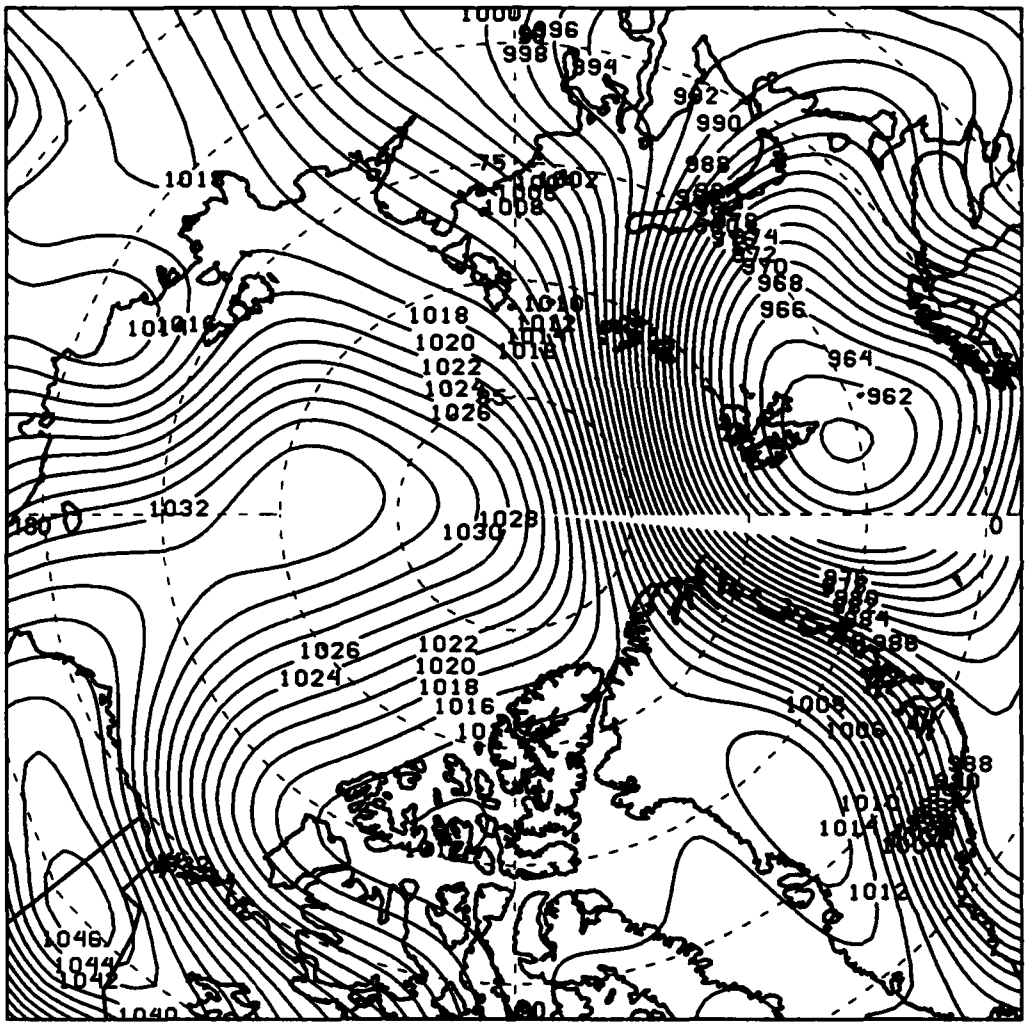

Figure 39. 1000 mb pressure field and fronts for 3 February 1993, 1200Z.

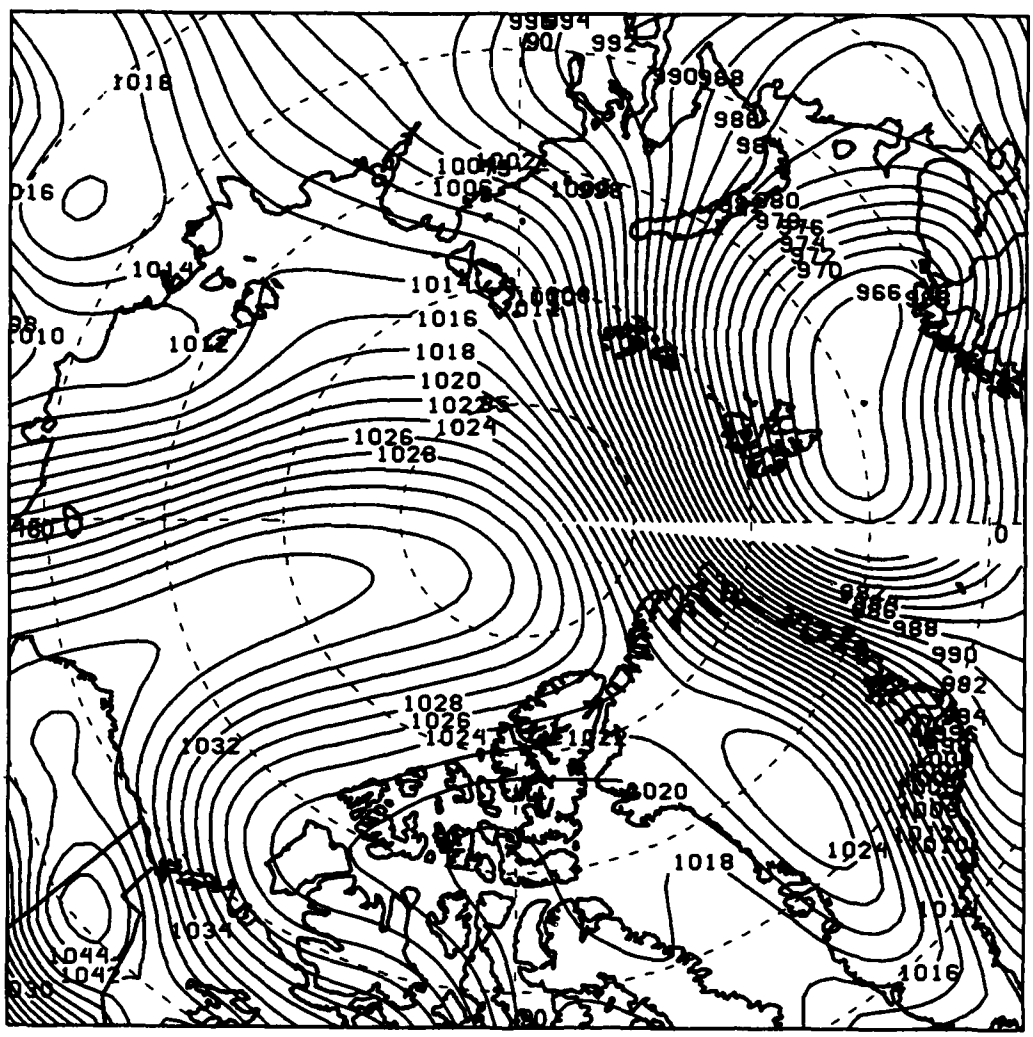

Figure 40. 1000 mb pressure field and fronts for 4 February 1993, 0000Z.

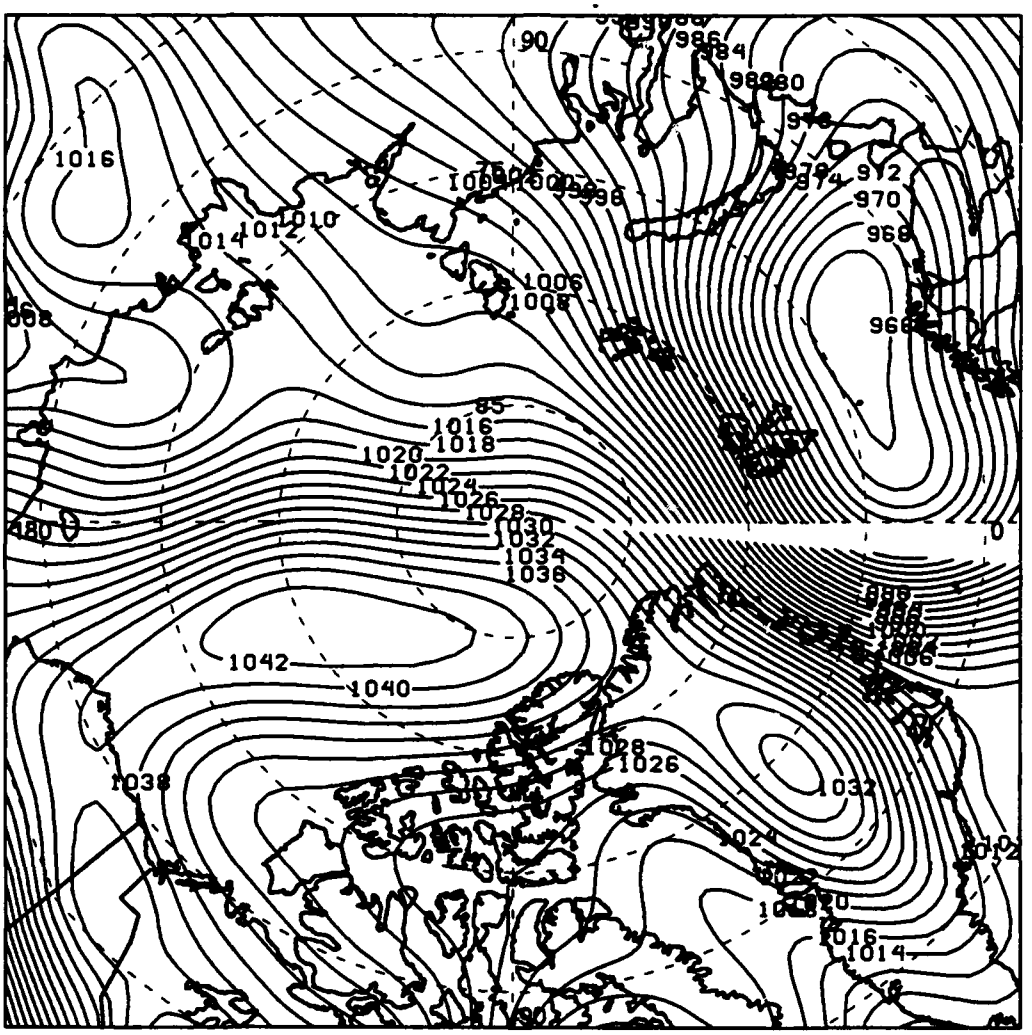

Figure 41. 1000 mb pressure field and fronts for 4 February 1993, 1200Z.

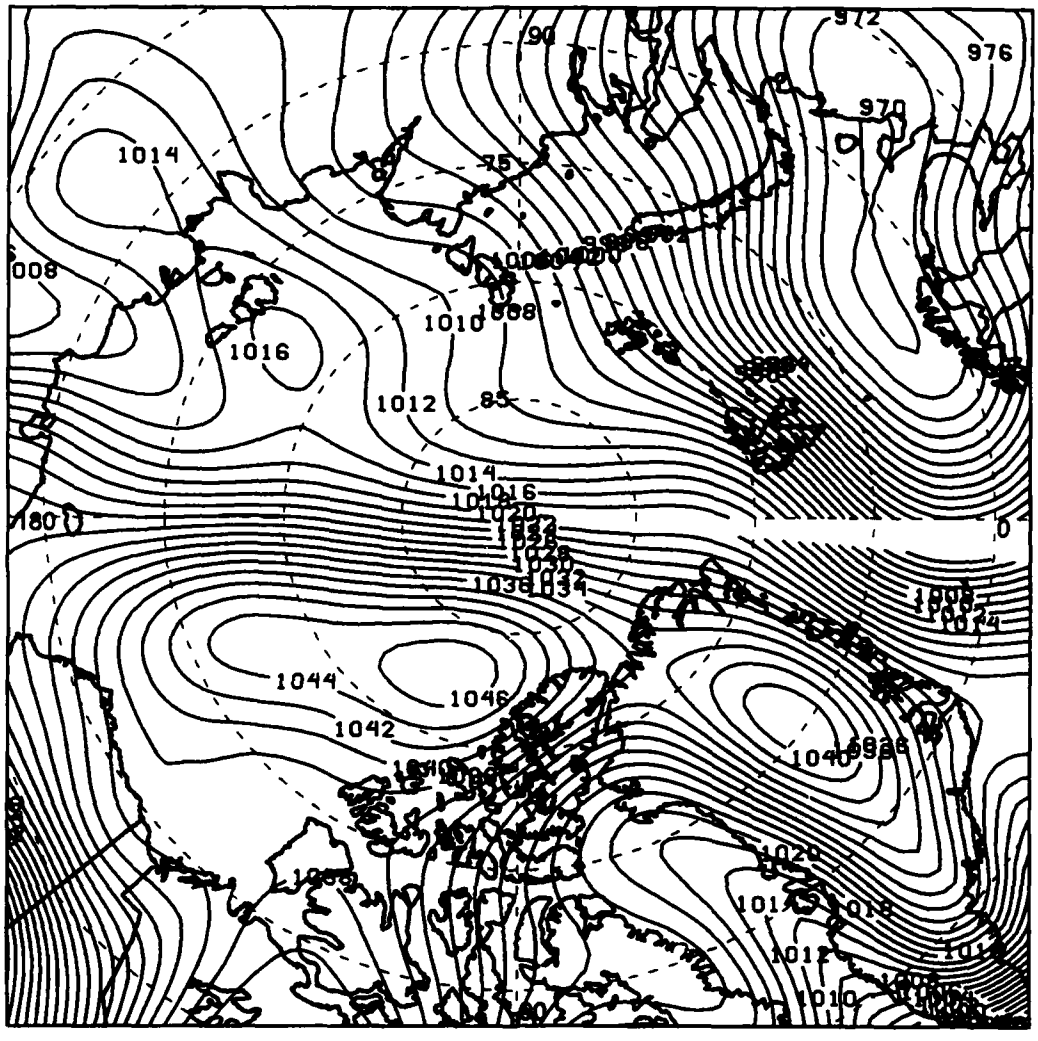

Figure 42. 1000 mb pressure field and fronts for 5 February 1993, 0000Z.

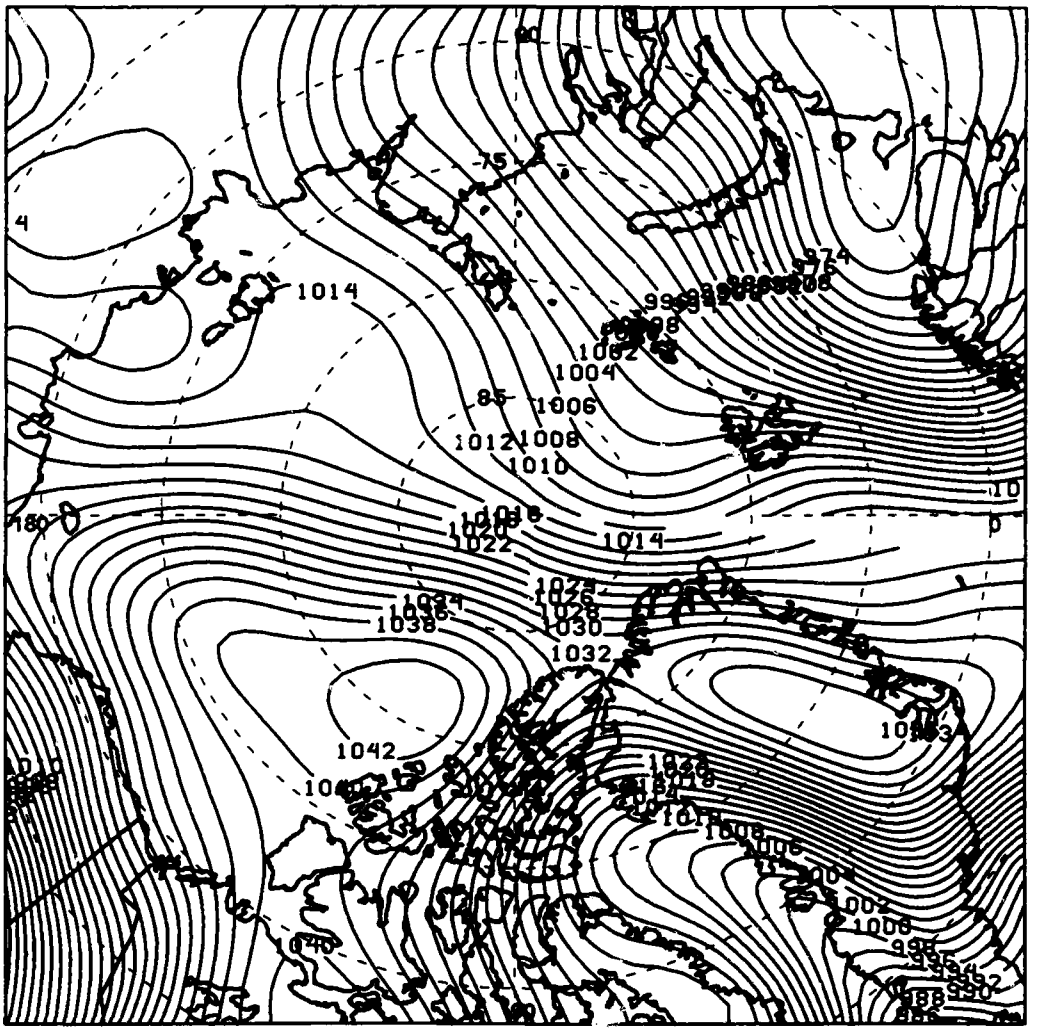

Figure 43. 1000 mb pressure field and fronts for 5 February 1993, 1200Z.

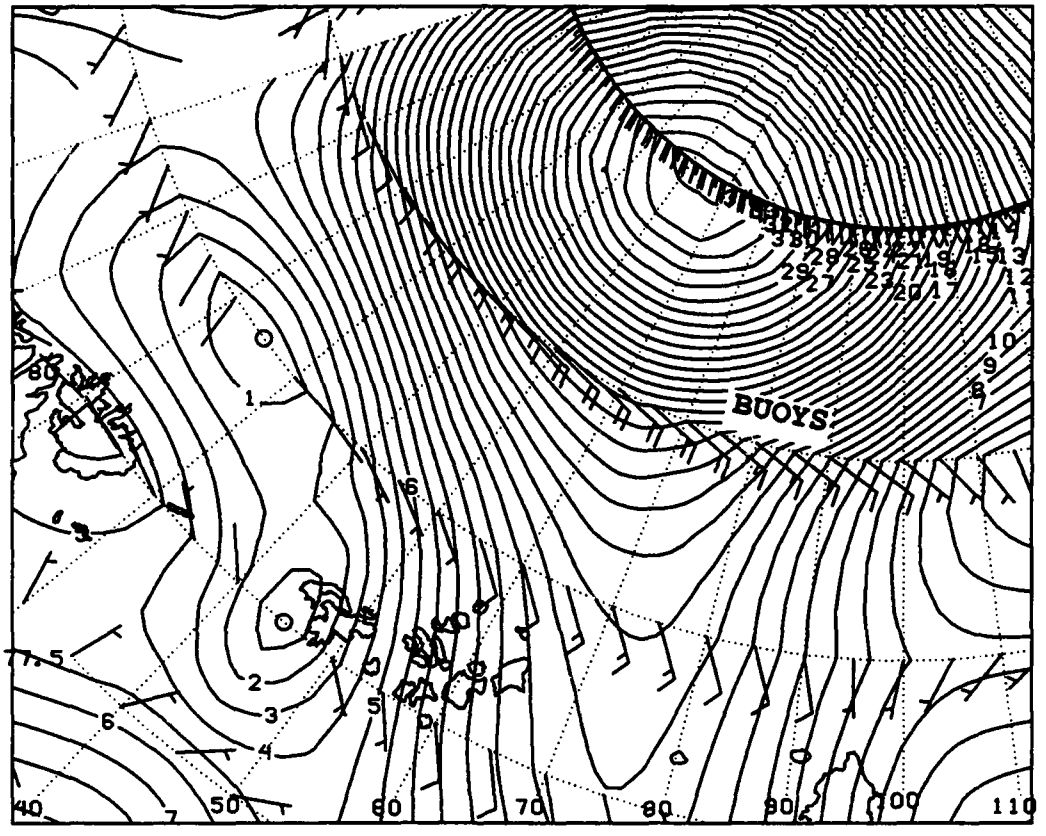

Figure 44. 1000 mb isotachs (m/s) and wind barbs for 28 January 1993, 0000Z.

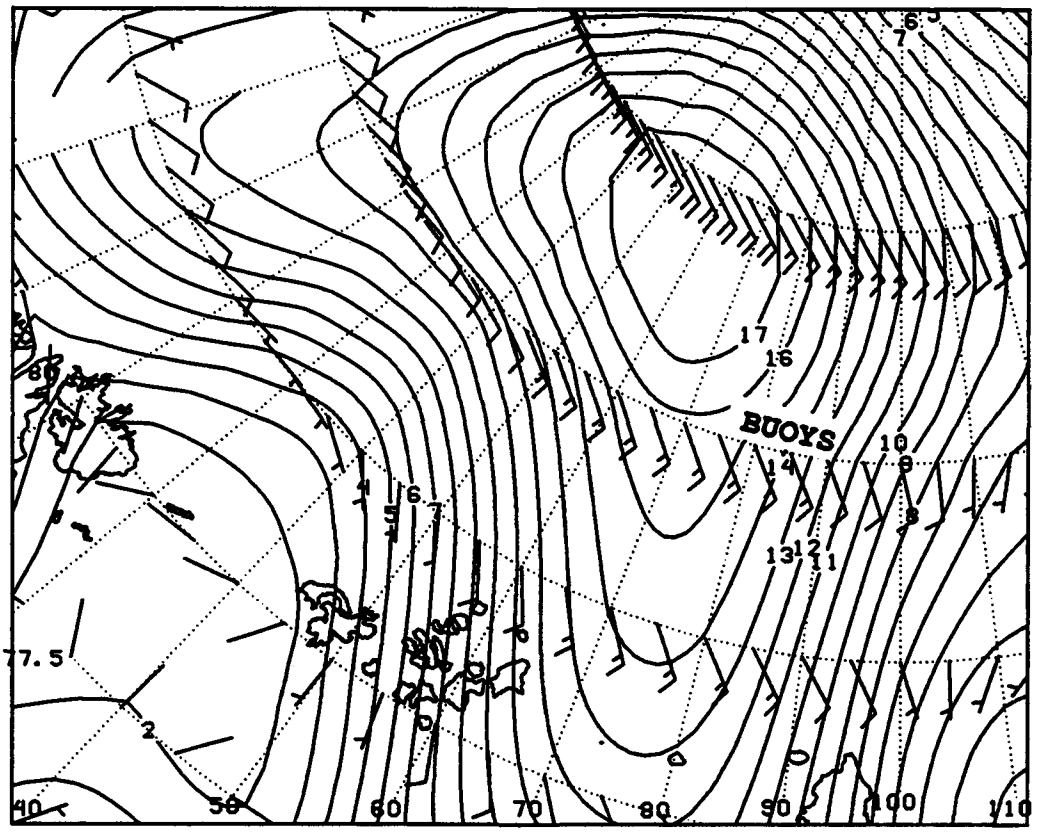

Figure 45. 1000 mb isotachs (m/s) and wind barbs for 28 January 1993, 1200Z.

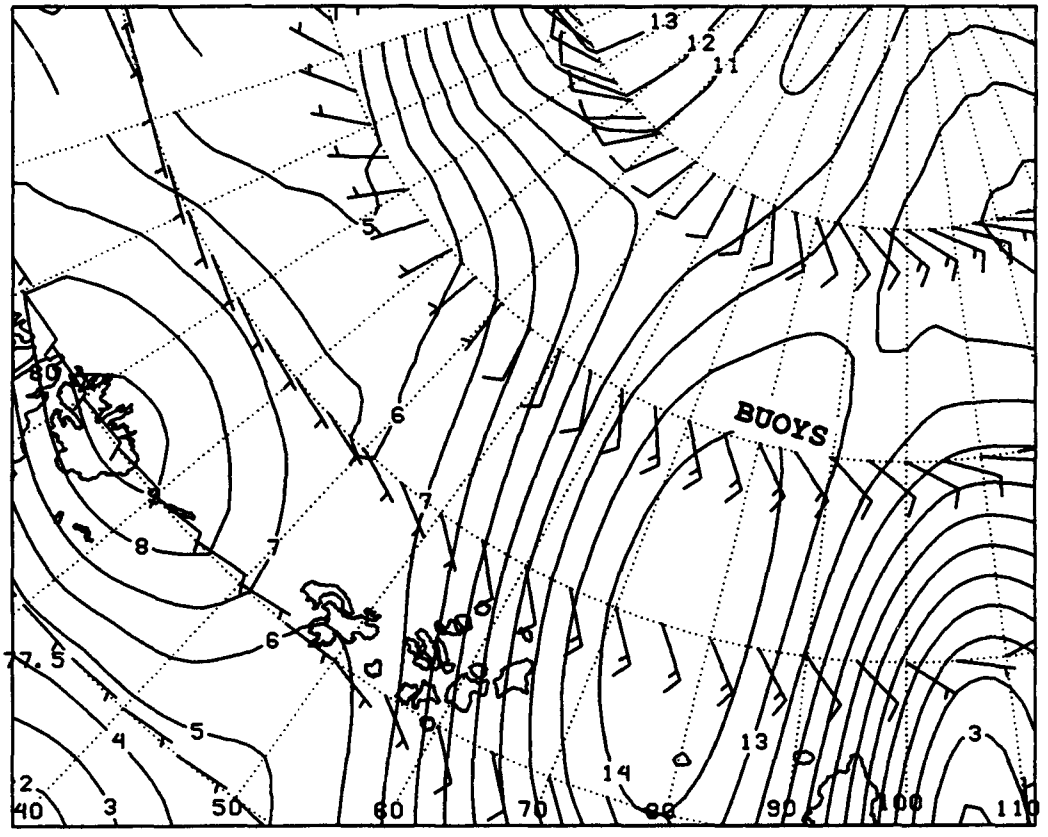

Figure 46. 1000 mb isotachs (m/s) and wind barbs for 29 January 1993, 0000Z.

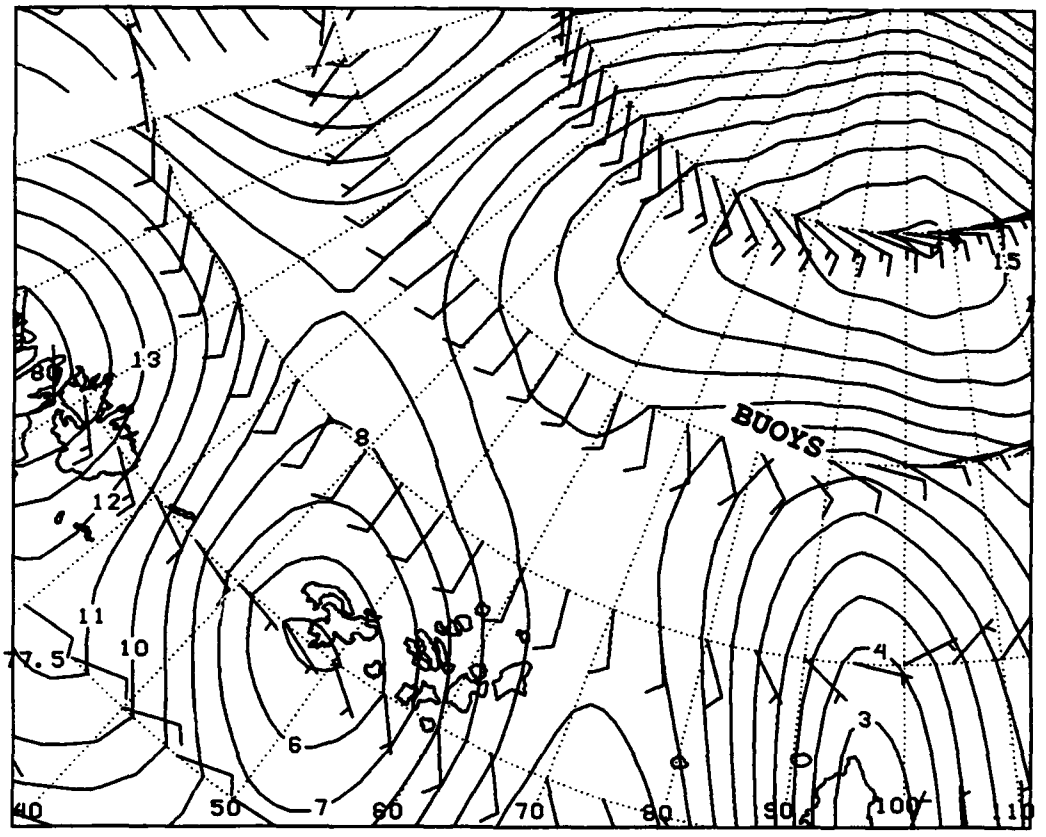

Figure 47. 1000 mb isotachs (m/s) and wind barbs for 29 January 1993, 1200Z.

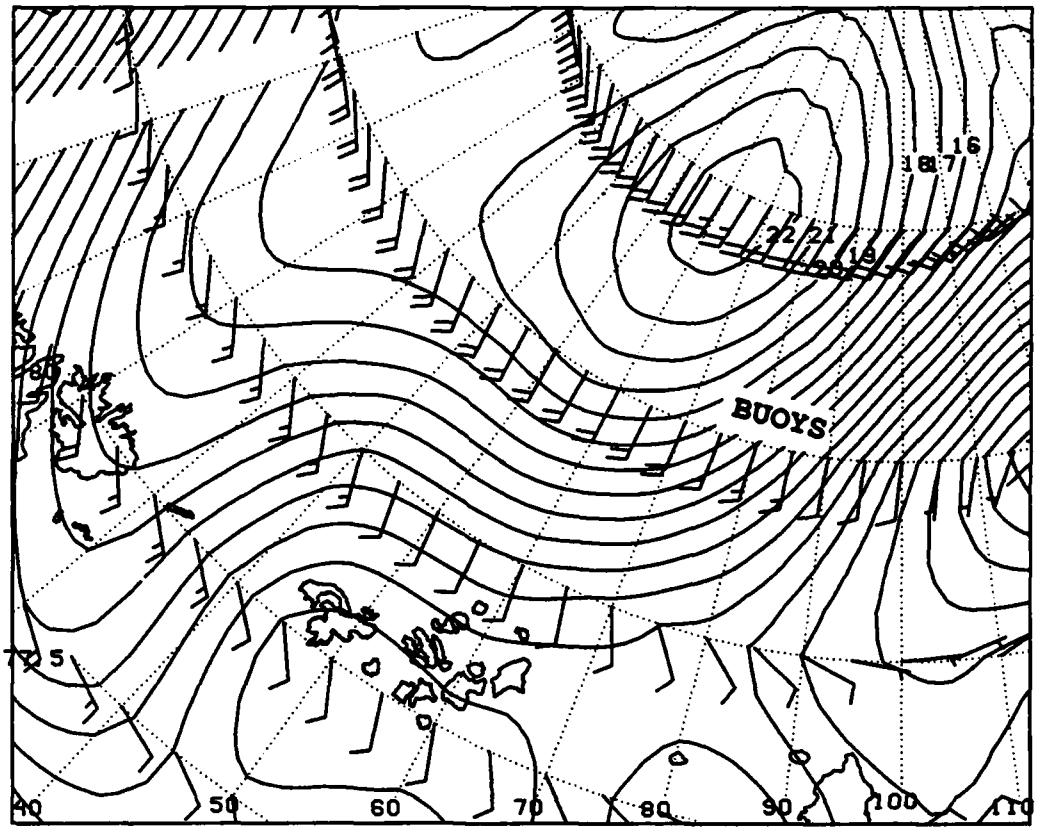

Figure 48. 1000 mb isotachs (m/s) and wind barbs for 30 January 1993, 0000Z.

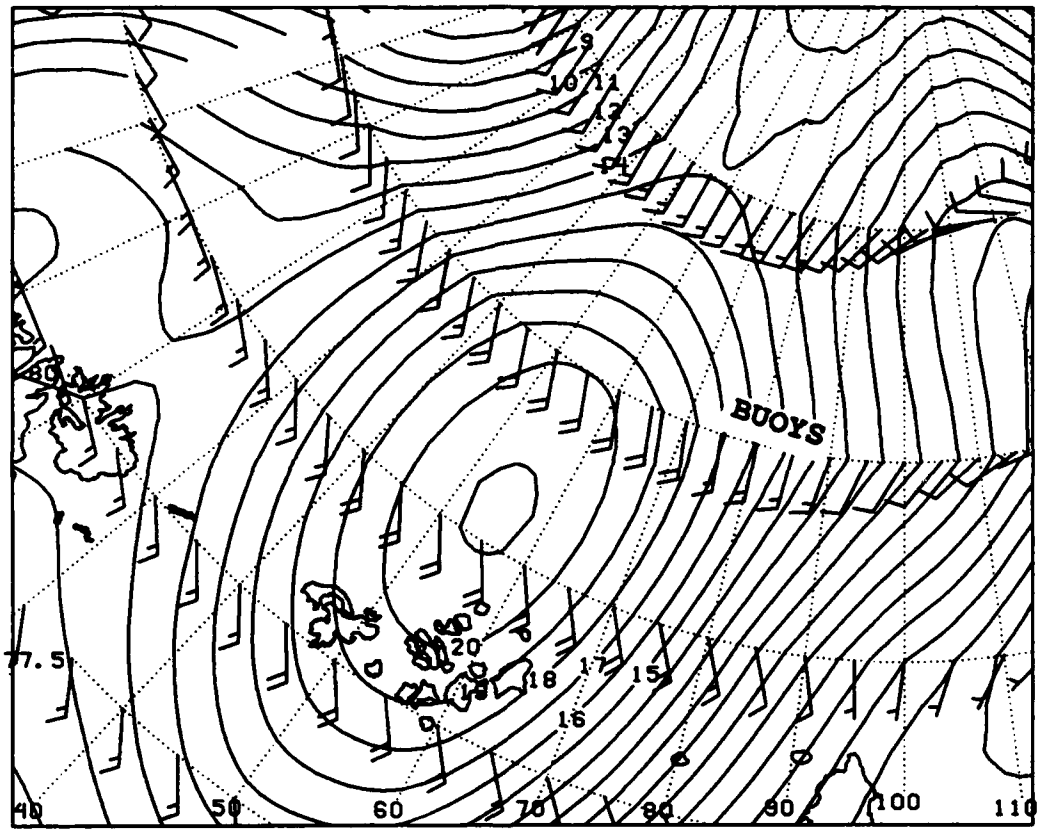

Figure 49. 1000 mb isotachs (m/s) and wind barbs for 30 January 1993, 1200Z.

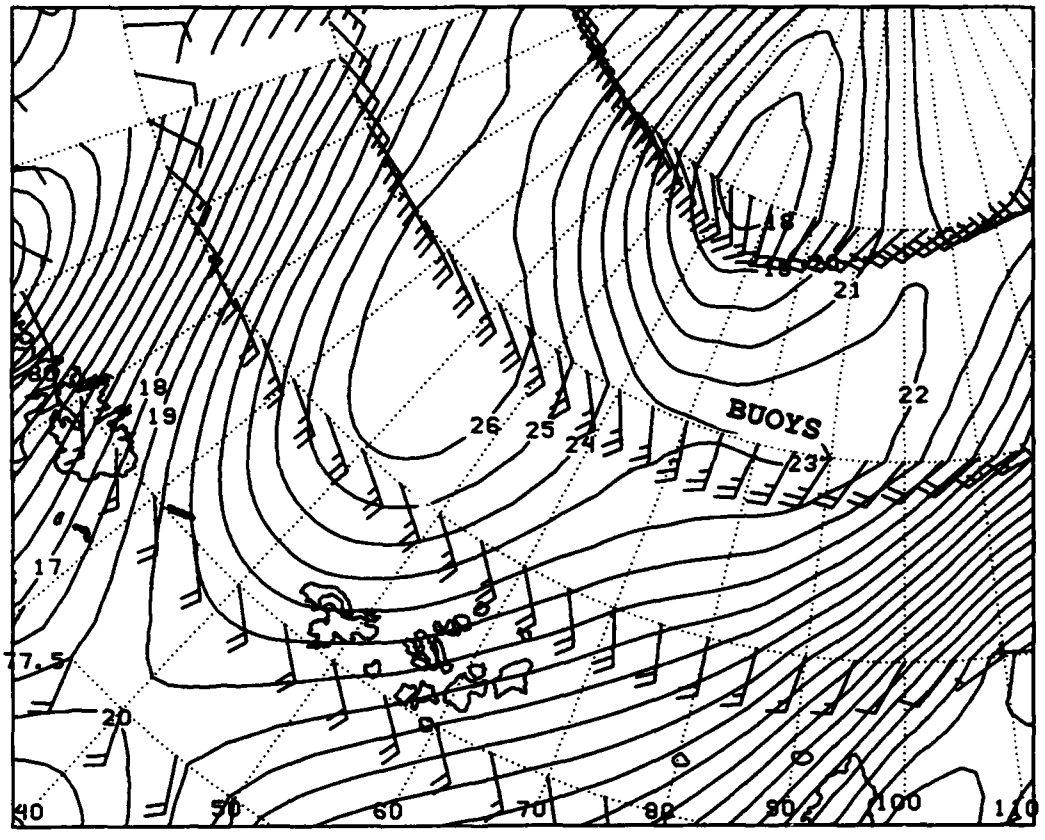

Figure 50. 1000 mb isotachs (m/s) and wind barbs for 31 January 1993, 0000Z.

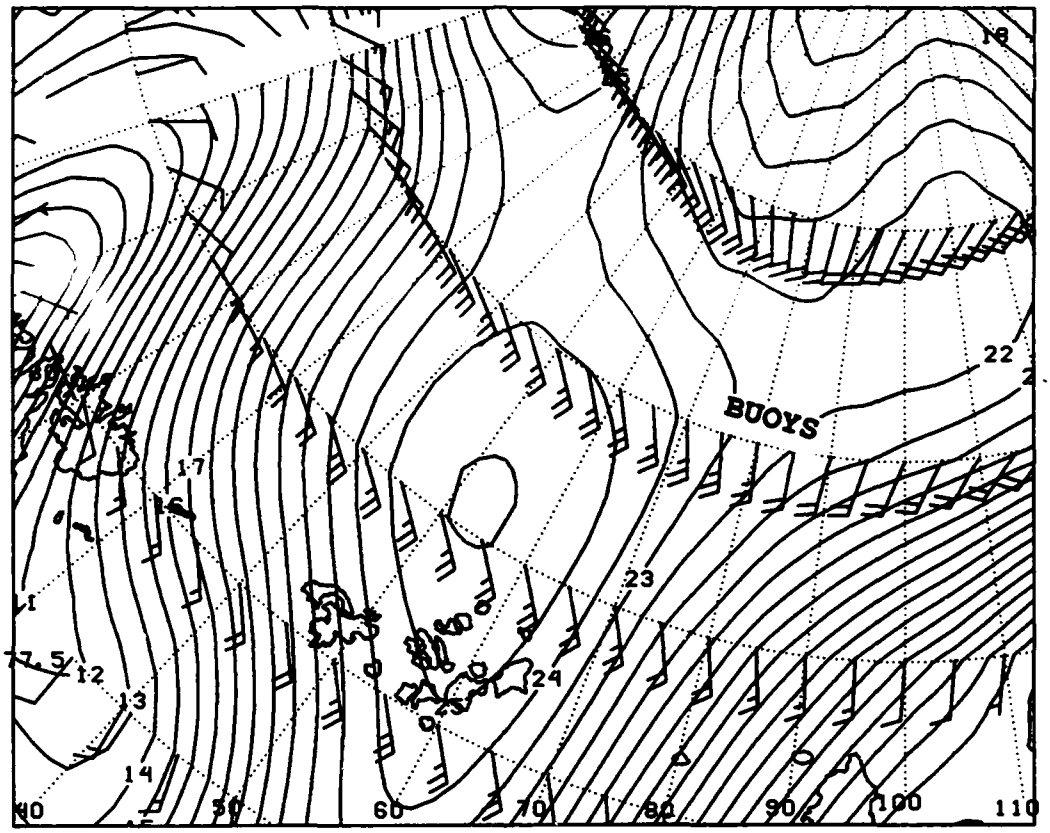

Figure 51. 1000 mb isotachs (m/s) and wind barbs for 31 January 1993, 1200Z.

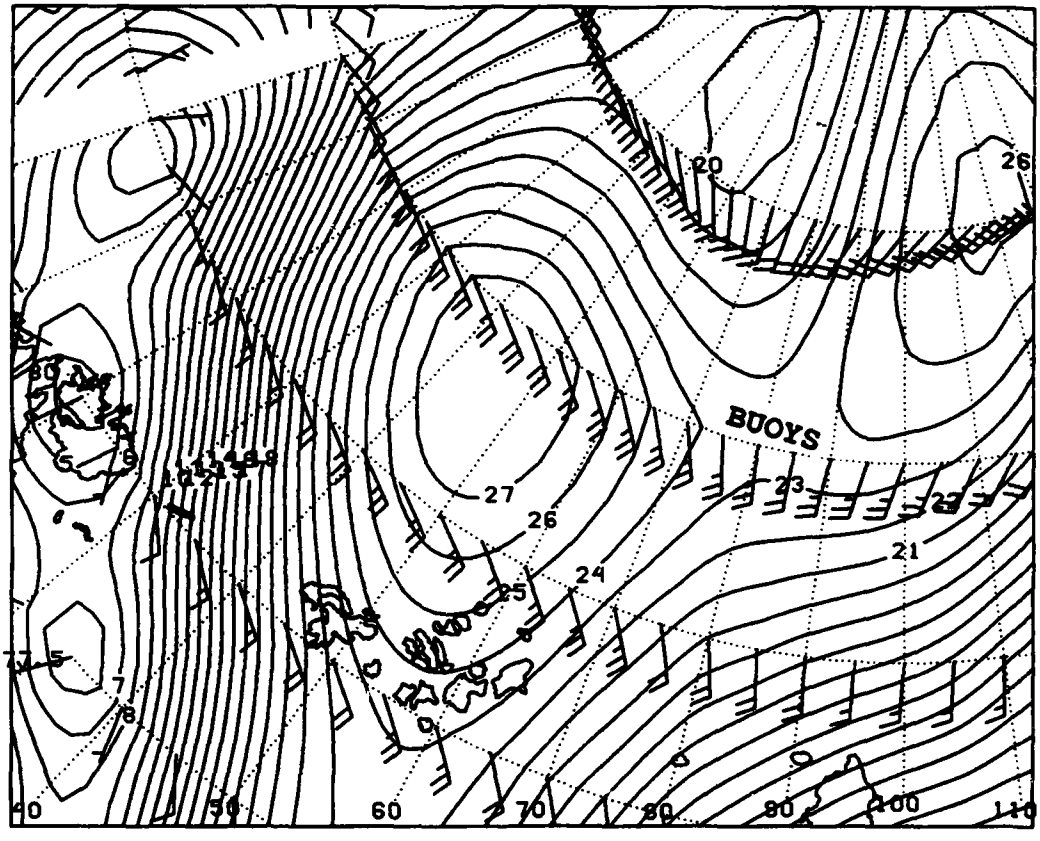

Figure 52. 1000 mb isotachs (m/s) and wind barbs for 1 February 1993, 0000Z.

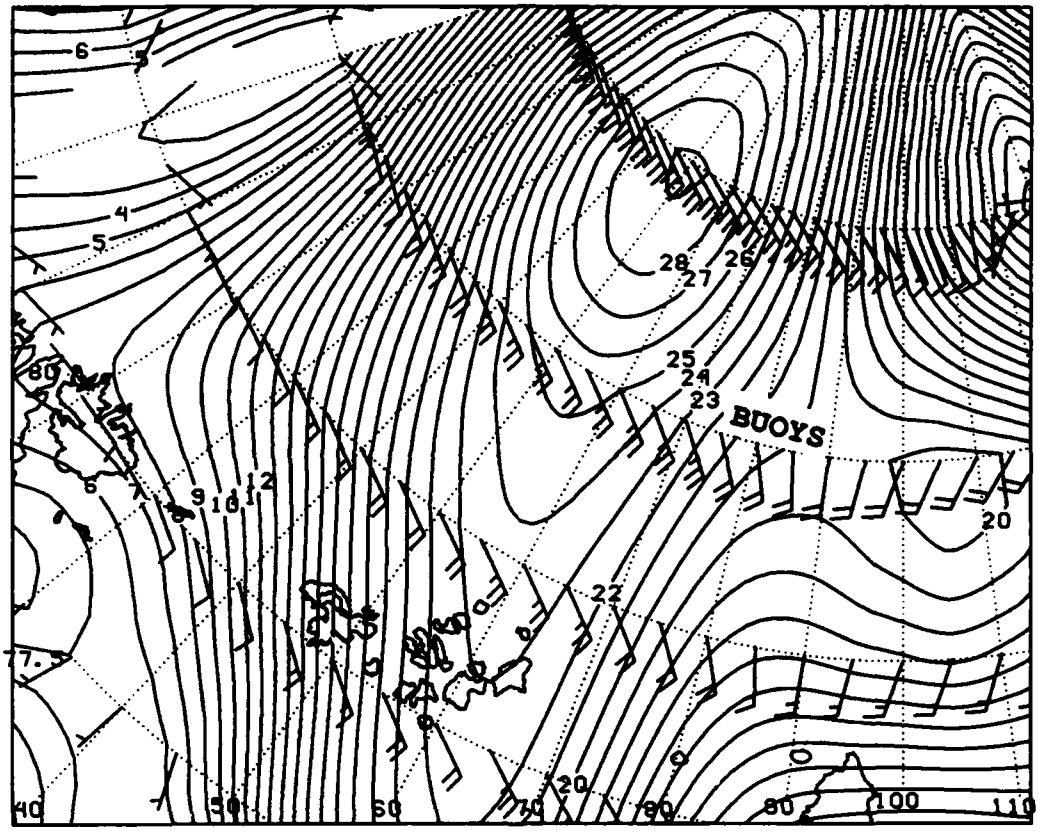

Figure 53. 1000 mb isotachs (m/s) and wind barbs for 1 February 1993, 1200Z.

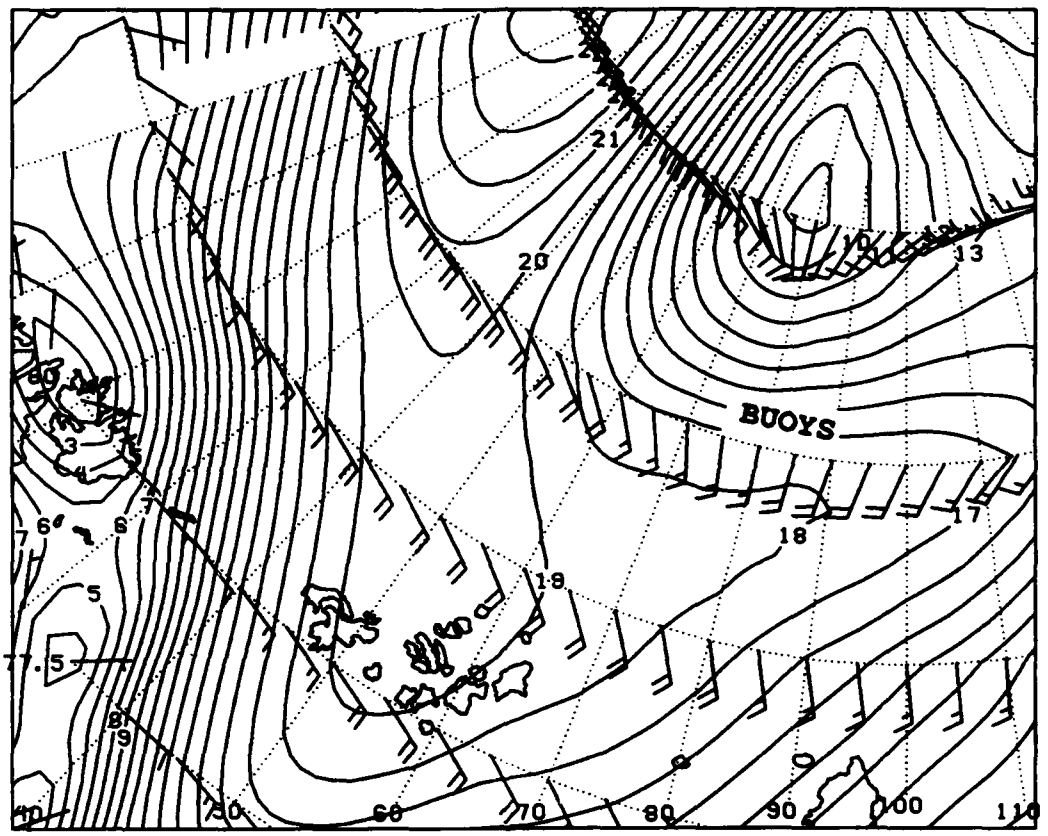

Figure 54. 1000 mb isotachs (m/s) and wind barbs for 2 February 1993, 0000Z.

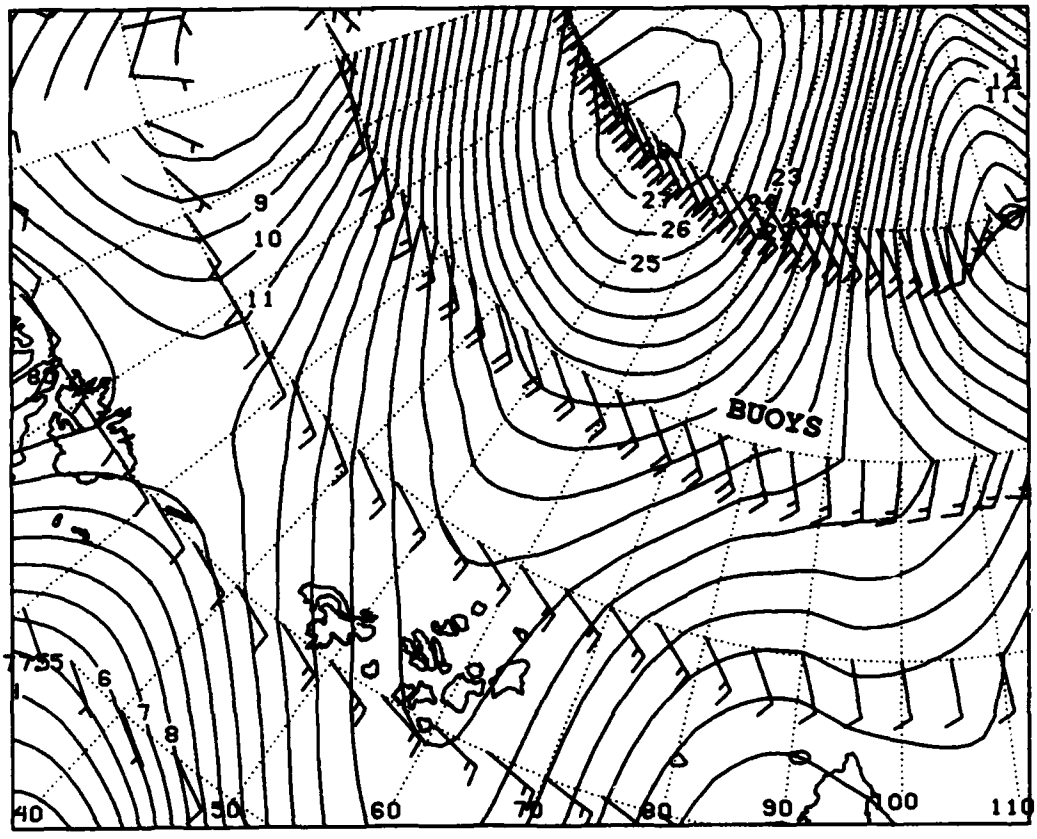

Figure 55. 1000 mb isotachs (m/s) and wind barbs for 2 February 1993, 1200Z.

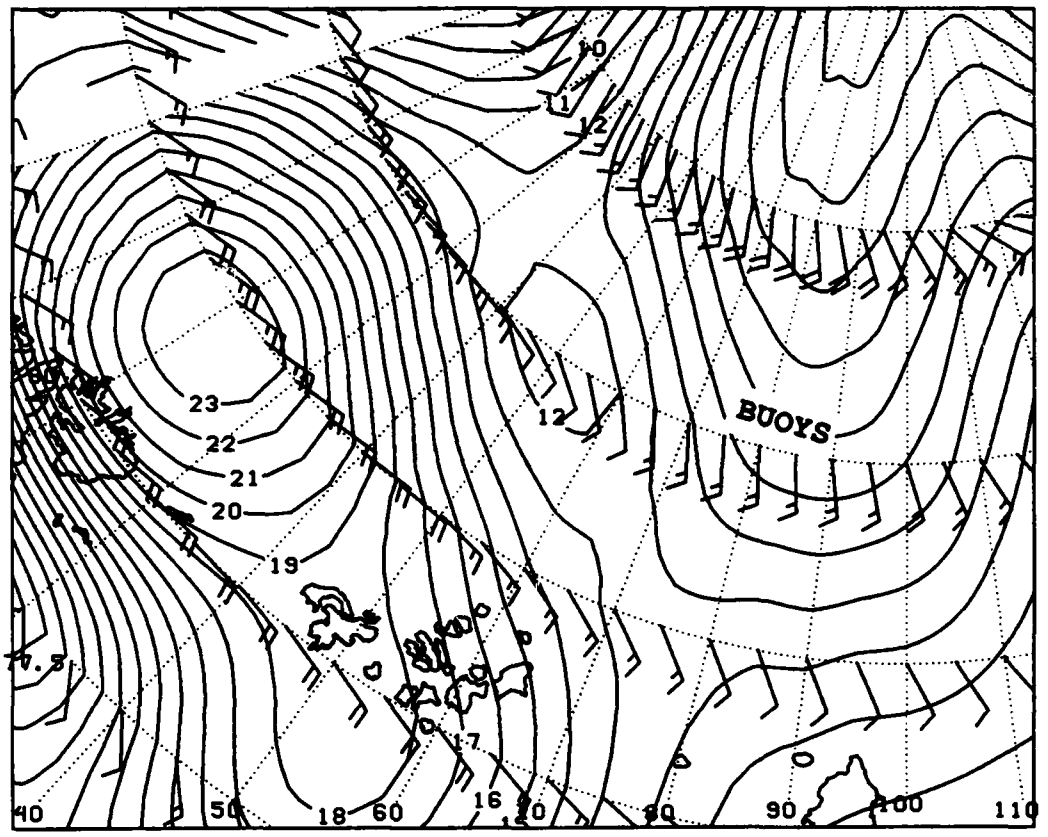

Figure 56. 1000 mb isotachs (m/s) and wind barbs for 3 February 1993, 0000Z.

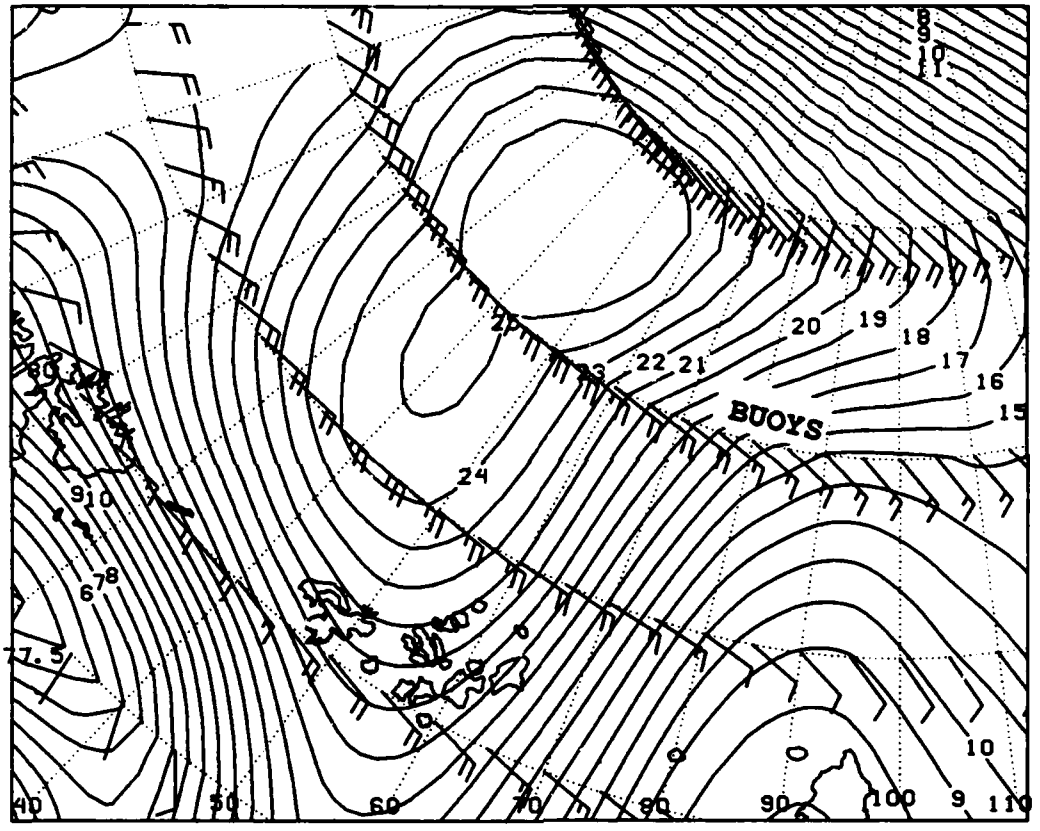

Figure 57. 1000 mb isotachs (m/s) and wind barbs for 3 February 1993, 1200Z.

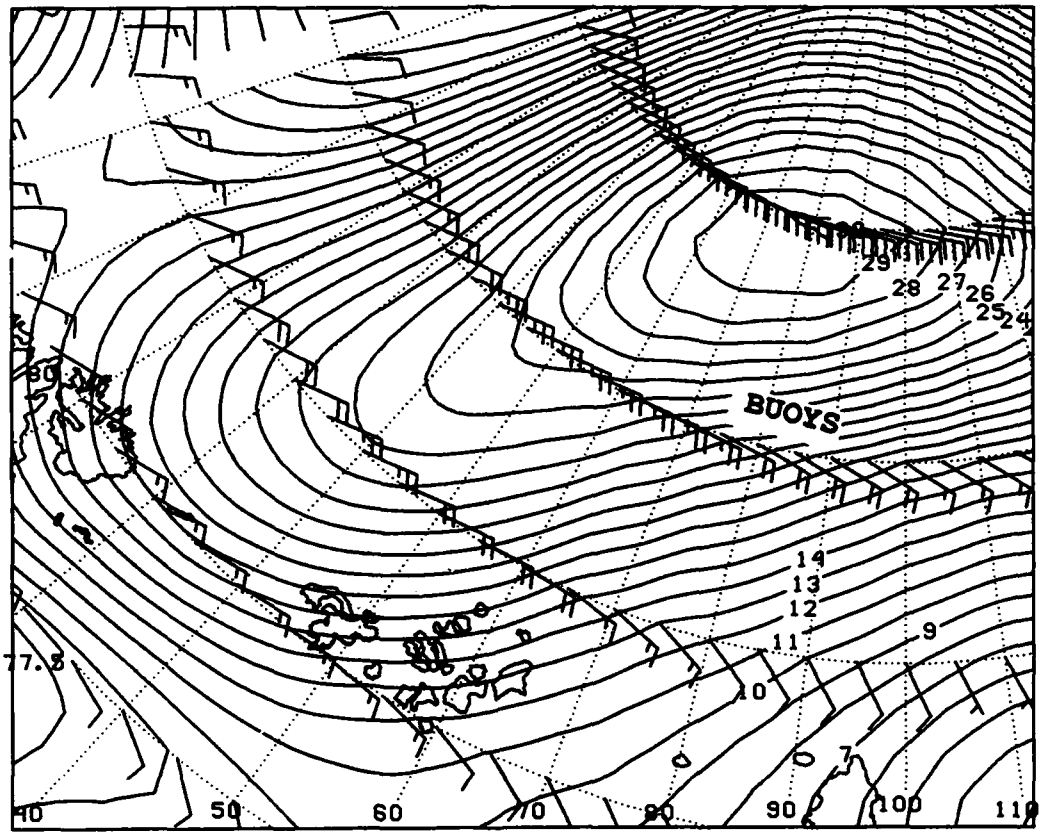

Figure 58. 1000 mb isotachs (m/s) and wind barbs for 4 February 1993, 0000Z.

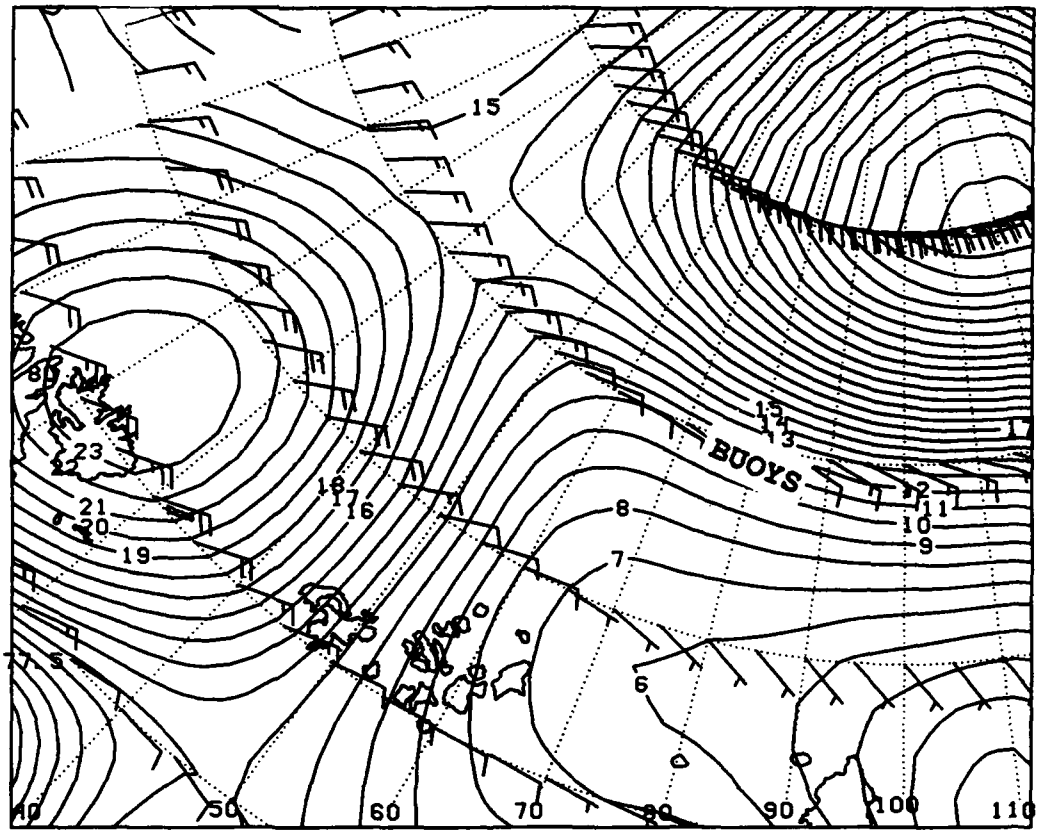

Figure 59. 1000 mb isotachs (m/s) and wind barbs for 4 February 1993, 1200Z.

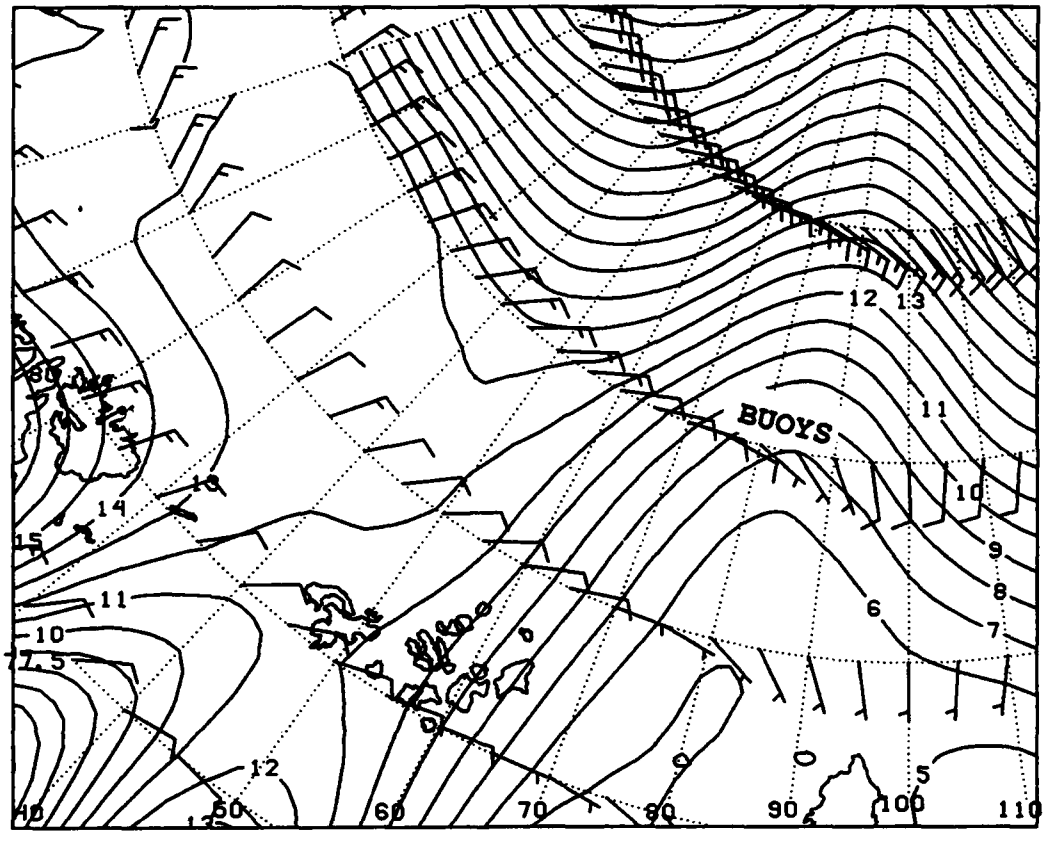

Figure 60. 1000 mb isotachs (m/s) and wind barbs for 5 February 1993, 0000Z.

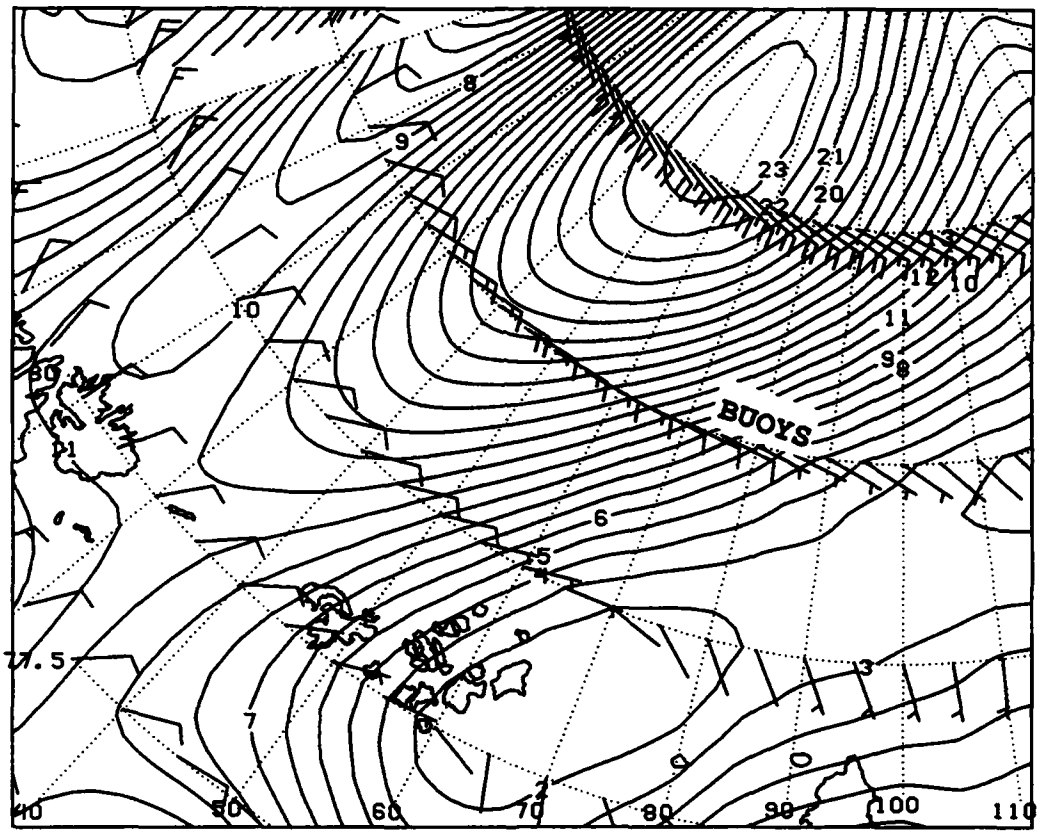

Figure 61. 1000 mb isotachs (m/s) and wind barbs for 5 February 1993, 1200Z.

APPENDIX C

EVENT #2 WEATHER CHARTS

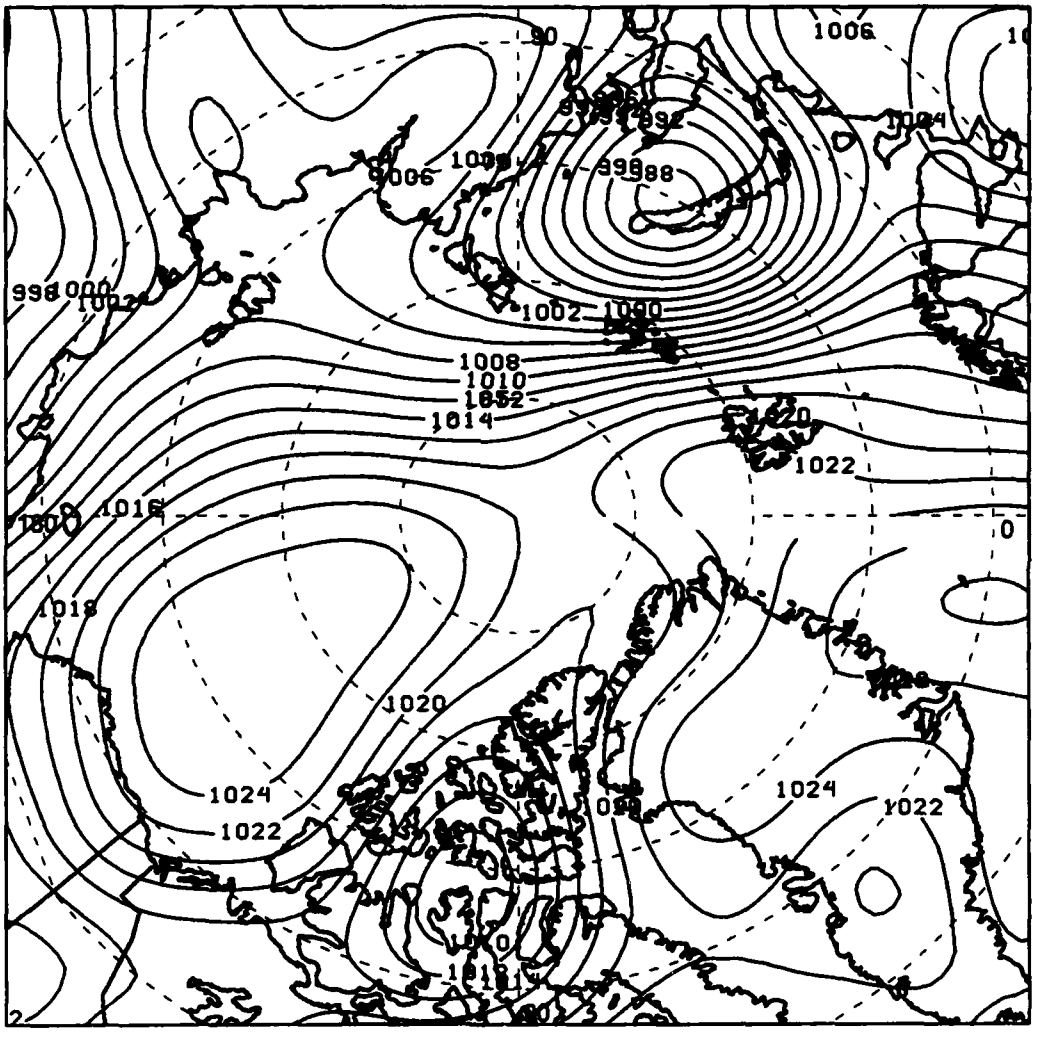

Figure 62. 1000 mb pressure field and fronts for 3 July 1992, 0000Z.

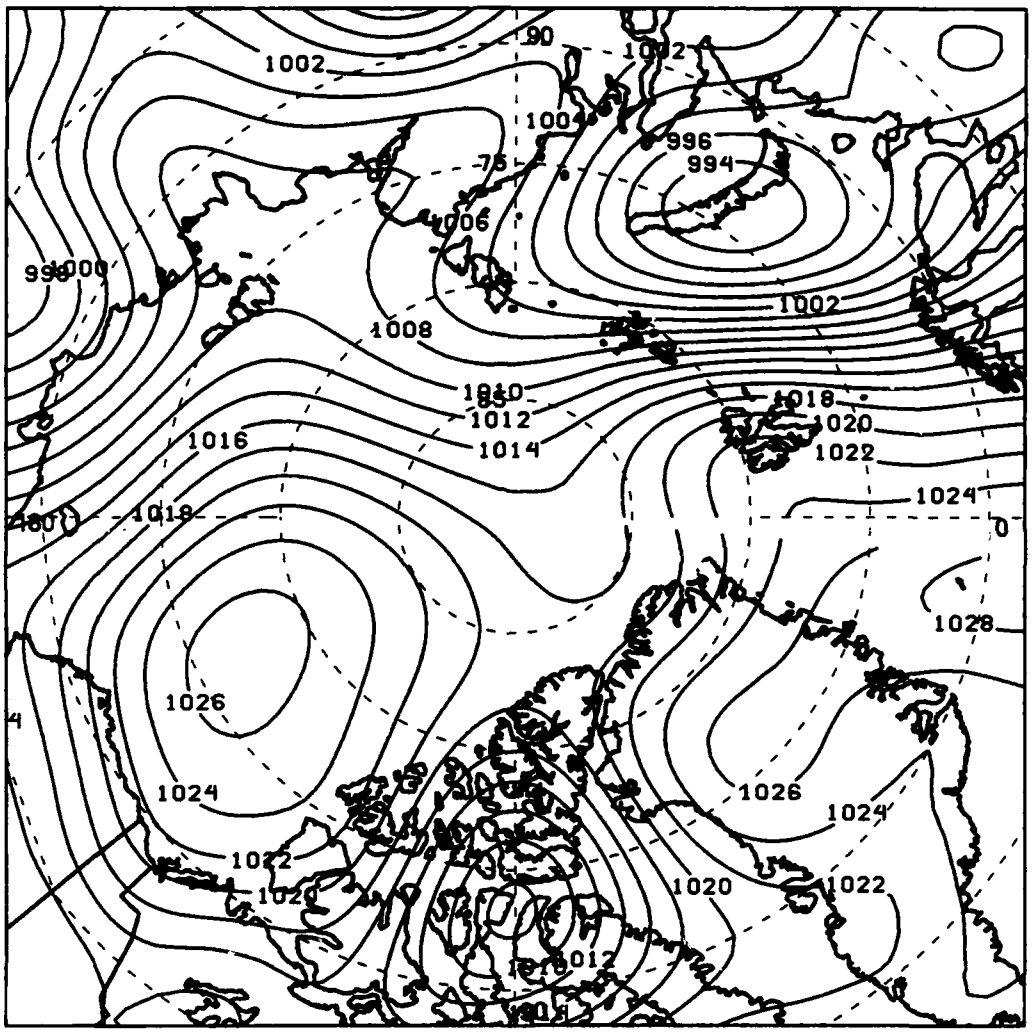

Figure 63. 1000 mb pressure field and fronts for 3 July 1992, 1200Z.

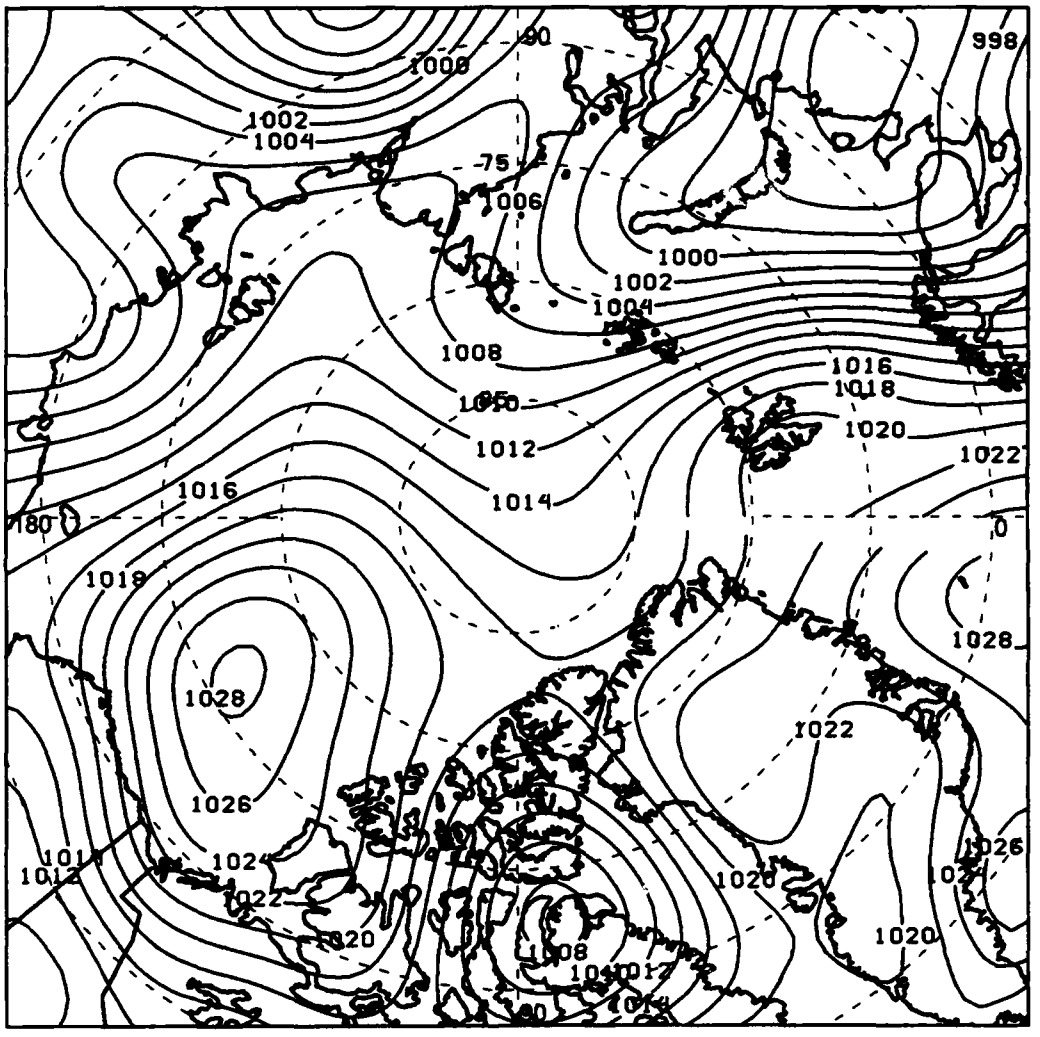

Figure 64. 1000 mb pressure field and fronts for 4 July 1992, 0000Z.

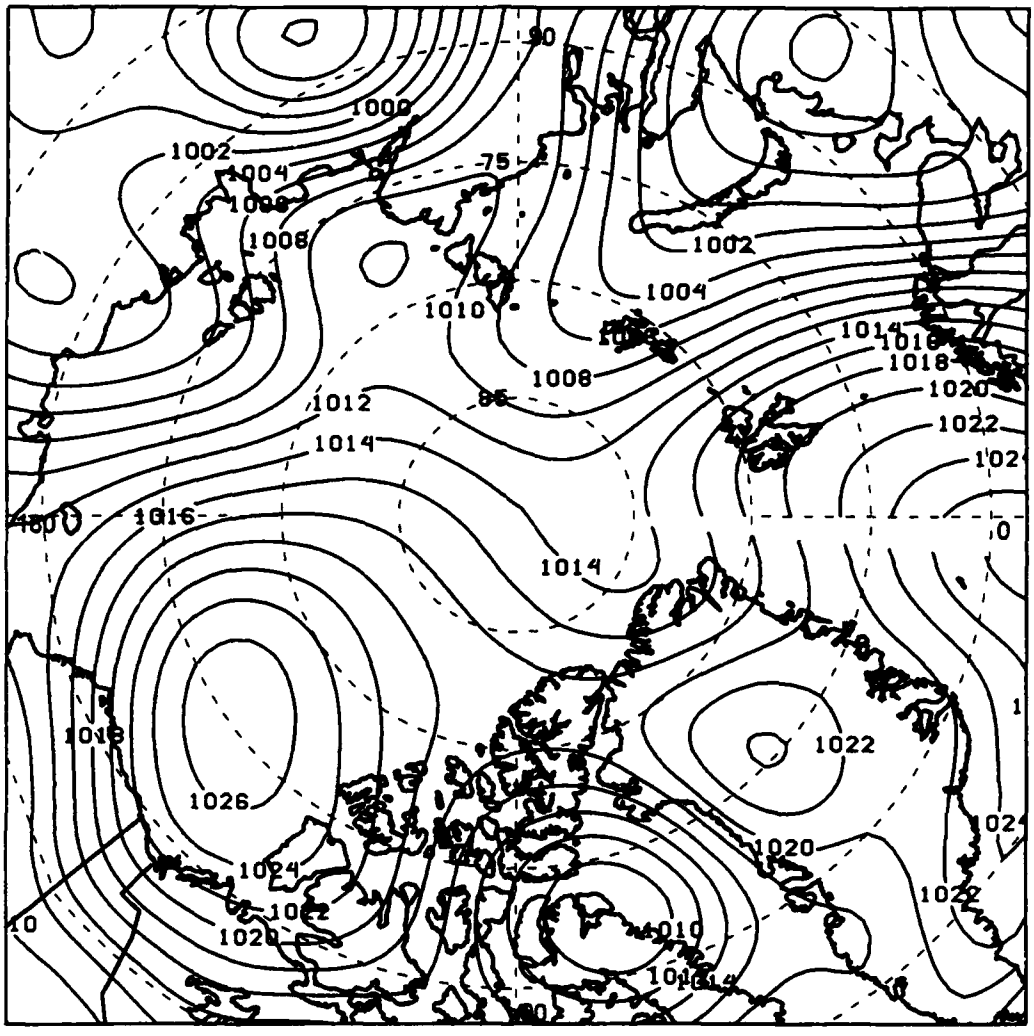

Figure 65. 1000 mb pressure field and fronts for 4 July 1992, 1200Z.

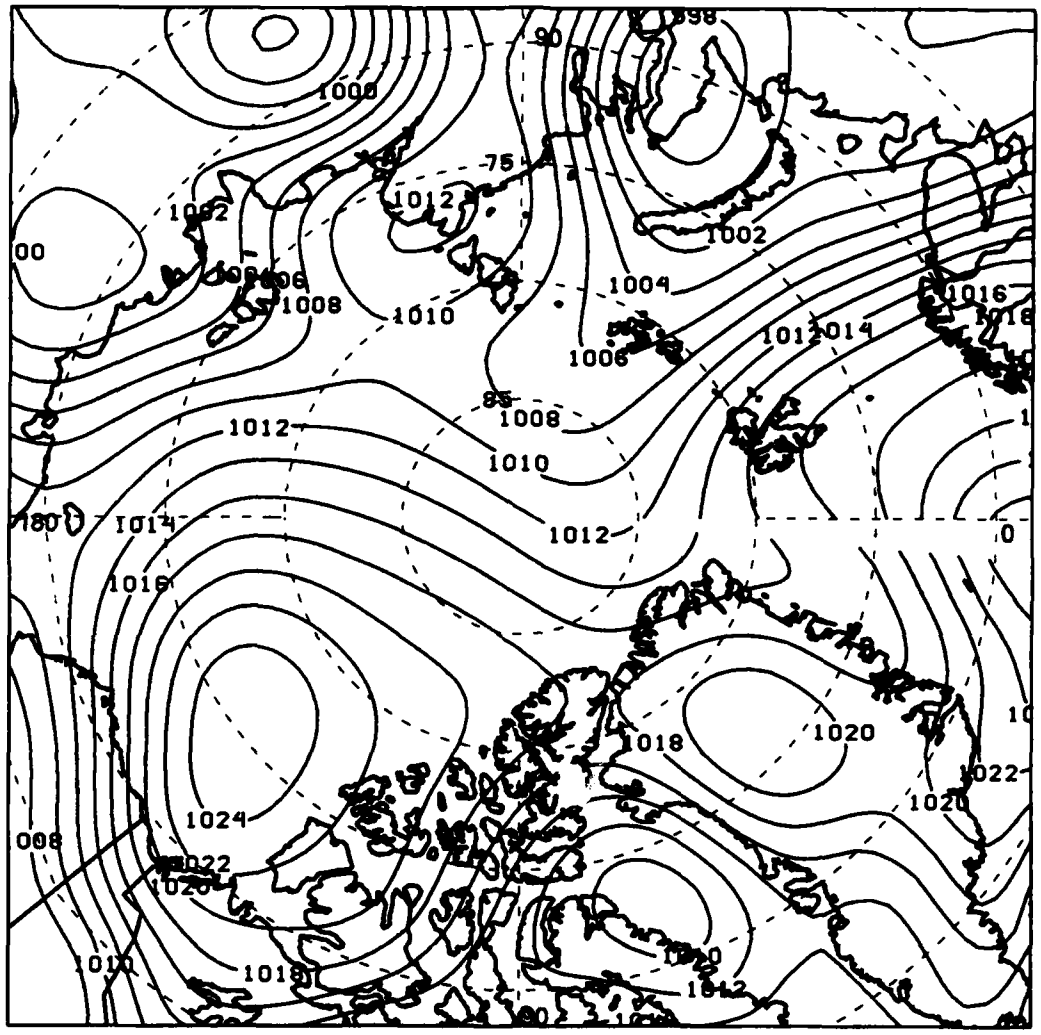

Figure 66. 1000 mb pressure field and fronts for 5 July 1992, 0000Z.

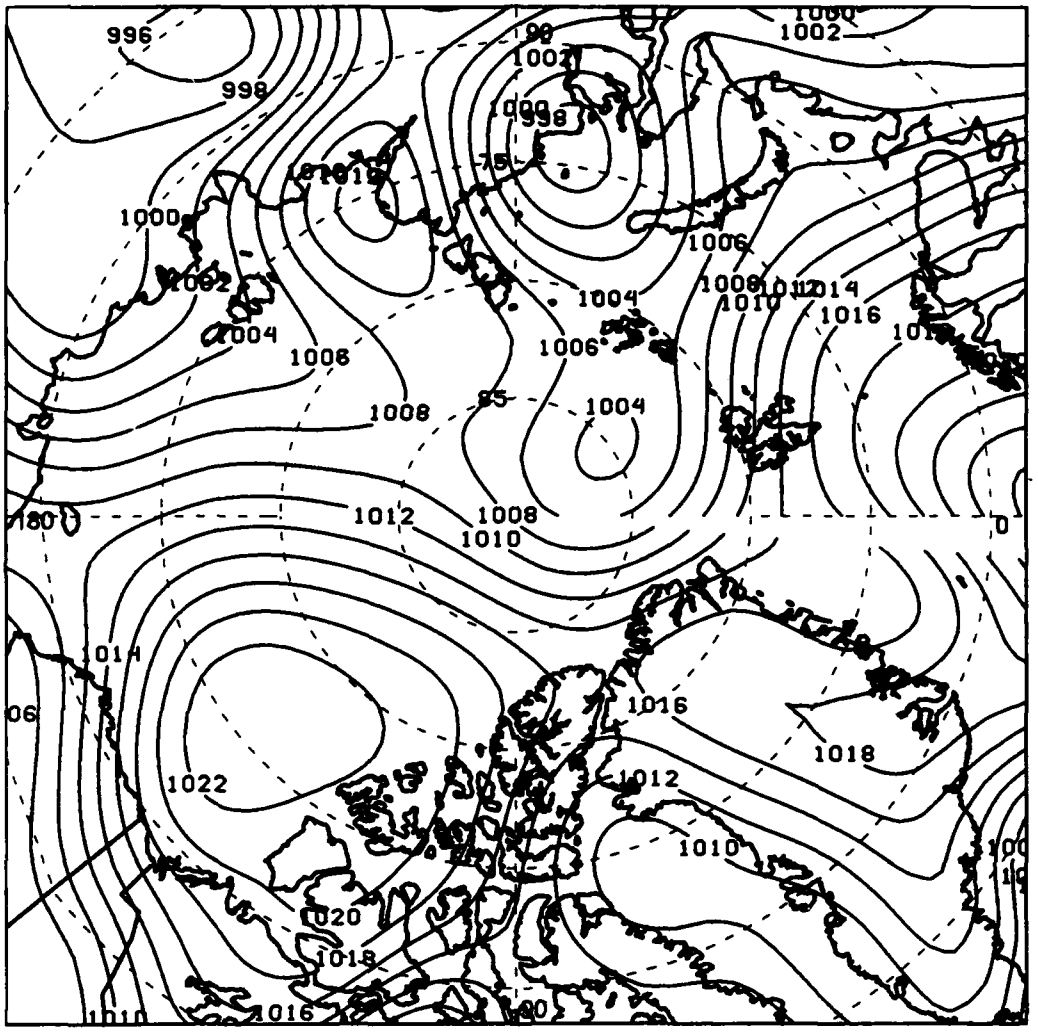

Figure 67. 1000 mb pressure field and fronts for 5 July 1992, 1200Z.

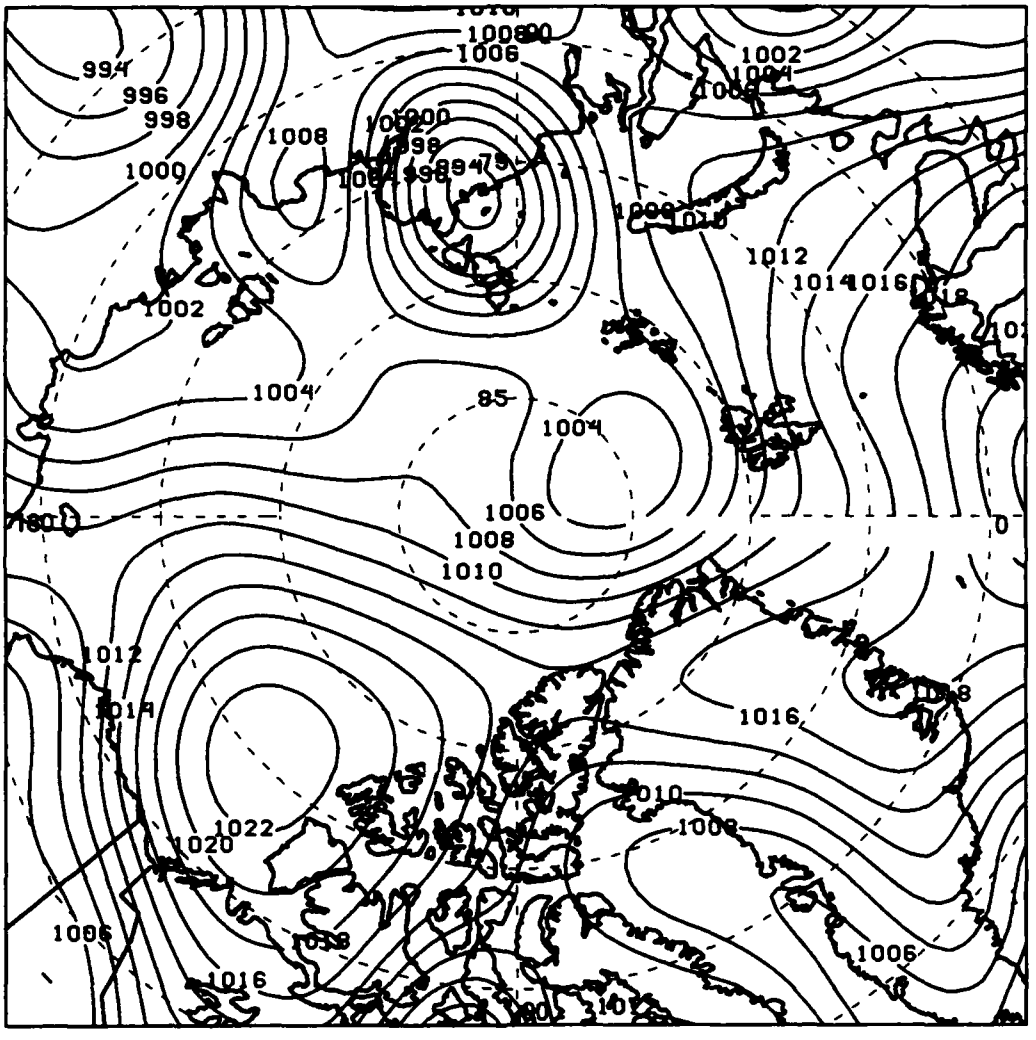

Figure 68. 1000 mb pressure field and fronts for 6 July 1992, 0000Z.

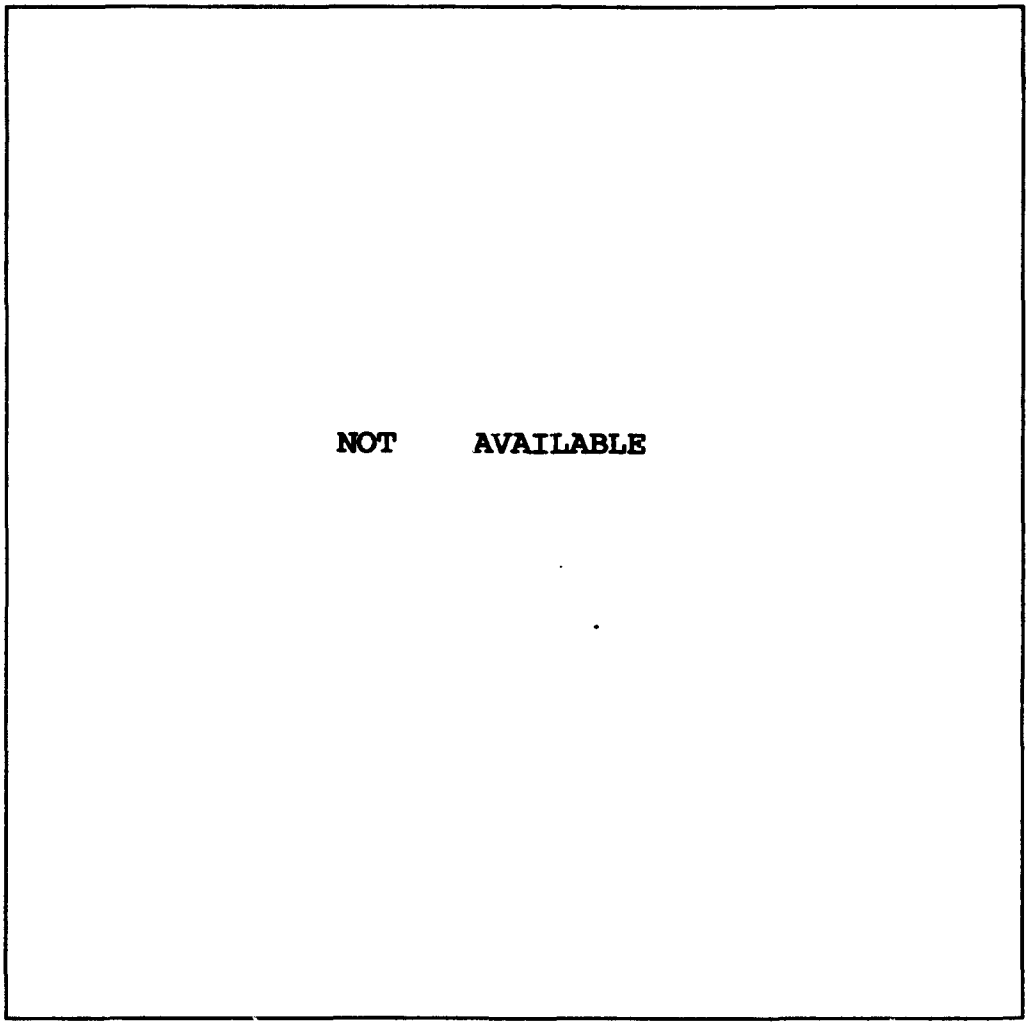

Figure 69. 1000 mb pressure field and fronts for 6 July 1992, 1200Z.

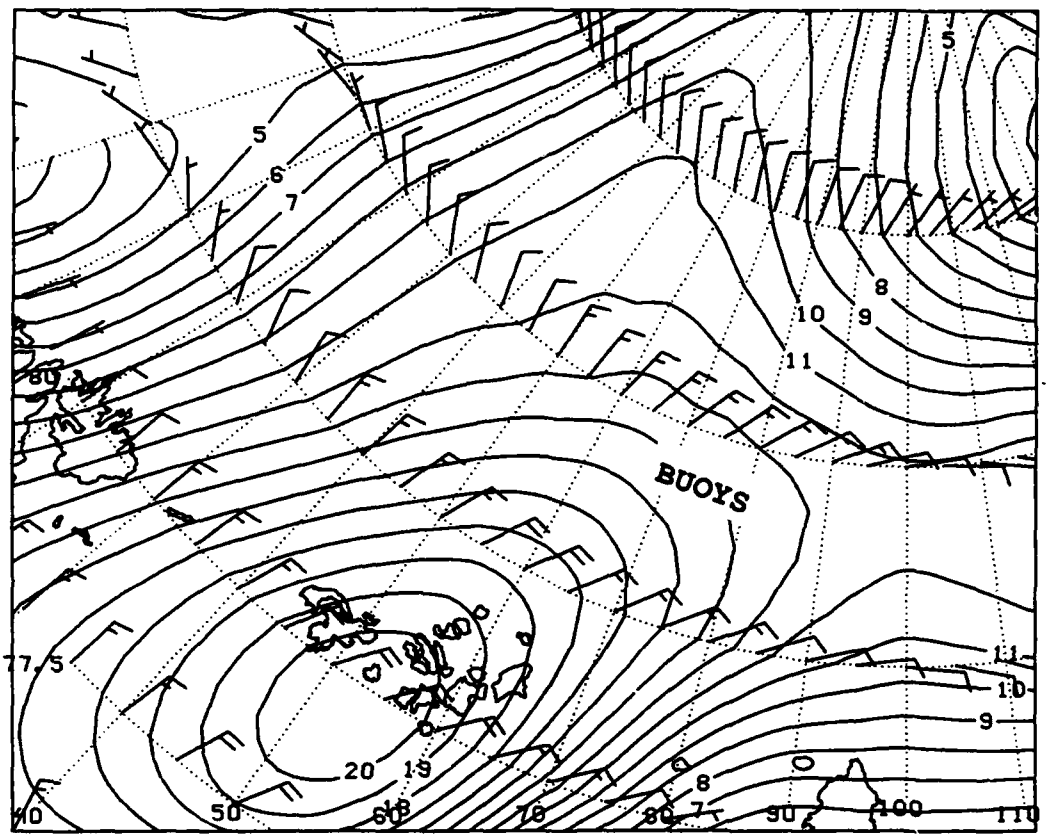

Figure 70. 1000 mb isotachs (m/s) and wind barbs for 3 July 1992, 0000Z.

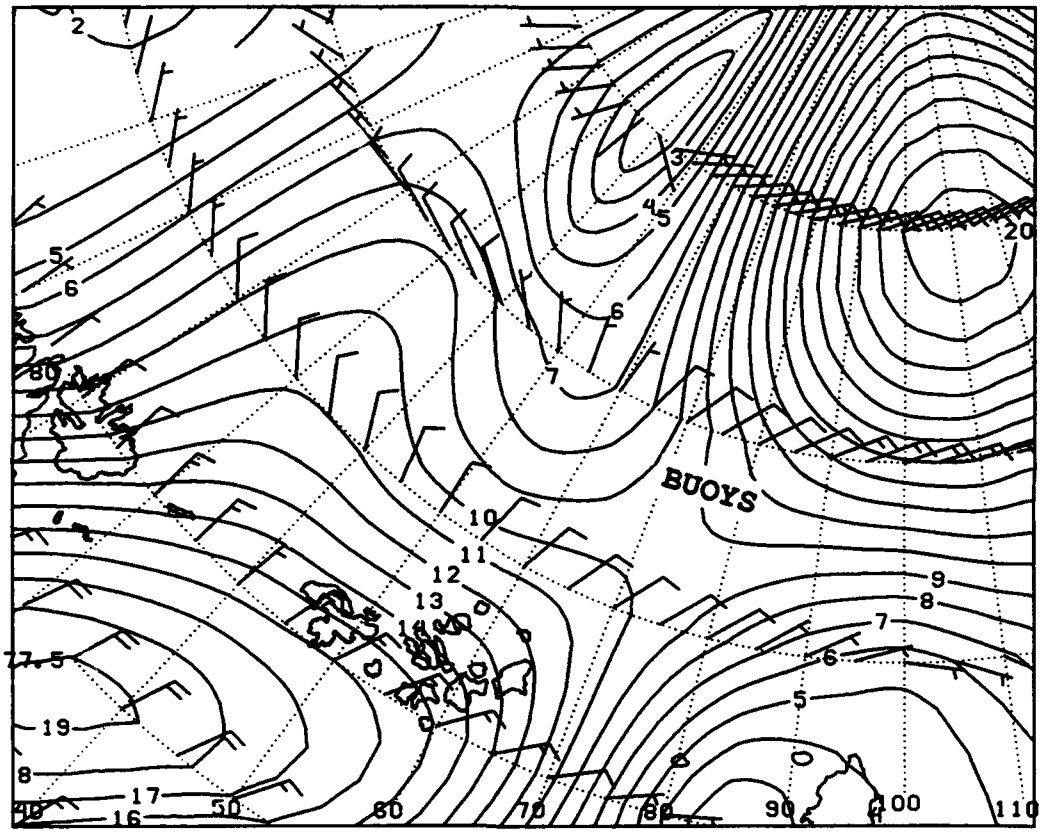

Figure 71. 1000 mb isotachs (m/s) and wind barbs for 3 July 1992, 1200Z.

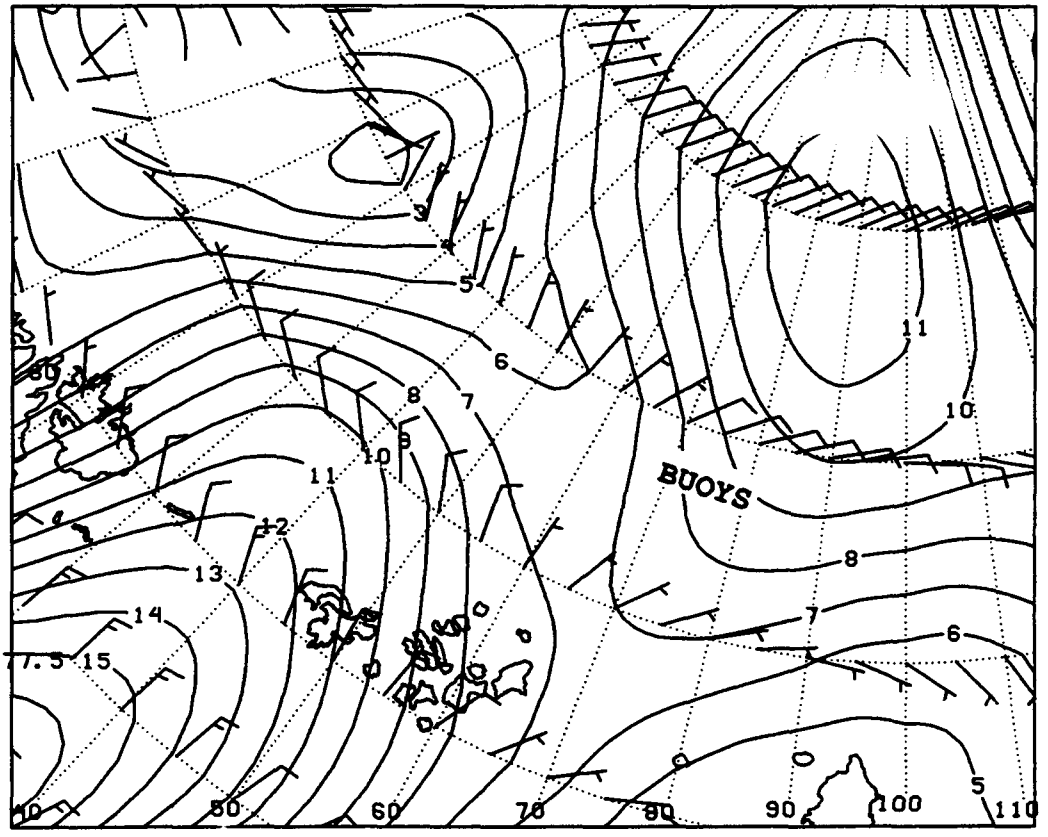

Figure 72. 1000 mb isotachs (m/s) and wind barbs for 4 July 1992, 0000Z.

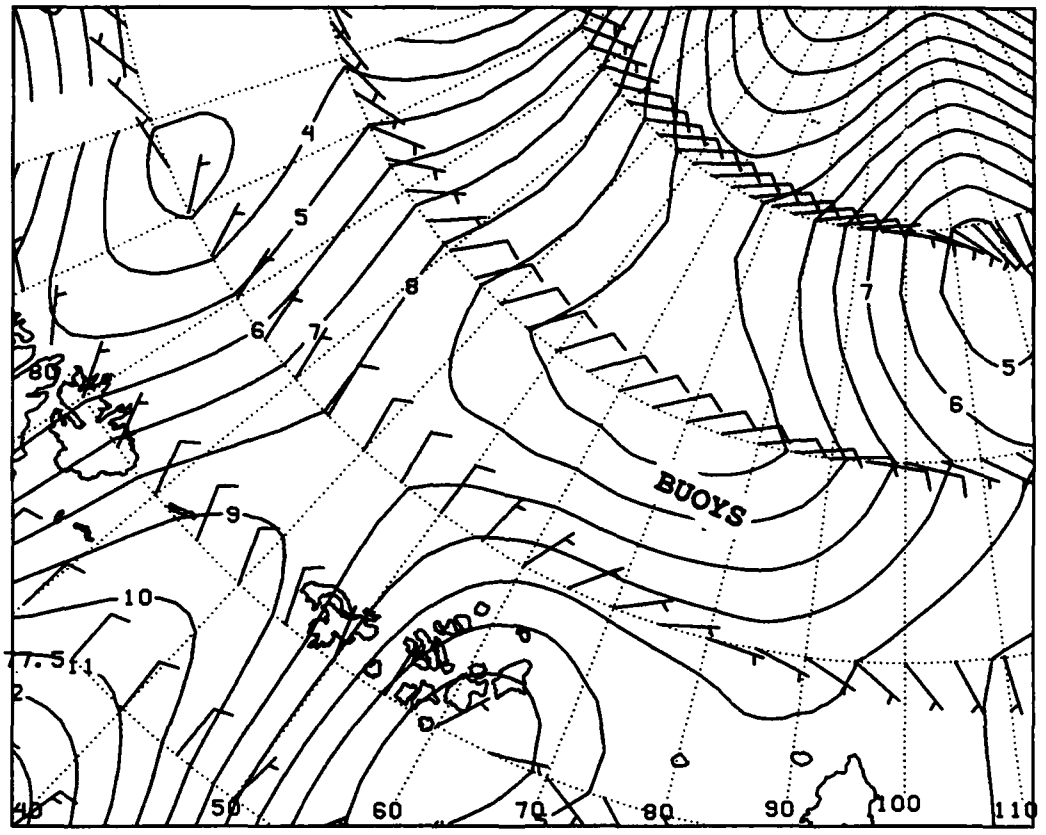

Figure 73. 1000 mb isotachs (m/s) and wind barbs for 4 July 1992, 1200Z.

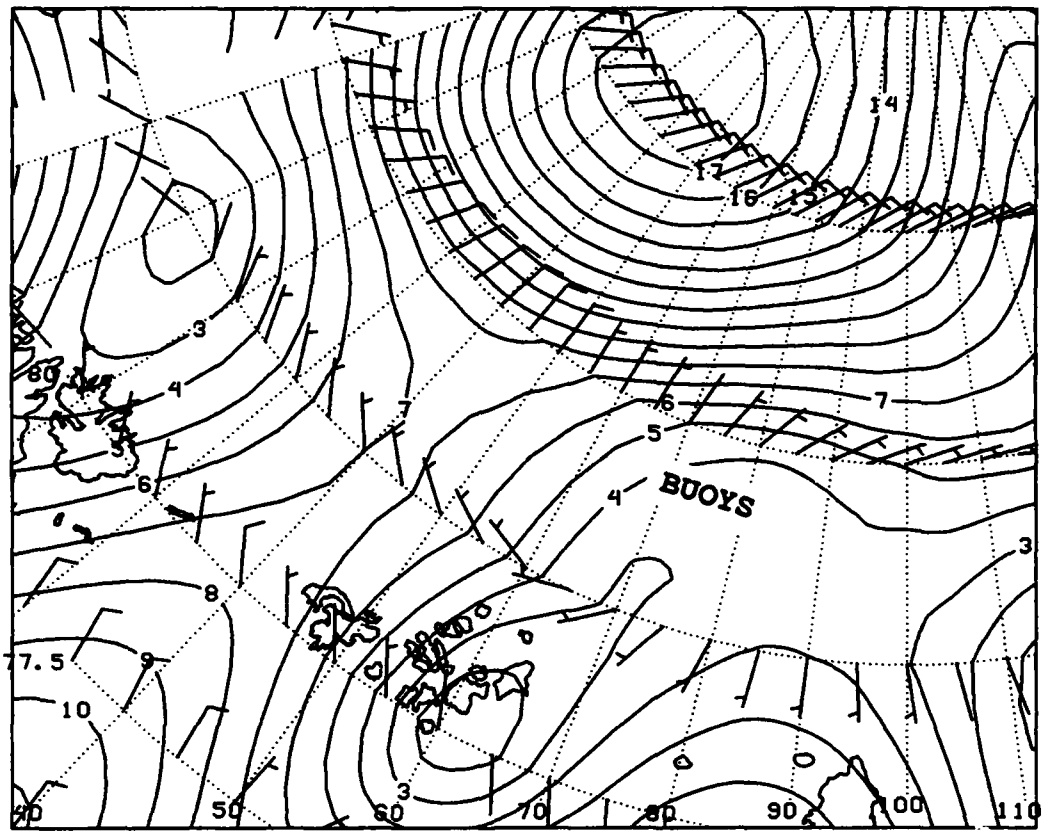

Figure 74. 1000 mb isotachs (m/s) and wind barbs for 5 July 1992, 0000Z.

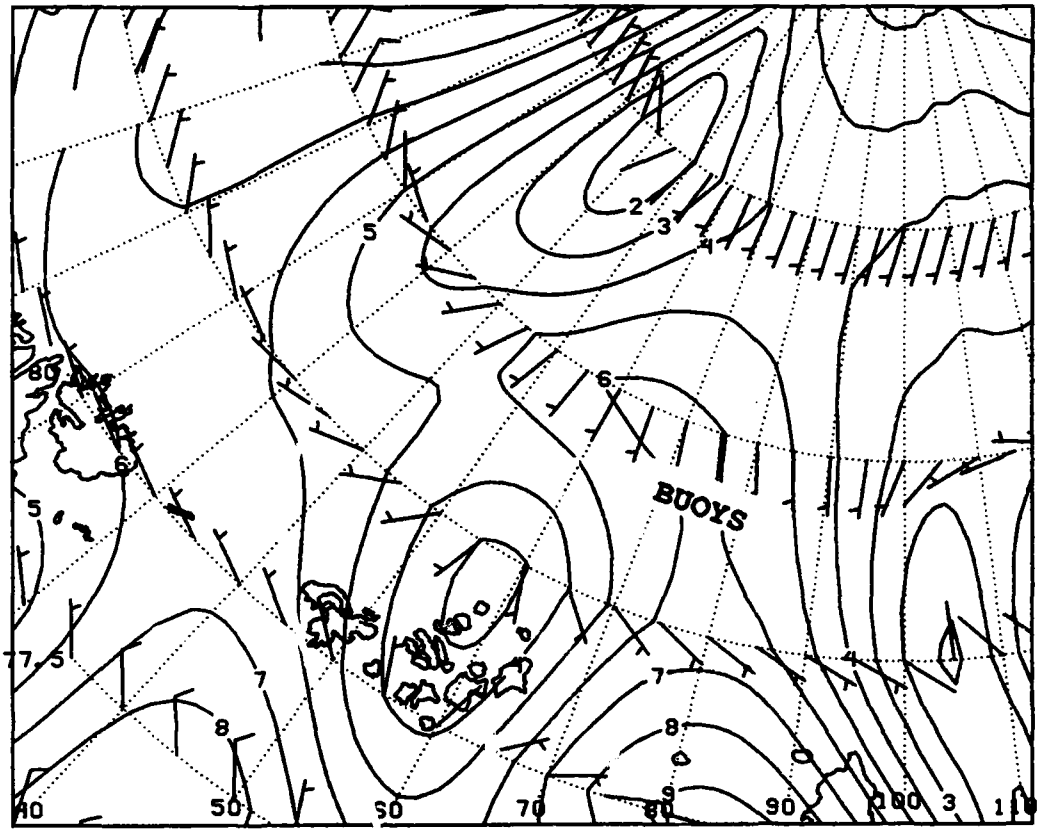

Figure 75. 1000 mb isotachs (m/s) and wind barbs for 5 July 1992, 1200Z.

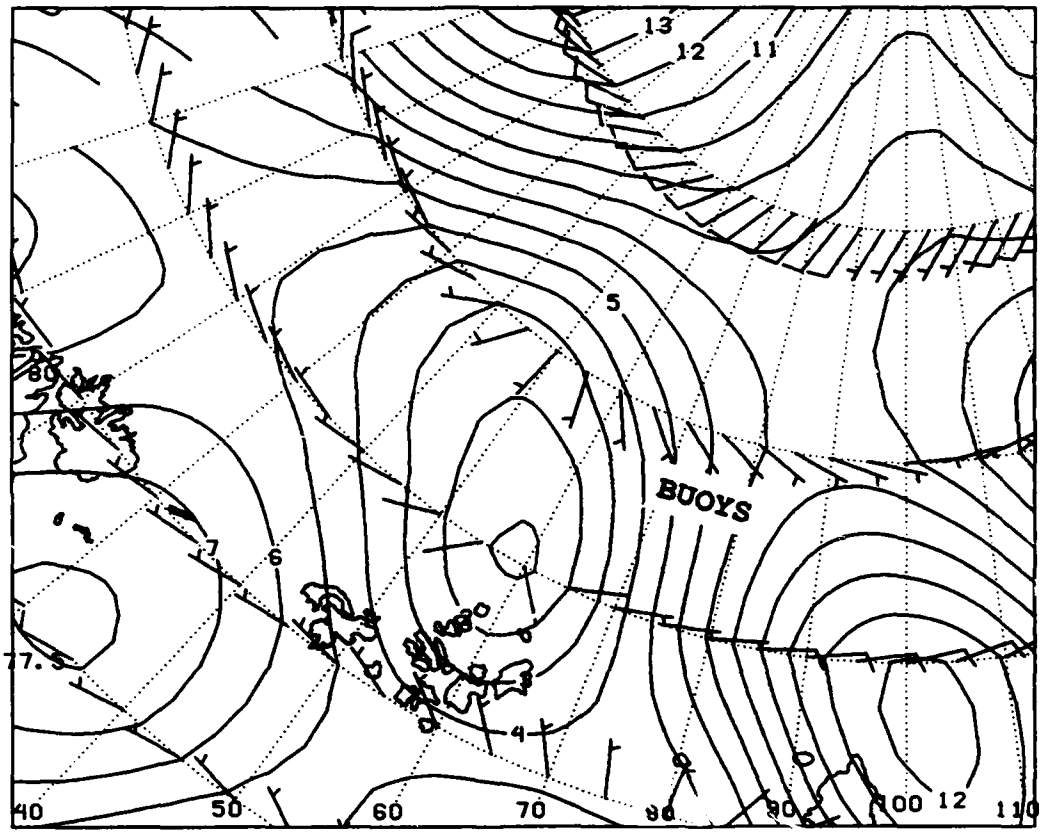

Figure 76. 1000 mb isotachs (m/s) and wind barbs for 6 July 1992, 0000Z.

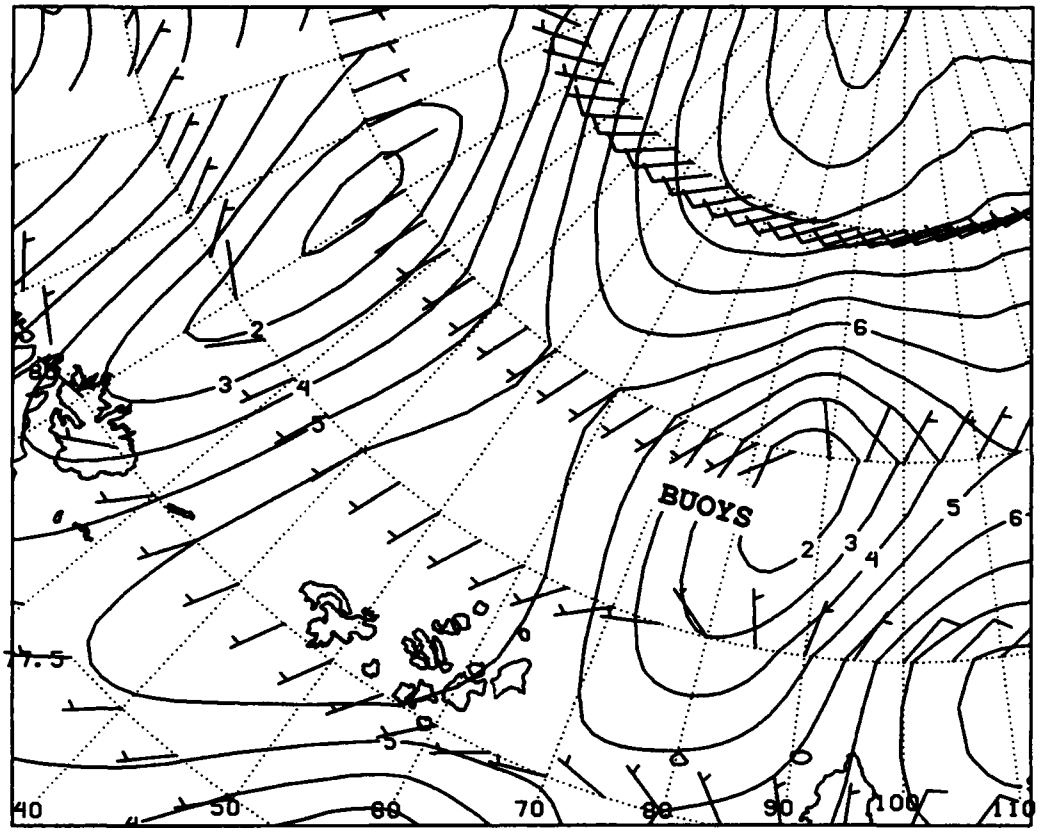

Figure 77. 1000 mb isotachs (m/s) and wind barbs for 6 July 1992, 1200Z.

APPENDIX D

EVENT #3 WEATHER CHARTS

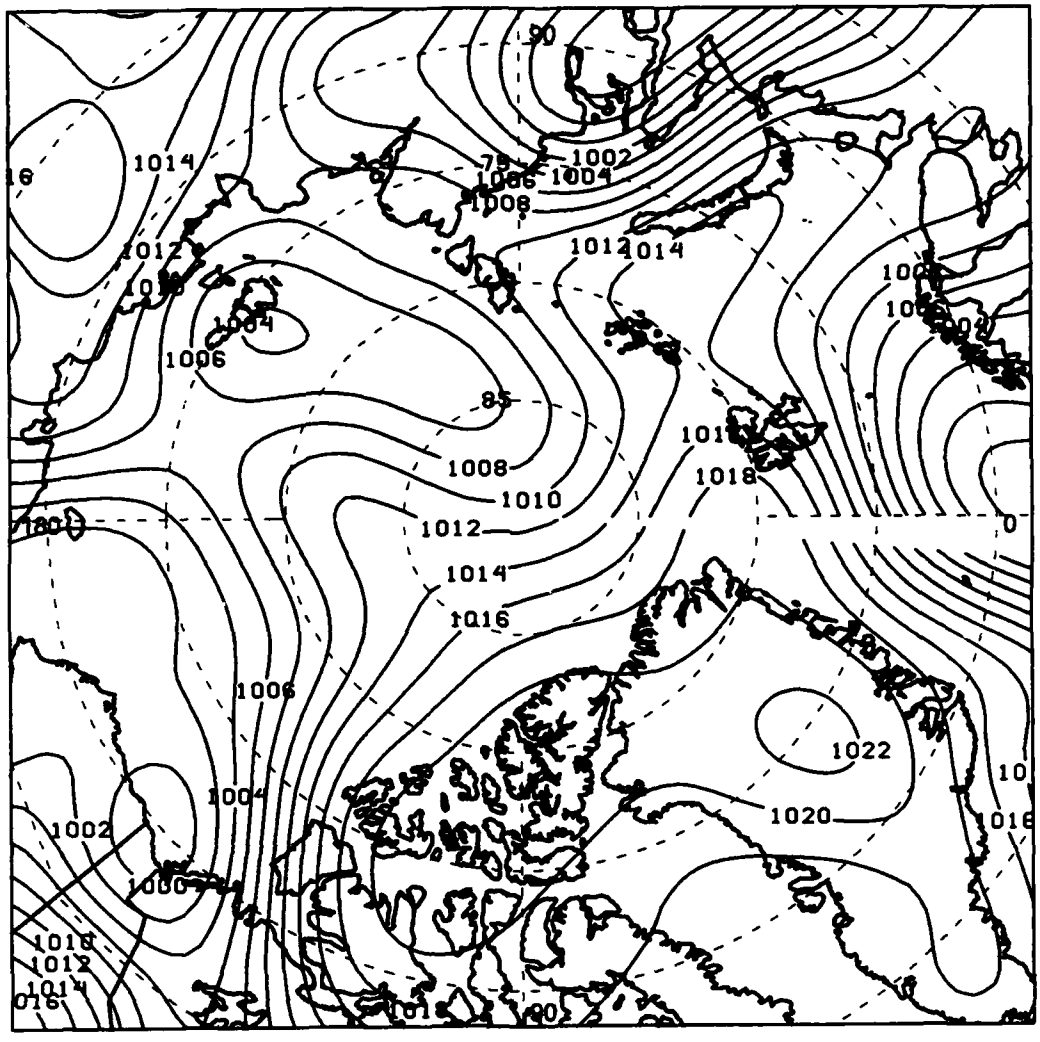

Figure 78. 1000 mb pressure field and fronts for 26 August 1992, 0000Z.

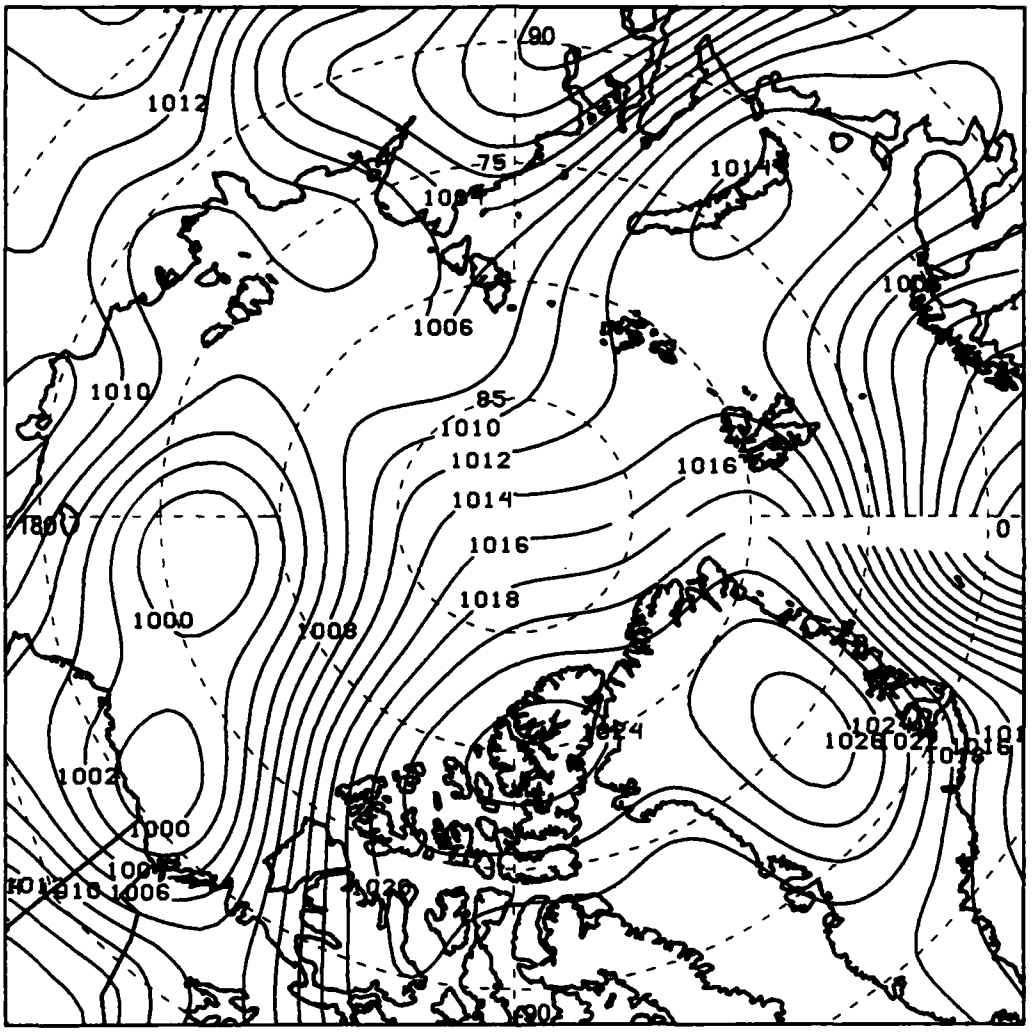

Figure 79. 1000 mb pressure field and fronts for 26 August 1992, 1200Z.

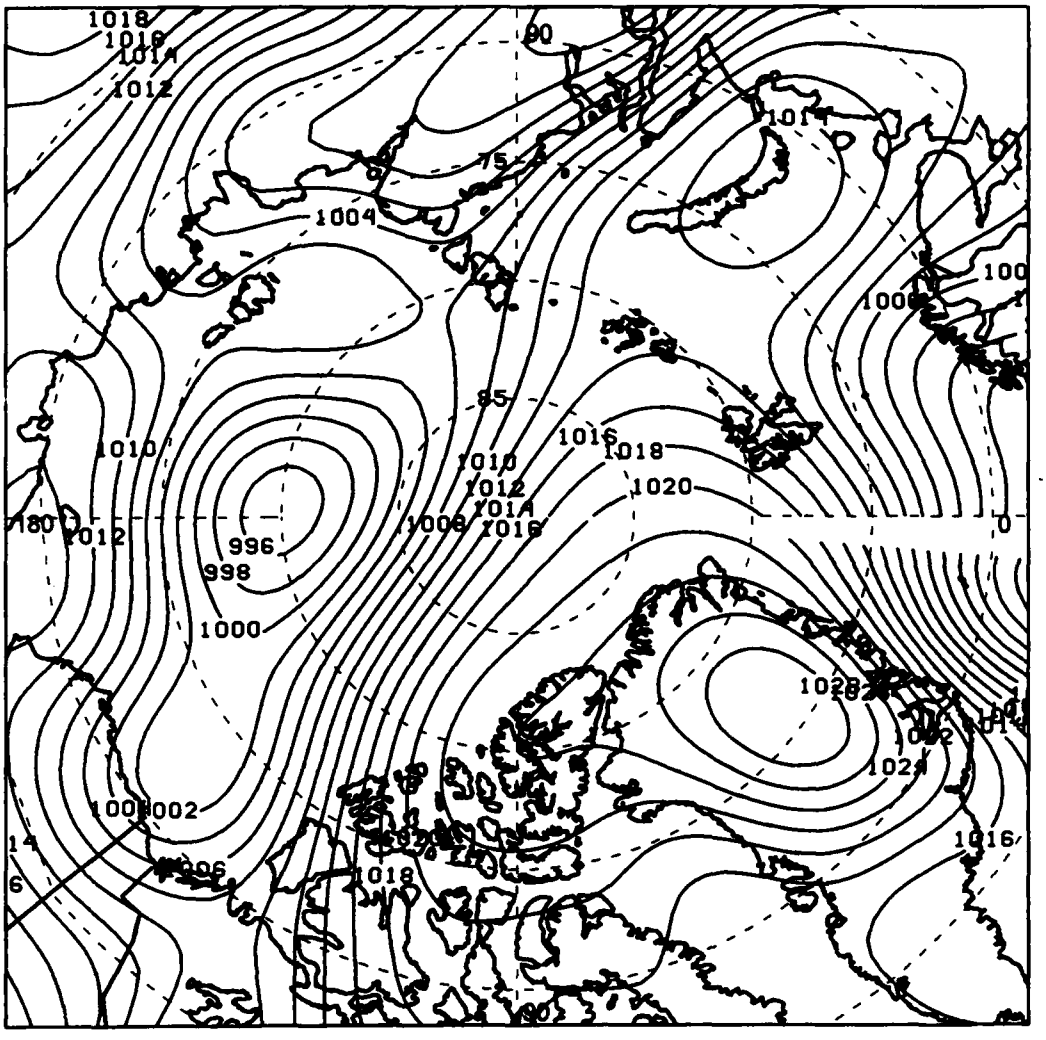

Figure 80. 1000 mb pressure field and fronts for 27 August 1992, 0000Z.

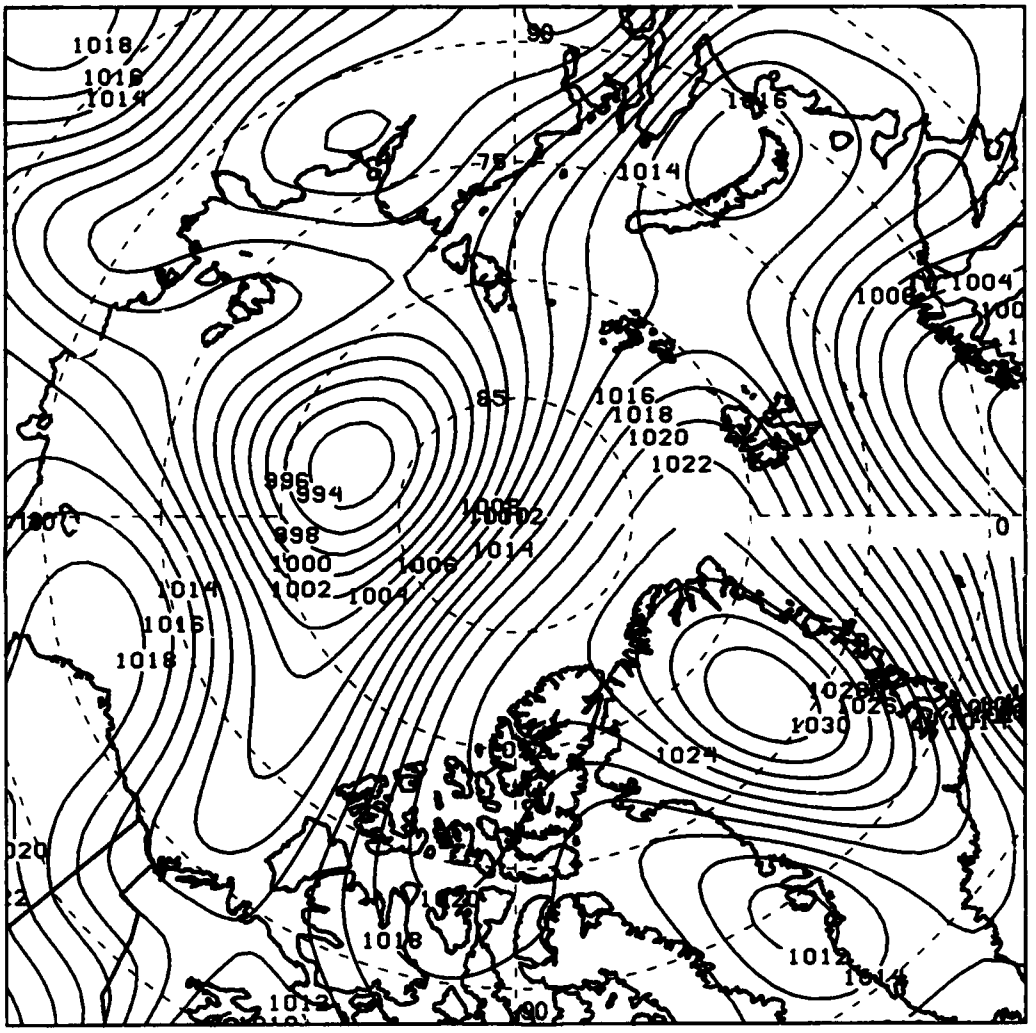

Figure 81. 1000 mb pressure field and fronts for 27 August 1992, 1200Z.

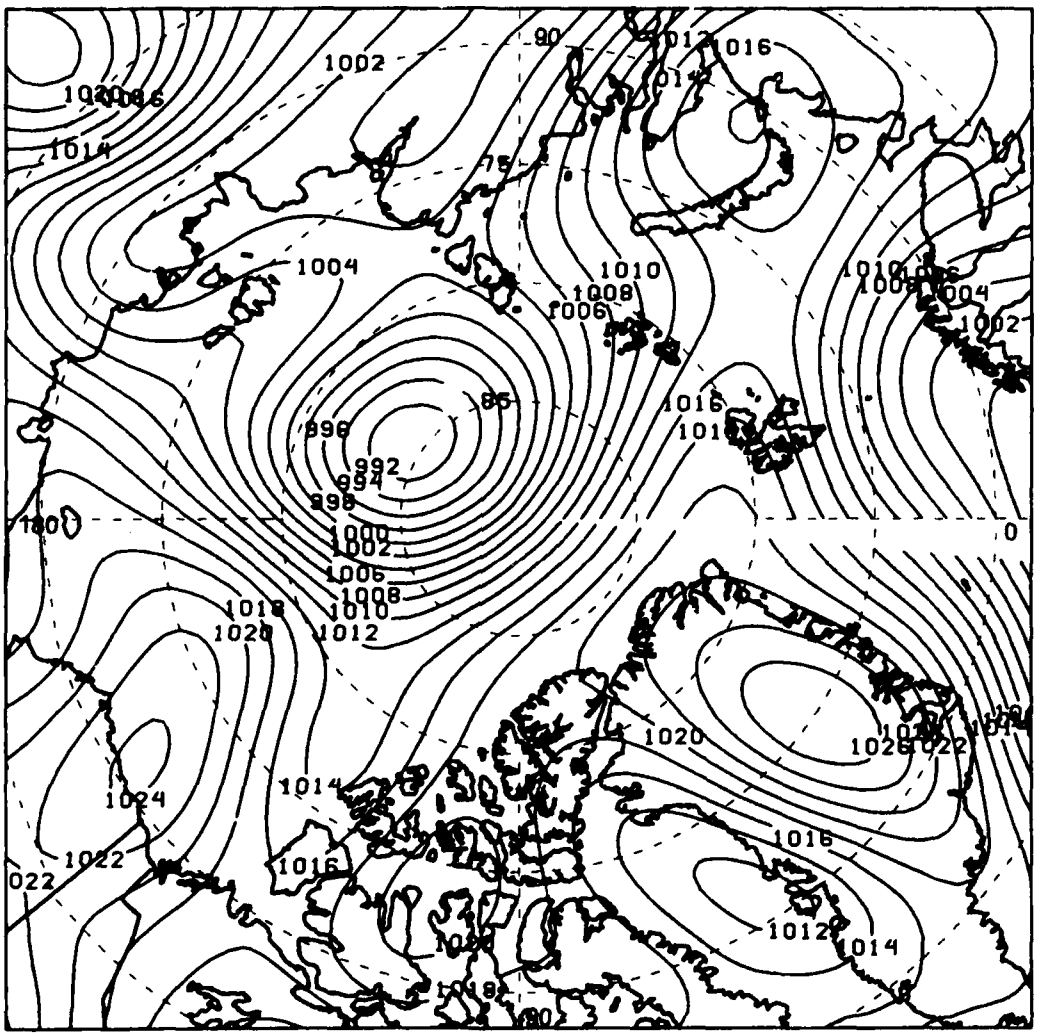

Figure 82. 1000 mb pressure field and fronts for 28 August 1992, 0000Z.

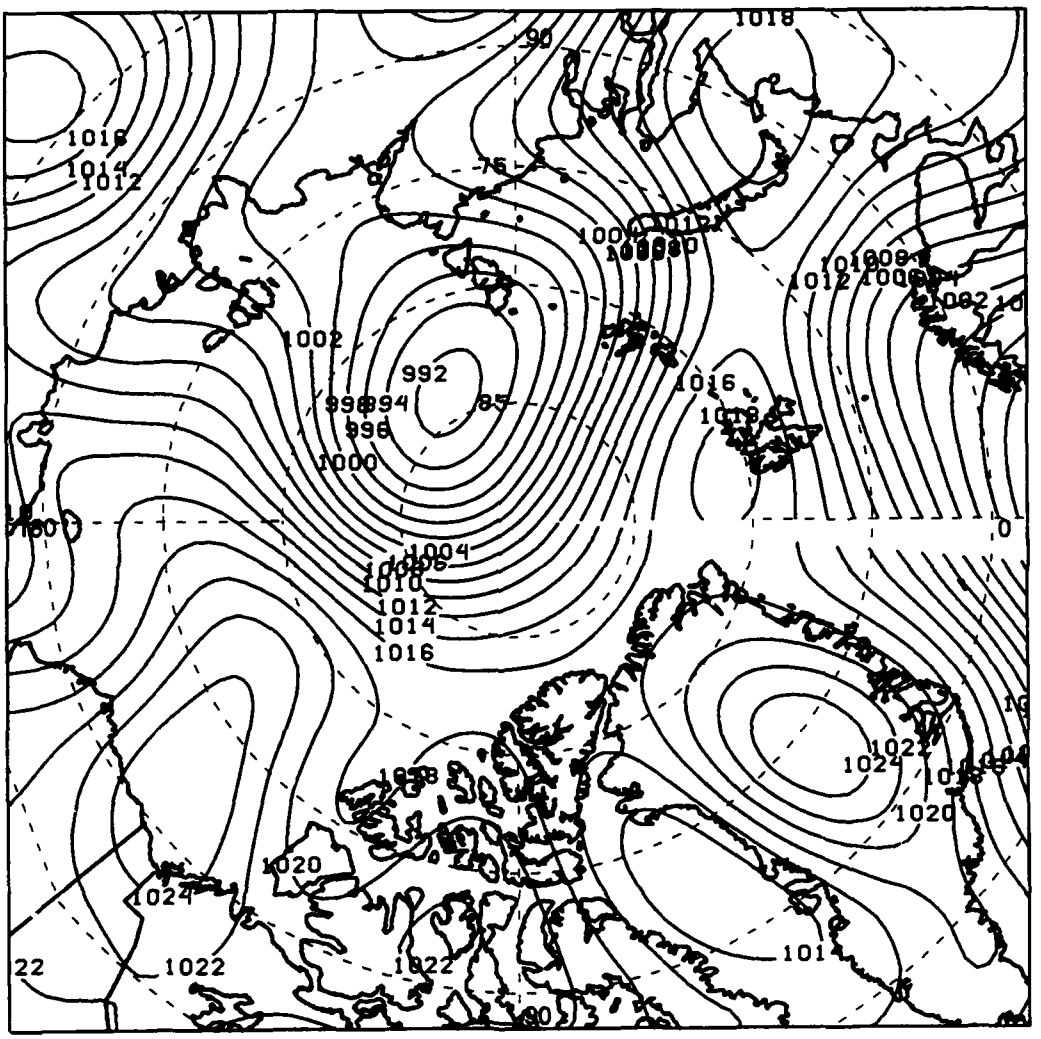

Figure 83. 1000 mb pressure field and fronts for 28 August 1992, 1200Z.

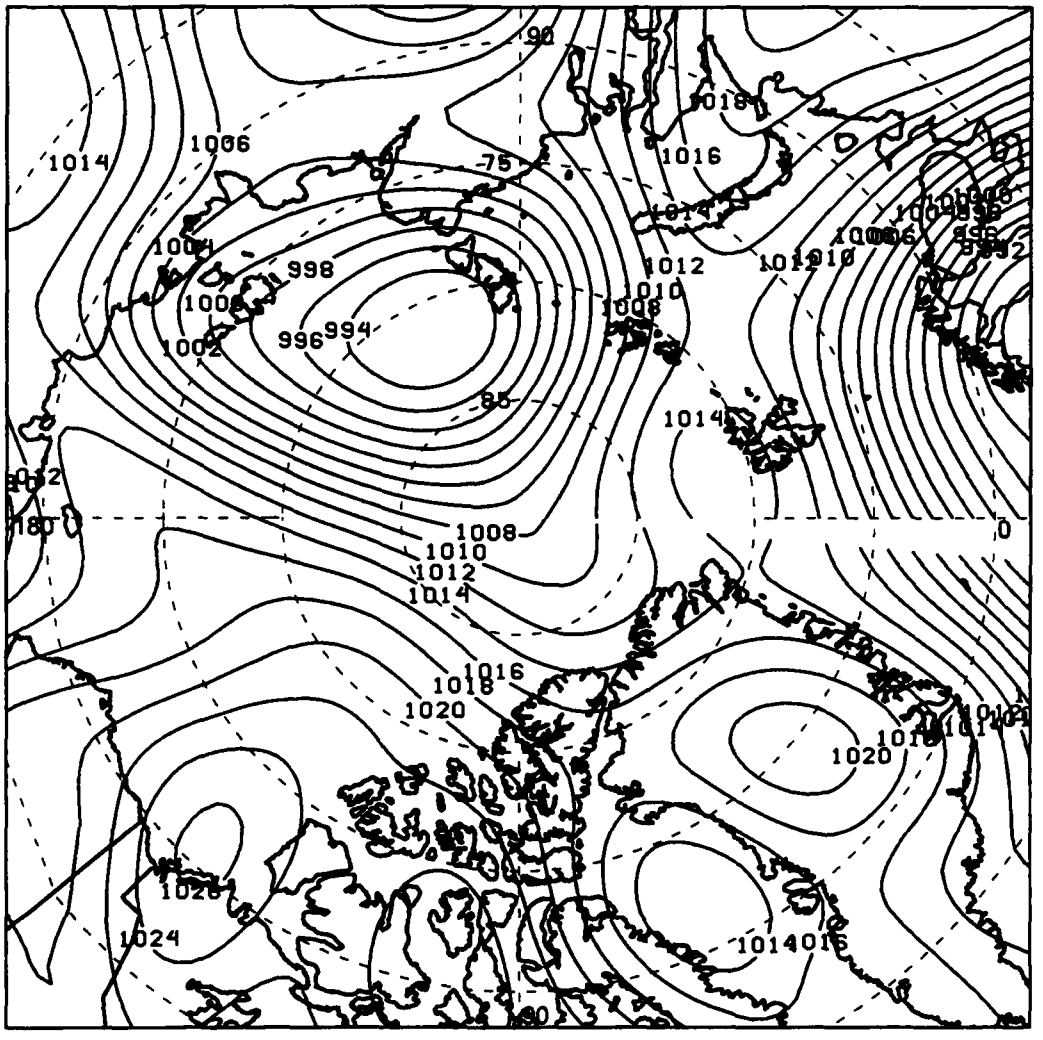

Figure 84. 1000 mb pressure field and fronts for 29 August 1992, 0000Z.

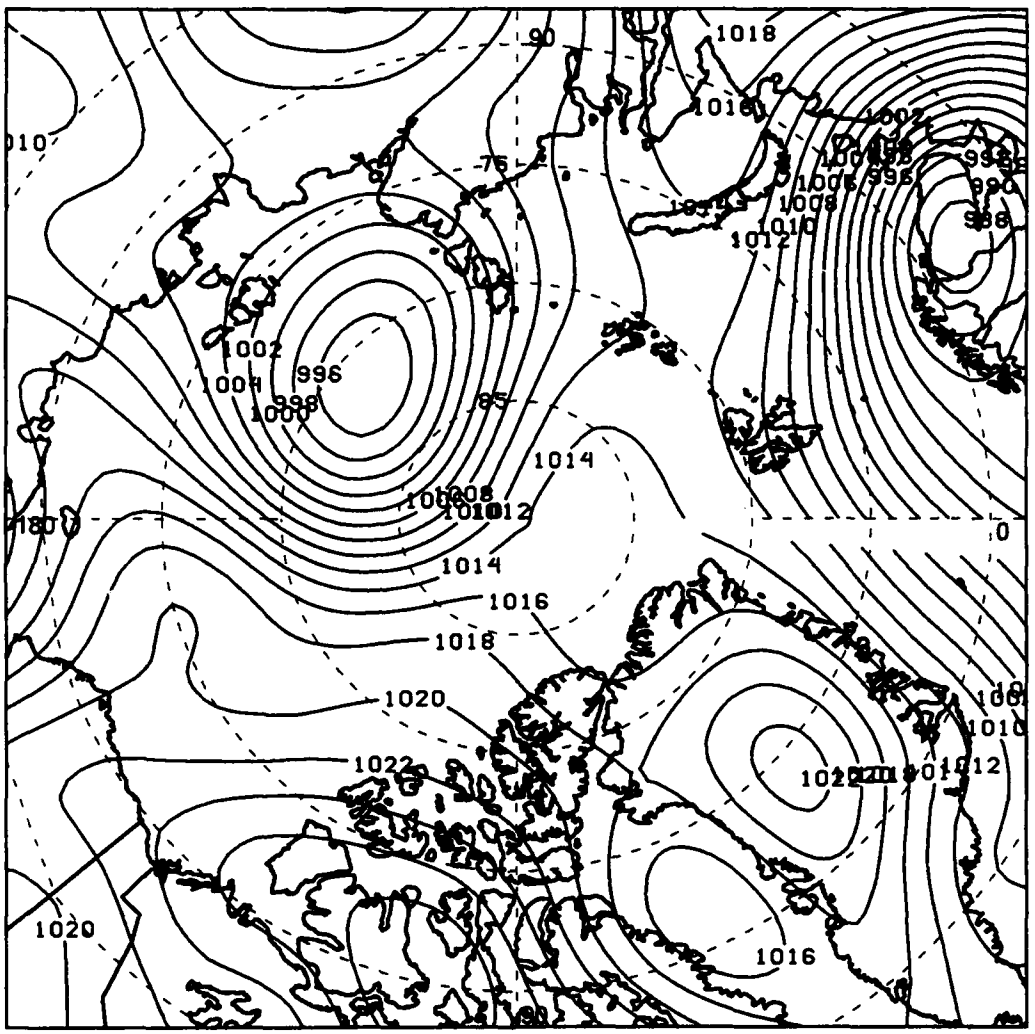

Figure 85. 1000 mb pressure field and fronts for 29 August 1992, 1200Z.

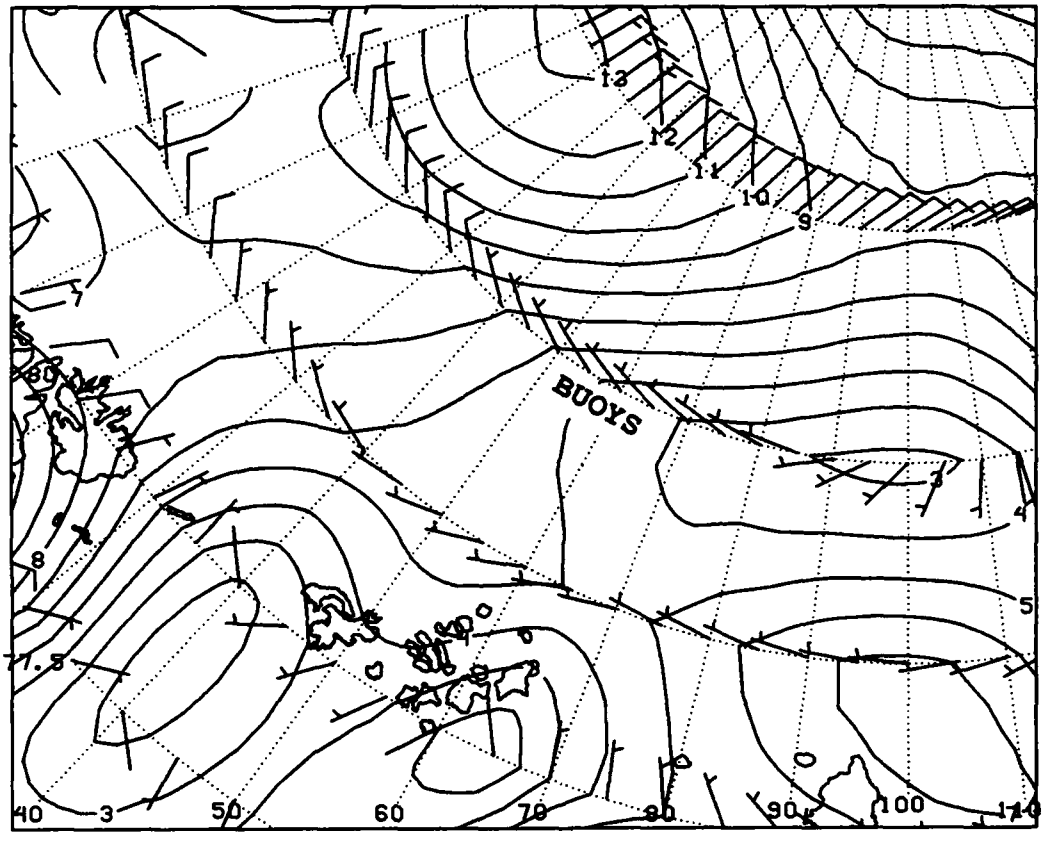

Figure 86. 1000 mb isotachs (m/s) and wind barbs for 26 August 1992, 0000Z.

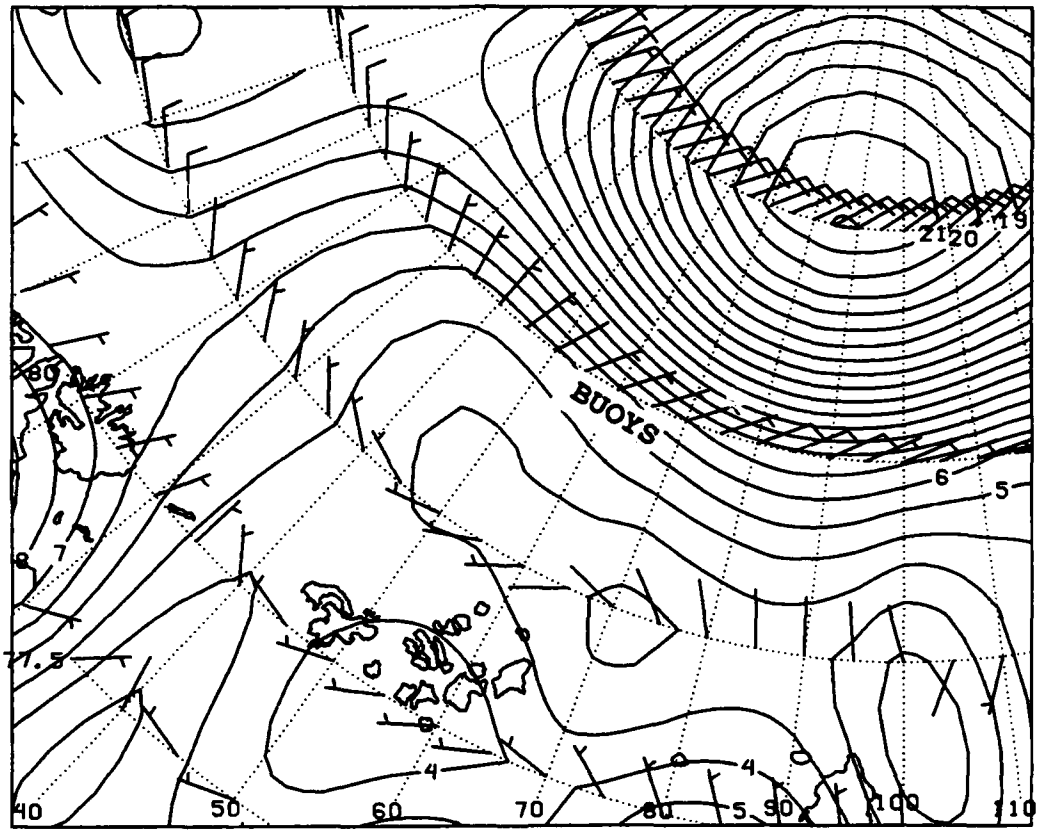

Figure 87. 1000 mb isotachs (m/s) and wind barbs for 26 August 1992, 1200Z.

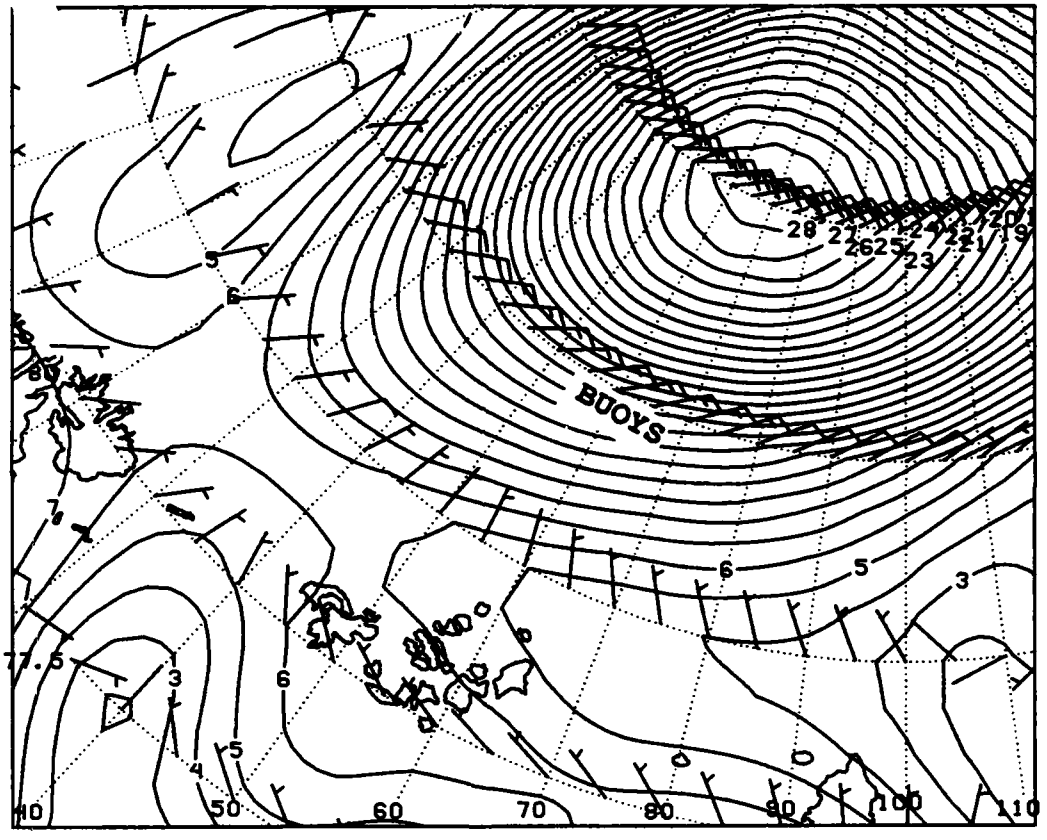

Figure 88. 1000 mb isotachs (m/s) and wind barbs for 27 August 1992, 0000Z.

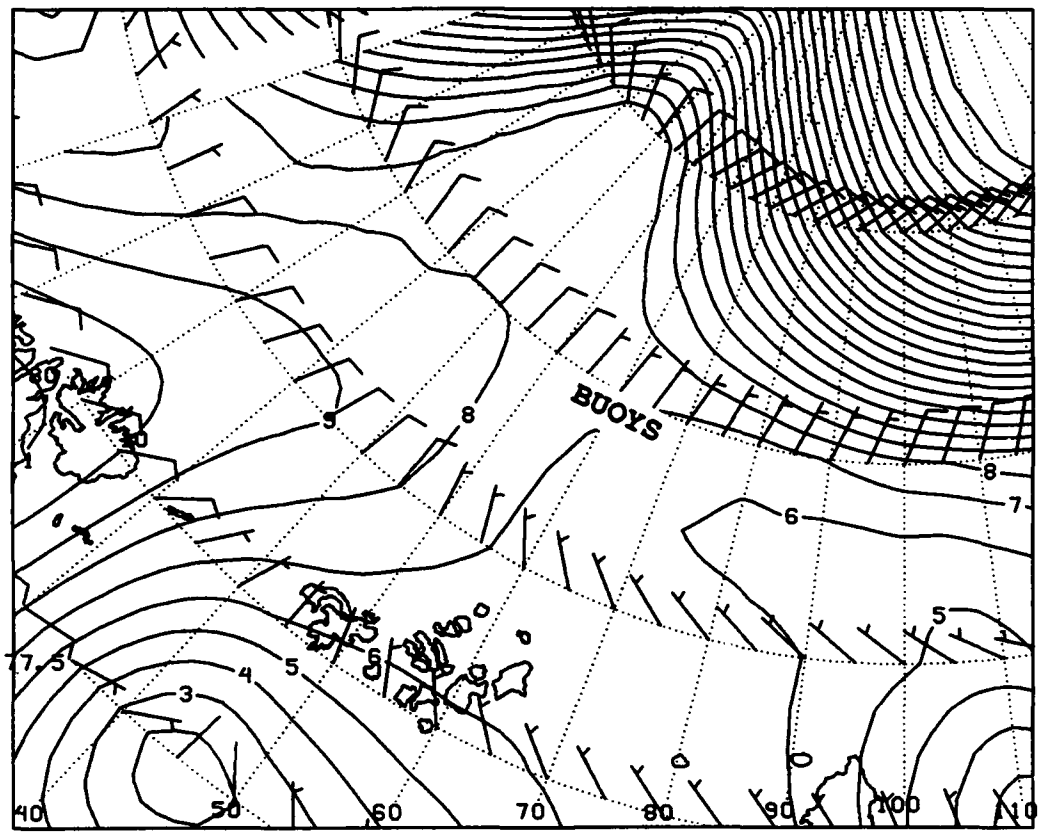

Figure 89. 1000 mb isotachs (m/s) and wind barbs for 27 August 1992, 1200Z.

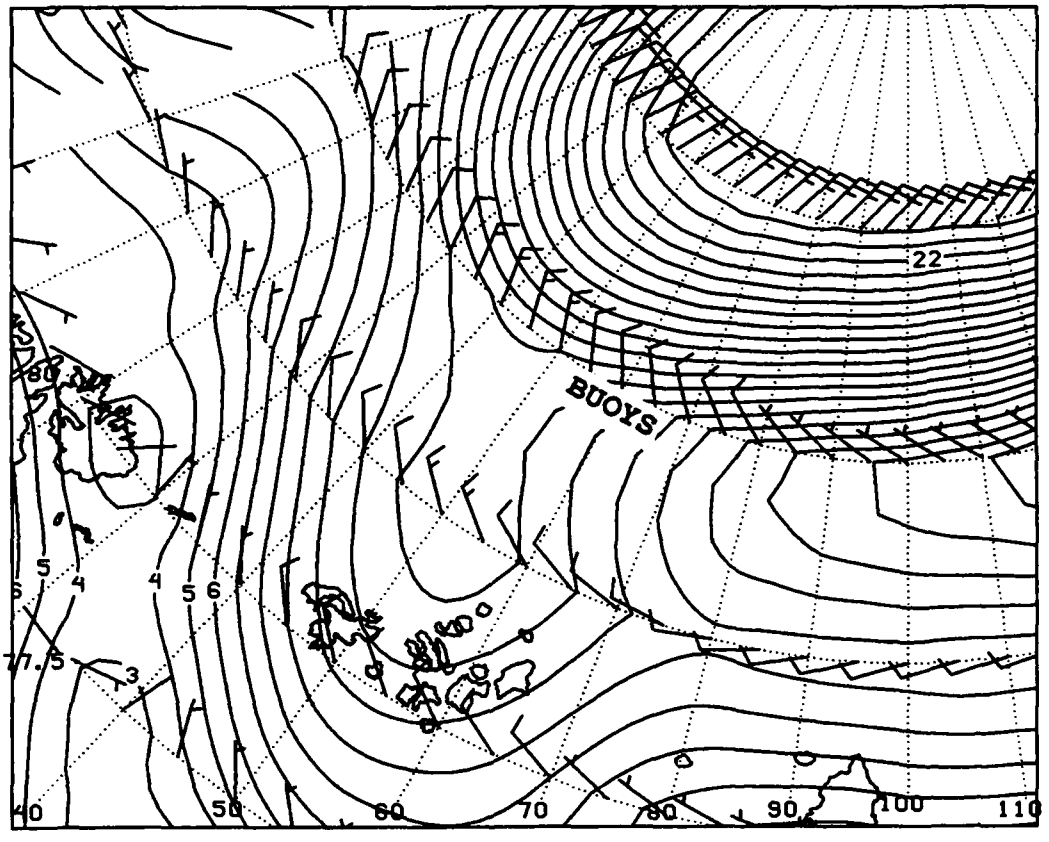

Figure 90. 1000 mb isotachs (m/s) and wind barbs for 28 August 1992, 0000Z.

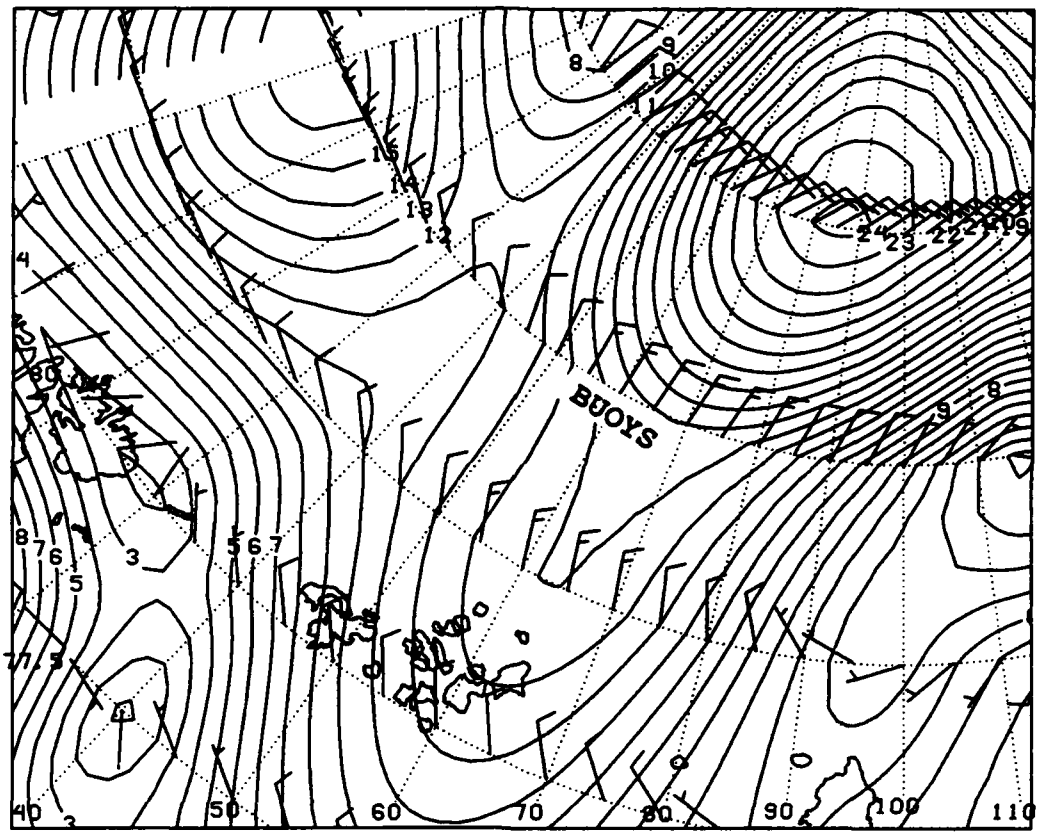

Figure 91. 1000 mb isotachs (m/s) and wind barbs for 28 August 1992, 1200Z.

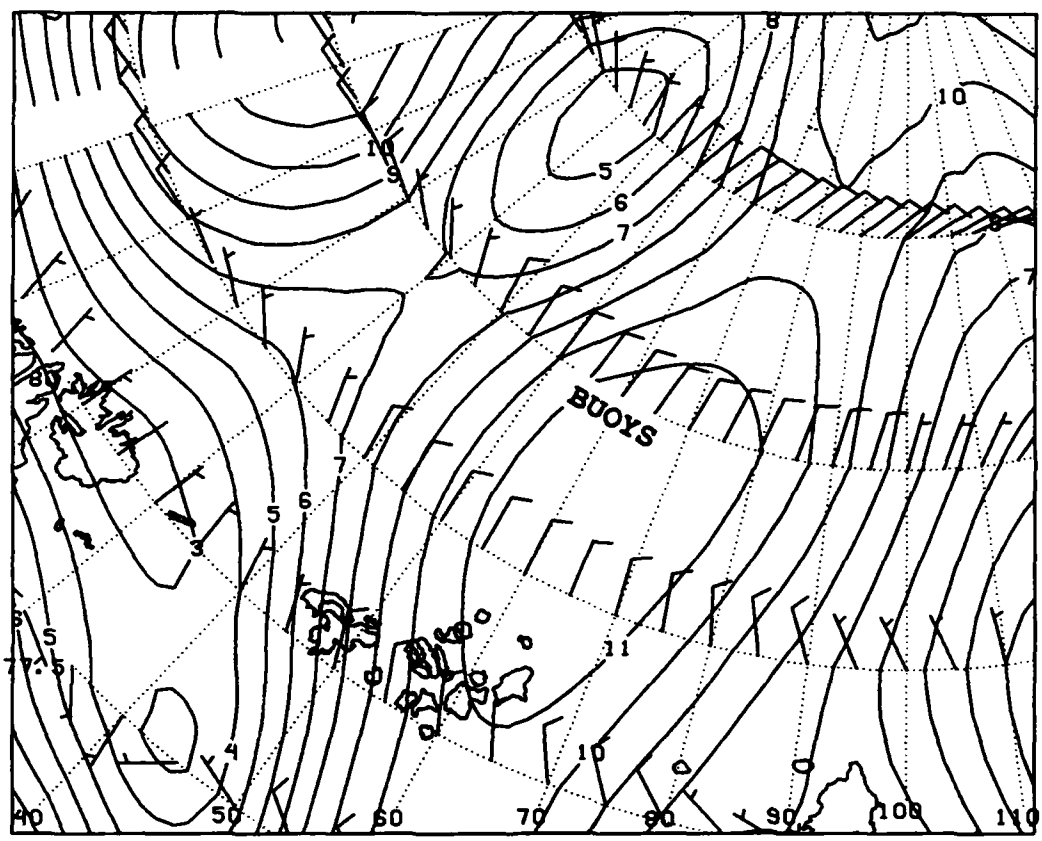

Figure 92. 1000 mb isotachs (m/s) and wind barbs for 29 August 1992, 0000Z.

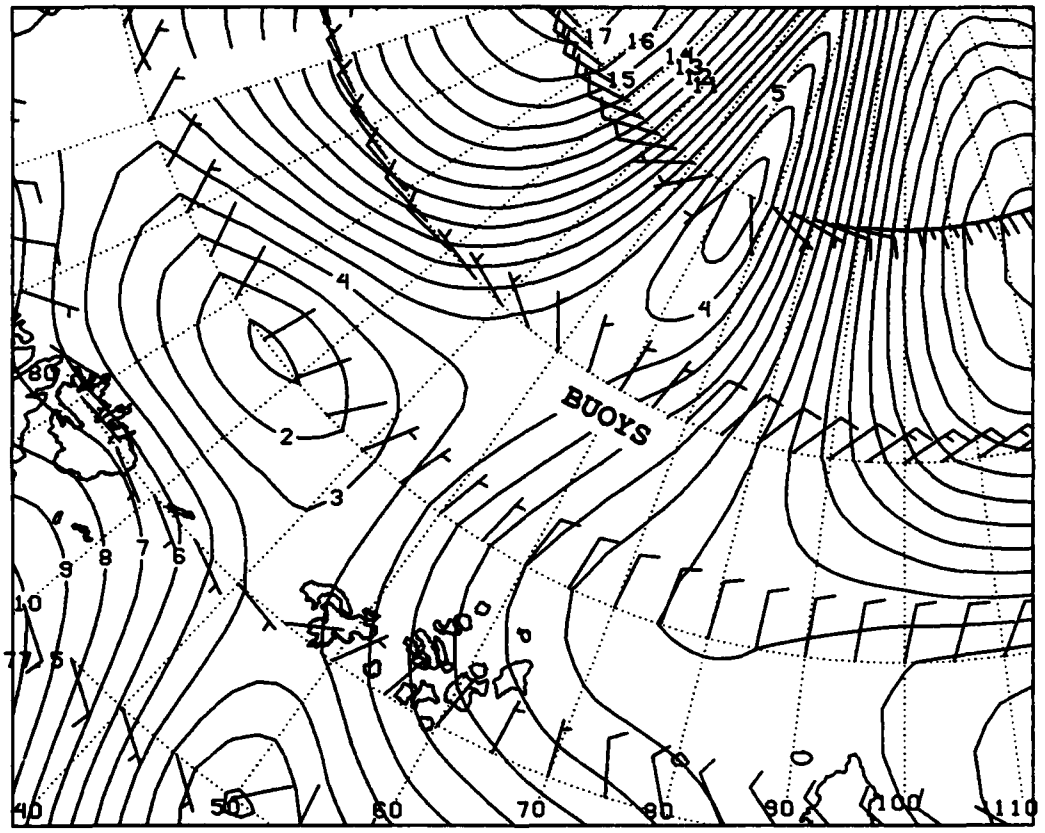

Figure 93. 1000 mb isotachs (m/s) and wind barbs for 29 August 1992, 1200Z.

LIST OF REFERENCES

Barron, M., (private communtication, 1993).

Bourke, R.H. and A.R. Parsons, "Ambient Noise Characteristics of the Northwestern Barents Sea," J. Acoust. Soc. Am., **94**, 2799-2808 (1993).

Buck, B.M. and M.W. Clarke, "Arctic Ambient Noise Level Statistics Based on NIMBUS-6 RAMS and NOAA-ARGOS Ambient Noise Data Buoys, 1975-1985,"(U) Polar Research Laboratory Tech. Rept. 69, Naval Oceanographic Office, Bay St. Louis, MS (1986) (confidential).

Buck, B.M. and M.W. Clarke, "Relating Arctic Under-Ice Ambient Noise with Environmental Factors,"(U) Tech. Rept. 114, Naval Oceanographic Office, Bay St. Louis, MS (1989) (confidential).

Buck, B.M. and J.H. Wilson, "Nearfield Noise Measurements from an Arctic Pressure Ridge," Polar Research Laboratory Tech. Rept. 57, Naval Ocean Research and Development Activity, NSTL Station, Bay St. Louis, MS (1984).

Buck, B.M. and J.H. Wilson, "Nearfield Noise Measurements from an Arctic Pressure Ridge," J. Acoust. Soc. Am., **80**, 256-264 (1986).

Buckingham, M.J. and C. Chen, "Acoustic Ambient Noise in the Arctic Ocean Below the Marginal Ice Zone," in *Sea Surface Sound, Natural Mechanisms of Surface Generated Noise in the Ocean*, edited by B.R. Kerman (Kluwer Academic Publishers, Netherlands, 1988), p. 585.

Cousins, J.D., "CEAREX Ambient Noise Data Measured Northeast of Svalbard," Master's Thesis, Naval Postgraduate School, Monterey, CA, (March 1991).

Diachok, O.I. and R.S. Winokur, "Spatial Variability of Under-Water Ambient Noise at the Ice-Water Boundary," J. Acoust. Soc. Am., **55**, 750-753, (1974).

Dyer, I., "The Song of Sea Ice and Other Arctic melodies," *The Robert Bruce Lecture: 2 March 1983, Arctic technology and Policy*, edited by I. Dyer and C. Chryssostomidis (Hemisphere Publishing, Washington, D.C., 1983), pp. 11-37.

Dyer, I., "Speculations on the Origin of Low Frequency Arctic Ocean Noise," in *Sea Surface Sound, Natural Mechanisms of Surface Generated Noise in the Ocean*, edited by B.R. Kerman (Kluwer Academic Publishers, Netherlands, 1988), pp. 513-530.

Lewis, J.K. and W. G. Denner, "Arctic Ambient Noise in the Beaufort Sea: Seasonal Space and Time Scales," J. Acoust. Soc. Am., **82**, 988-997 (1987).

Lewis, J.K. and W.G. Denner, "Arctic Ocean Noise Generation due to Pack Ice Kinematics and Heat Fluxes," J. Acoust. Soc. Am., **88**, 549-565 (1988).

Makris, N.C. and I. Dyer, "Environmental Correlates of Pack Ice Noise," J. Acoust. Soc. Am., **79,** 3288-3298 (1986).

Makris, N.C. and I. Dyer, "Environmental Correlates of Arctic Ice-edge Noise," J. Acoust. Soc. Am., **90**, 1434-1440 (1991).

Oard, V.T., "Characteristic Spectral Signatures of Arctic Noise Generating Mechanisms," Master's Thesis, Naval Postgraduate School, Monterey, CA, (June 1987).

Parsons, A.R., "Environmental Forcing of Ambient Noise in the Barents Sea," Master's Thesis, Naval Postgraduate School, Monterey, CA, (June 1992).

Poffenberger, D.L., "Analysis of Arctic Ambient Noise Measured from Drifting Buoys in the Greenland Sea ans Eurasian Basin,"(U) Master's Thesis, Naval Postgraduate School, Monterey, CA, (December 1987). (confidential)

Poffenberger, D.L., R.H. Bourke and J.H. Wilson, "Ambient Noise in the Eurasian Basin,"(U) USN J. Underwater Acoust., **38**(4), 433-455 (1988) (confidential).

Urick, R.J., Principles of Underwater Sound, 3rd Edition (McGraw-Hill Book Company, New York, 1983), pp. 202-233.

Williams, R.T., (private communication, 1994).

INITIAL DISTRIBUTION LIST

1.	Defense Technical Information Center Cameron Station Alexandria, VA 22304-6145	2
2.	Library, Code 52 Naval Postgraduate School Monterey, CA 93943-5002	2
3.	Chairman (Code OC/BF) Department of Oceanography Naval Postgraduate School Monterey, CA 93943-5000	3
4.	Dr. James H. Wilson Neptune Sciences, Inc. 3834 Vista Azul San Clemente, CA 92674	2
5.	LT David Feller 1396 Liberty Ave North Bellmore, NY 11710	1
6.	Commander Naval Oceanography Command Code 7170 Stennis Space Ctr, MS 39529-5000 Att: Mr. Jack McDermid	1
7.	Commanding Officer Attn: Mr. Charles O'Neill Naval Oceanographic Office Stennis Space Ctr Bay St. Louis, MS 39522-5001	1
7.	Commanding Officer Attn: Dr. Nelson Letourneau Naval Oceanographic Office Stennis Space Ctr Bay St. Louis, MS 39522-5001	1
8.	Commanding Officer Naval Polar Oceanography Center, Suitland Washington, DC 20373	1
9.	Dr. Robert S. Pritchard Ice Casting, Inc. 11042 Sand Point Way NE Seattle, WA 98125	1

10. Dr. Warren W. Denner — 1
Earth Ocean Science
P.O. Box 1378
Carmel Valley, CA 93924

11. Dr. James K. Lewis — 1
207 South Seashore Ave
Long Beach, MS 39560

12. Mr. Beaumont M. Buck — 1
Polar Associates, Inc.
1828 State St
Santa Barbara, CA 93101

13. Dr. Nicholas C. Makris — 1
Naval Research Laboratory
Code 5160
Washington, DC 20375-5000

14. Dr. Lloyd D. Keigwin — 1
Department of Geology and Geophysics
Woods Hole Oceanographic Institution
Woods Hole, MA 02543

15. Dr. Thomas B. Curtin — 1
Code 322 HL
Office of Naval Research
800 N. Quincy St.
Arlington, VA 22217-5660

16. Mr. Jim Donald — 2
Naval Undersea Warfare Center
New London Lab
Code 01Y
New London, CT 06320

17. Mr. Barry Blumenthal — 1
Code C124A
Advanced Environmental Acoustic Support Program
Office of Naval Research
800 N. Quincy St.
Arlington, VA 22217-5660

18. Mr. Ed Chauka/Mr. Bobby Wheatley — 2
Advanced Environmental Acoustic Support Program
Code ONR - DET
Building 1020 - Room 184
Stennis Space Center, MS 39529-5000